The Effect of LIPUS on TMJ Arthritis in Juvenile Rats

by

Jacqueline Crossman

A thesis submitted in partial fulfillment of the requirements for the degree of

Doctor of Philosophy

Medical Sciences – Oral Biology

University of Alberta

Abstract:

Juvenile idiopathic arthritis (JIA) is an inflammatory disease that can affect the temporomandibular joint (TMJ). TMJ-JIA can cause mandibular growth disturbances. Treatment options include medications targeting inflammation, orthodontic intervention, and surgeries; however, these medications are ineffective in many patients, none of these options stimulate mandibular growth, and surgery is risky, painful, and costly. This thesis aimed to investigate the effect of low intensity pulsed ultrasound (LIPUS) on TMJ-JIA in juvenile rats. LIPUS has been shown to have stimulatory effects on osteoblasts, chondrocytes, and synovial cells, and it has been demonstrated to have an anti-inflammatory effect on arthritis in animal models and more importantly LIPUS can stimulate mandibular growth.

We first aimed to validate the collagen-induced arthritis (CIA) juvenile rat model of TMJ arthritis. Twenty-seven 3-week-old male Wistar rats were used. After *in vivo* micro-computed tomography (MicroCT) scanning, we divided them into 3 groups (n=9): the CIA group, the Saline group, and the Healthy group. The CIA group received CIA-TMJ injections (right and left) with an emulsion of type II collagen (Col-II) and Complete Freund's Adjuvant, the Saline group received saline TMJ injections, and the Healthy group remained untreated. After 4 weeks, the rats were euthanized and *ex vivo* MicroCT scanned, and the TMJ tissues were prepared for analysis. Our results demonstrated that CIA rats had significantly less mandibular growth ($p < 0.01$), their synovial tissues were inflamed, there was an increased expression of interleukin (IL)-1β, matrix metalloproteinase (MMP)-13 and tumor necrosis factor (TNF)-α ($p < 0.05$), there was acute cartilage thickening, and Col-II expression was decreased. These results demonstrate the degenerative changes in TMJ cartilage due to CIA in the TMJ.

Next, we studied the effect of LIPUS on CIA-induced TMJ arthritis. Seventy-two 3-week-old male Wistar rats underwent *in-vivo* MicroCT scans and were divided into 8 groups (n=9). Group 1 received CIA injections into the TMJs and immediate LIPUS treatment to the TMJs (20 minutes/day, 4 weeks); Group 2 received saline TMJ injections and immediate LIPUS treatment; Group 3 received CIA-TMJ injections and no immediate LIPUS (isoflurane anesthesia only, 20 minutes/day, 4 weeks); and Group 4 received saline TMJ injections and no LIPUS treatment. Group 5 received CIA-TMJ injections and after 4 weeks, received LIPUS treatment (delayed LIPUS application); Group 6 received saline TMJ injections and delayed LIPUS; Group 7 received CIA-TMJ injections and no delayed LIPUS (isoflurane only, 20 minutes/day, 4 weeks); and Group 8 received saline TMJ injections and no delayed LIPUS. The animals were euthanized, then *ex vivo* MicroCT scans were completed and tissues were prepared for analysis. We histologically analyzed H&E-stained TMJs, measured cartilage cell layer thicknesses and performed toluidine blue staining. Immunohistochemistry was completed to analyze expression of Col-II, Col-X, MMP-13, receptor activator of NF-κB ligand (RANKL), vascular endothelial growth factor (VEGF), transforming growth factor (TGF)-β1, IL-1β, IL-17, and TNF-α. ELISAs quantified levels of TNF-α and IL-1β in the blood serum, TGF-β1 (active/inactive forms) in the plasma, and IL-6 and IL-1β in the articular disc. We calculated mandibular and condylar growth using MicroCT analysis.

In general, synovitis and condylar bone erosion were observed in the CIA TMJs, but less severe synovitis and minimal erosion was present in the LIPUS-treated TMJs. Immediate LIPUS treatment prevented acute cartilage thickening due to CIA ($p < 0.05$); increased proteoglycan production and Col-II, Col-X, and TGF-β1 expression; decreased MMP-13 and VEGF expression; and stimulated mandibular growth in CIA TMJs ($p < 0.005$). Delayed LIPUS treatment increased

Col-II and TGF-β1 expression, but it did not affect cartilage thickness nor stimulate mandibular growth.

This study validated the CIA juvenile rat model of TMJ arthritis. Our results show that LIPUS prevented mandibular growth disturbances and acute cartilage changes caused by CIA. The inflammatory effects from CIA didn't appear to persist in the rats that received delayed LIPUS, so we observed minimal effects of CIA and LIPUS in these older rats. This study's results have increased the understanding of this animal model of arthritis, its uses and limitations, as well as providing a greater understanding of LIPUS and its effects on the TMJ and mandibular growth in CIA-induced TMJ arthritic rats. These results will help to design future studies to further investigate LIPUS and TMJ arthritis, towards developing a new treatment for children TMJ-JIA.

Preface:

This thesis in an original work by Jacqueline Crossman. This research received ethics approval from the University of Alberta Animal Care and Use Committee (AUP00002169).

Chapter 3 of this research has been published in the journal Tissue Engineering: Part C [Crossman J, Lai H, Kulka M, Jomha N, Flood P, El-Bialy T. Collagen-induced temporomandibular joint arthritis juvenile rat animal model. *Tissue Engineering: Part C.* 2021; 27 (2): 115-123]. Doi: 10.1089/ten.tec.2020.0294. Jacqueline Crossman designed and performed the experiments, collected and analyzed the data, and wrote the article. H. Lai helped design the experiments, performed statistical analysis, and edited the article. M. Kulka helped analyze the data and edited the article. N. Jomha helped analyze the data and edited the article. P. Flood helped design the experiments, helped analyze the data, and edited the article. T. El-Bialy helped design the experiments, analyzed data, edited the article, supervised the project, and provided financial support beyond the received external peer reviewed funds.

Chapter 4 has been prepared as manuscript for future publication in a peer-reviewed scientific journal. Jacqueline Crossman designed and performed the experiments, collected and analyzed the data, and wrote this manuscript. H. Lai helped design the experiments, performed statistical analysis, and edited this manuscript. M. Kulka helped analyze the data and edited the manuscript. N. Jomha helped analyze the data and edited the manuscript. P. Flood helped design the experiments, helped analyze the data, and edited the manuscript. T. El-Bialy helped design the experiments, analyzed data, edited the manuscript, supervised the project, and provided financial support beyond the received external peer reviewed funds.

Dedication:

This thesis is dedicated to my wonderful husband, Andrew, who has been my constant source of support and encouragement before, during, and after my graduate studies. I am truly thankful to have you in my life and cannot imagine it any other way. I look forward to the wonderful things to come. I also dedicate this work to my parents, Allan and Barbara, and my in-laws, Roland and Barbie, who continue to love and support me unconditionally, and whose lives are perfect examples of hard work and dedication that I aspire to achieve in my own life.

Acknowledgement:

First, I would like to thank my supervisor, Dr. Tarek El-Bialy, for his continual guidance and support throughout this program and beyond. I express my sincere gratitude to my supervisory committee members, Dr. Patrick Flood, Dr. Hollis Lai, Dr. Marianna Kulka, and Dr. Nadr Johma, for their discussion, direction, suggestions, and assistance with my research and writing.

My sincere thanks to the past El-Bialy lab members for their support, the members of neighbouring labs within the Department of Dentistry for their help with lab techniques, and my program advisors and directors for their guidance.

I would also like to acknowledge my funding sources: Graduate Students' Association (GSA), School of Dentistry, Women and Children's Health Research Institute (WCHRI), Faculty of Medicine and Dentistry, Mitacs Inc., Canadian Association for Dental Research (CADR) and Network for Canadian Oral Health Research (NCOHR) , and Faculty of Graduate Studies and Research. Thank you.

Table of Contents

CHAPTER ONE: INTRODUCTION 1
1. Background and literature review.....2
1.1 Rheumatoid Arthritis and Juvenile Idiopathic Arthritis 2
1.1.1 Disease Subsets and Characterization 2
1.1.1 Genetics 3
1.1.3 Pathology and Immunology 4
1.1.4 Prevalence and Involvement of the Temporomandibular Joint (TMJ) 9
1.1.5 Management and Treatment of TMJ Arthritis 12
1.2 Low Intensity Pulsed Ultrasound (LIPUS) 14
1.2.1 Effect of LIPUS on Fracture Healing 16
1.2.2 Effect of LIPUS on Chondrocytes 21
1.2.3 Effect of LIPUS on Osteoblasts 22
1.2.4 Effect of LIPUS on Synovial Cells 23
1.2.5 Effect of LIPUS on Arthritis 24
1.2.6 Effect of LIPUS on Mandibular Growth 29
1.2.7 Effect of LIPUS on TMJ Arthritis 30
1.3 Animal Models of Rheumatoid Arthritis and Juvenile Idiopathic Arthritis 31
1.4 Collagen-induced Arthritis 32
1.5 Study Aims and Hypotheses.....35
1.6 References.....36
CHAPTER TWO: MATERIALS AND METHODS 42
2.1 Animal Care and Experimental Design 43
2.2 Part 1: Validation of TMJ arthritis in collagen induced arthritis (CIA) juvenile rats 43
2.2.1 Micro-computed tomography scanning.....43
2.2.2 Collagen-induced arthritis (CIA).....44
2.2.3 Tissue preparation and *ex vivo* MicroCT scanning 46

2.2.4 Histology and Immunohistochemistry....46
2.2.5. Analysis....48
2.3 Part 2: The effect of LIPUS on TMJ arthritis in juvenile rats....50
2.3.1 Micro-computed tomography scanning....50
2.3.2. Groups....50
2.3.3. Histology and Immunohistochemistry....54
2.3.4 Enzyme-linked immunosorbent assays (ELISAs)....55
2.3.5 MicroCT Analysis....56
2.3.6 Statistical Analysis....58
CHAPTER THREE: COLLAGEN-INDUCED TEMPOROMANDIBULAR JOINT ARTHRITIS JUVENILE RAT ANIMAL MODEL....59
3.1 Abstract....60
3.2 Impact Statement....60
3.3 Introduction....61
3.4 Methods....61
3.4.1 Collagen-induced arthritis....61
3.4.2 Experiment....61
3.4.2.1 Experimental design....61
3.4.2.2 Statistical analyses....63
3.4.2.3 Experimental results....63
3.5 Discussion....63
3.5.1 Limitations....67
3.6 Conclusion....67

3.7 Authors' Contributions 67

3.8 Disclosure Statement 67

3.9 Funding Information 67

3.10 References 67

CHAPTER FOUR: THE EFFECT OF LOW INTENSITY PULSED ULTRASOUND ON TMJ ARTHRITIS IN JUVENILE RATS 69

4.1 Abstract 70

4.2 Introduction 71

4.3 Materials and Methods 75

4.3.1 Animals and Study Design 75

4.3.2 Body Weights, Head Widths and MicroCT Scanning 75

4.3.3 Histology and Immunohistochemistry 77

4.3.4 Enzyme-linked Immunosorbent Assays (ELISAs) 79

4.3.5 MicroCT Analysis 80

4.3.6 Statistical Analysis 81

4.4 Results 82

4.5 Discussion 100

4.6 Conclusion 114

4.7 References 115

CHAPTER FIVE: GENERAL DISCUSSION AND CONCLUSION.....119

5.1 Limitations and Future Studies 128

5.2 Reference 129

BIBLIOGRAPHY 131

List of Tables

Chapter 2

Table	*Description*	*Page*
Table 2	Description of group allocation.	Pg. 50

Chapter 3

Table	*Description*	*Page*
Table 1	Mean, Standard Deviation, *F*-Values, and *P*-Values (*Post Hoc*) for Body Weight (g) (Before and After MicroCT Scanning) and Head Width (mm) at Days 1 and 2 Postinjection in Each Group (CIA, Saline, and Healthy)	Pg. 65

Chapter 4

Table	*Description*	*Page*
Table 4.1	Group allocation including 8 described groups (n=9) receiving Either CIA or Saline TMJ injections and LIPUS or no LIPUS treatment (isoflurane only) for 20 minutes/day.	Pg. 75

List of Figures

Chapter 1

Figure	*Description*	*Page*
Figure 1.1	Illustration showing cartilage cell layers of the mandibular condyle. A) Fibrocartilage, B) Proliferating chondrocytes, C) Mature chondrocytes, D) Hypertrophic chondrocytes.	Pg. 11
Figure 1.2	Illustration demonstrating 4 stages of fracture repair: 1) Inflammation, 2) Soft callus, 3) Hard callus, 4) Remodeling.	Pg. 17
Figure 1.3	Illustration demonstrating how LIPUS affects intracellular Signaling pathways in healthy chondrocytes.	Pg. 26
Figure 1.4	Illustration demonstrating how LIPUS affects intracellular signaling pathways in inflamed chondrocytes.	Pg. 27
Figure 1.5	Illustration demonstrating how LIPUS affects intracellular signaling pathways in healthy synovial cells.	Pg. 28
Figure 1.6	Illustration demonstrating how LIPUS affects intracellular signaling pathways in inflamed synovial cells.	Pg. 29

Chapter 2

Figure	*Description*	*Page*
Figure 2.1	Photos of isoflurane anesthesia unit (left) and knockdown Chamber (right).	Pg. 43

Figure 2.2	Illustration demonstrating TNF-α quantification analysis. Three fields of view (green boxes) on illustrated condyle placed at central axis, midpoint between central axis and anterior edge of condyle, and midpoint between central axis and posterior edge of condyle, as described above. Photomicrograph representing TNF-α-stained cartilage. Scale bar = 50 μm	Pg. 48
Figure 2.3	Illustration demonstrating mandibular length measurements from condylar point (a) to menton point (b).	Pg. 49
Figure 2.4	Illustration showing study design for Part 2.	Pg. 51
Figure 2.5	Photo of rats receiving LIPUS treatment (right) vs. Isoflurane only (left).	Pg. 52
Figure 2.6	Photo of rat receiving LIPUS treatment.	Pg. 53
Figure 2.7	Illustrative photo of example head width measurements at day 1 in a Saline (left) and CIA rat (right)	Pg. 53
Figure 2.8	Illustration demonstrating segmentation of mandibular condyle (pink) from mandible (yellow) for calculation of condylar volume.	Pg. 57

Chapter 3

Figure	*Description*	*Page*
Figure 1	(A) 3D Reconstruction. Representative hemimandibles from each group (CIA, Saline, and Healthy). (B) Mandibular length. Illustration showing mandibular length; a—condylar point, b—menton point. Average mandibular growth (mm) in each group. $**p < 0.01$. (C) TMJ condyles. Representative bony changes between TMJ condyles (only condyle shown) in each group. 3D, three-dimensional; CIA, collagen-induced arthritis; TMJ, temporomandibular joint.	Pg. 62

Figure 2 (A) Schematic il- lustration showing direction of histological Sectioning (sagittal plane). (B) Re- presentative H&E-stained TMJs from CIA, Saline, and Healthy groups. Articular cartilage and synovial tissue. *White* scale bar = 200 mm and *black* scale bar = 100 mm. Pg. 63

Figure 3 (A) Illustration representing the seven condylar cartilage measurements performed for each cartilage cell layer of the mandibular condyle. (B) TMJ condylar cartilage cell layer thicknesses (mm) (fibrocartilage, proliferative, chondrogenic, and hypertrophic cell layers) for CIA, Saline, and Healthy groups. ***$p < 0.005$. Pg. 64

Figure 4 Rat body weight and head widths. Average body weight (g) (A) And Head widths (mm) (B) measured at each time point before and after TMJ injections. *$p < 0.05$, **$p < 0.01$, ***$p < 0.005$. Pg. 65

Figure 5 (A) TB-stained TMJ condyles and immunohistochemical staining For Col-II, MMP-13, and IL-1b. Immunohistochemistry Photomicrographs from each group (CIA, Saline, and Healthy groups). Negative control involved the absence of primary antibody. Representative photomicrographs for the negative control and from each group are shown for each immunostain. Scale bars = 200 mm (TB only) and 50 mm. (B) Representative images for CIA, Saline, and Healthy groups for TNF-a immunohistochemical staining. Quantification of chondrocytes positive for TNF-a in articular cartilage. Means – SDs are shown. Scale bar = 50 mm. *$p < 0.05$. Col-II, type II collagen; IL-1b, interleukin-1b; MMP-13, matrix metalloproteinase 13; SD, standard deviation; TB, Toluidine blue; TNF-a, tumor necrosis factor-a. Pg. 66

Chapter 4

Figure	*Description*	*Page*
Figure 4.1	Photographic example of a rat receiving LIPUS treatment to right and left TMJs under isoflurane anesthesia. LIPUS transducers with ultrasound gel were applied to shaved TMJ areas.	Pg. 77
Figure 4.2	Illustration demonstrating how the thickness of fibrocartilage, proliferative, chondrogenic and hypertrophic cell layers were measured at 7 points on the mandibular condylar cartilage [Crossman et al., 2021].	Pg. 78
Figure 4.3	Illustration demonstrating how mandibular length (A) was performed and how the mandibular condyle (pink) was segmented from the mandible (yellow) to calculate condyle volume [B]. a = condylar point, b = menton point.	Pg. 81
Figure 4.4	Head width increases compared to baseline (pre-injection) head widths in each group through the study at the indicated days. Days 1-22 (black) began the day after TMJ inections. Days 1-21 (red) were days 1-21 of delayed LIPUS/isoflurane treatment.	Pg. 83
Figure 4.5	Body weight increases from each group throughout the study and are shown as a percent increase from their weights pre-injection.	Pg. 84
Figure 4.6	Representative photomicrographs of H&E-stained histological sections of the TMJ from each group. Scale bar = 2 mm.	Pg. 85
Figure 4.7	Representative photomicrographs of H&E-stained histological sections of TMJ condylar cartilage from each group. Scale bar = 200 μm.	Pg. 86
Figure 4.8	The cartilage cell layer (fibrocartilage, proliferative,	Pg. 87

chondrogenic, hypertrophic) thicknesses in each group. Data is represented as the mean ± S.D. * = $p < 0.05$, ** = $p < 0.01$, *** = $p < 0.005$

Figure 4.9 Representative photomicrographs of T.B.-stained histological sections of TMJ cartilage from each group. Scale bar = 200 μm. Pg. 88

Figure 4.10 Representative photomicrographs of immunohistochemically-stained TMJ cartilage from each group. A) Col-II, B) Col-X, C) MMP-13. Scale bar = 100 μm (A, C), 200 μm (B). Pg. 89

Figure 4.11 Representative photomicrographs of immunohistochemically-stained TMJ cartilage from each group. A) RANKL, B) VEGF, C) TGF-β1. Scale bar = 500 μm (A), 50 μm (B), 100 μm (C). Pg. 91

Figure 4.12 Representative photomicrographs of immunohistochemically-stained TMJ cartilage from each group. A) IL-1β (synovium), B) IL-1β (articular disc), C) IL-17 (synovium), D) IL-17 (articular disc), E) TNF-α (cartilage), F) TNF-α (synovium). Scale bar = 100 μm (A-D, F), 20 μm (D). Pg. 93

Figure 4.13 Level of TNF-α (pg/mL) in blood serum. Data is represented as the mean ± S.D. * = $p < 0.05$ Pg. 94

Figure 4.14 Level of TGF-β1-LAP (ng/mL) in blood plasma. Data is represented as the mean ± S.D. Pg. 96

Figure 4.15 Representative 3D reconstructions of hemimandibles from each group showing condylar erosion (red arrows). Pg. 97

Figure 4.16	Mandibular growth (lengthwise) (mm) in each group. *** = $p < 0.005$	Pg. 98
Figure 4.17	Condylar growth (volume-wise) (mm^3) in each group. * = $p < 0.05$, ** = $p < 0.01$, *** = $p < 0.005$	Pg. 99
Figure 5.1	Illustration of proposed mechanism of the effect of CIA on the TMJ and mandibular growth in Part 1.	Pg. 123
Figure 5.2	Illustration of proposed mechanism of the effect of immediate LIPUS treatment on CIA in the TMJ and mandibular growth in Part 2.	Pg. 125

List of Abbreviations

AA: Arachindonic acid

ACPA: Antibodies to citrullinated protein antigens

ANOVA: Analysis of variance

APC: Antigen presenting cell

CD: Cluster of differentiation

CFA: Complete Freund's adjuvant

CIA: Collagen-induced arthritis

Col-I/II/X: Type I/II/X collagen

COX: Cyclooxygenase

CT: computed tomography

DAB: Diaminobenzidine

DC: dendritic cell

DMARD: Disease-modifying antirheumatic drug

DNA: Deoxyribonucleic acid

ECM: Extracellular matrix

ELISA: Enzyme-linked immunosorbent assay

ERK: Extracellular signal regulating kinase

FAK: Focal adhesion kinase

FDA: Food and drug administration

H&E: Hematoxylin and eosin

HA: Hyaluronan

HLA: Human leukocyte antigen

HRP: Horseradish peroxidase

IAS: Intra-articular steroid

IFA: Incomplete Freund's adjuvant

IFN: Interferon

IgA: Immunoglobulin A

IgG: Immunoglobulin G

IL: Interleukin

JIA: Juvenile idiopathic arthritis

KO: Knockout

LAP: Latency associated peptide

LIPUS: Low intensity pulsed ultrasound

M1/M2: Macrophage type ½

MAPK: Mitogen-activated protein kinase

MHC: Major histocompatibility complex

MicroCT: Micro-computed tomography

MMP: Matrix metalloproteinase

MRI: magnetic resonance imaging

NK: Natural killer

NSAID: Non-steroidal anti-inflammatory drug

OA: Osteoarthritis

OPG: Orthopantomogram or osteoprotegerin

PBS: Phosphate-buffered saline

PG: Prostaglandin

PGE2: Prostaglandin E2

PI3K: Phosphoinositol 3 kinase

PKA: protein kinase A

RA: Rheumatoid arthritis

RANKL: Receptor activator of NF-κB ligand

RCT: Randomized controlled trial

RF: Rheumatoid factor

SATA: Spatial average-temporal average

TB: Toluidine blue

TBS: Tris-buffered saline

TGF: Transforming growth factor

Th: T helper

TMJ: Temporomandibular joint

TNF: Tumor necrosis factor

VEGF: Vascular endothelial growth factor

CHAPTER 1: INTRODUCTION

1. *Background and literature review*

1.1 Rheumatoid Arthritis and Juvenile Idiopathic Arthritis

1.1.1 Disease Subsets and Characterization

Rheumatoid arthritis (RA) is a chronic, autoimmune disease that is characterized by joint and systemic inflammation and the production of autoantibodies. This syndrome encompasses multiple subsets, each of which involves inflammatory cascades, initiated by the complement-mediate immune system, that ultimately lead to a common pathway that results in persistent synovial inflammation and accompanying damage to articular cartilage and underlying bone [Guo et al., 2018; Scott, Wolfe & Huizinga, 2010; Demoruelle, Deane & Holers, 2014]. In general, these disease subsets are further divided into 'seropositive' and 'seronegative', meaning that the blood serum from a patient with arthritis is either positive or negative for rheumatoid factor (RF+ and RF-), an autoantibody associated with the development of RA [Nigrovic, Raychaudhuri & Thompson, 2018; Guo et al., 2018]. Other types of arthritis that do not fall under the category of RA are combined into a group termed 'spondyloarthritis'. Historically, RA affects adults, but the primary inflammatory arthritides that involve the pediatric population are grouped as juvenile idiopathic arthritis (JIA). JIA is further subcategorized into seven categories: systemic arthritis, oligoarthritis, polyarthritis rheumatoid factor (RF)- positive, polyarthritis RF-negative, enthesitis-related arthritis, psoriatic arthritis, and undifferentiated arthritis. Sharply dividing disease terms for inflammatory arthritis between the adult and juvenile populations may pose a problem when we consider the extensive phenotypic overlap and genetic associations between RA and JIA [Nigrovic, Raychaudhuri & Thompson, 2018].

RA is generally polyarthritis that affects joints symmetrically. The most common joints to be affected are the metacarpophalangeal (knuckles) and proximal interphalangeal (finger joints immediately distal to the knuckle). JIA can affect any joint but is mostly observed in larger joints. RA and JIA less frequently affect the shoulder and hip joints. Subcutaneous nodules, rheumatoid vasculitis, pericardial involvement, and ocular manifestations can be observed in both RA and JIA patients, but the frequency and prevalence of these clinical features vary between RA and JIA and between their own subcategories (ie. seronegative/positive, etc.) [Prahalad & Glass, 2002]. Even further similarities between RA and JIA occur when considering pathological features of each disease. Both diseases present hypertrophy and hyperplasia of the synovial lining, along with early cellular infiltration of mainly T lymphocytes. As inflammation of the joint progresses, bone erosion and cartilage destruction result. Typically, this type of joint damage happens later in JIA compared to RA, but this may be simply due to the increased thickness of juvenile articular cartilage compared to that in adults. Additionally, it is believed that both diseases primarily involve type 1 T helper (Th1) lymphocytes, as well as pro-inflammatory cytokines, including tumor necrosis factor (TNF)-α and interleukin (IL)-1 [Prahalad & Glass, 2002].

1.1.2 Genetics

Recent studies in the field of genetics have begun to shed light on distinguishing patterns across the age spectrum between JIA and RA, revealing that the age divide between RA and JIA may not be correct. The human leukocyte antigen (HLA) haplotypes were the first to be associated with an increased risk of developing arthritis. These associations include rheumatoid arthritis with HLA-DRB1 and related alleles. These encode amino acid sequences that enhance the presentation of citrullinated peptides that are involved in the development of systemic pathogenic autoimmunity

in JIA and RA [Nigrovic, Raychaudhuri & Thompson, 2018; Demoruelle, Deane & Holers, 2014]. Another example of arthritis traversing the age-divide is shown by seropositive RA patients and seropositive polyarticular JIA patients both being RF+. Furthermore, it has been shown that oligoarticular JIA, seronegative polyarticular JIA, and seronegative RA patients all share many HLA associations [Nigrovic, Raychaudhuri & Thompson, 2018]. These examples suggest that a better categorization of arthritis may be the forms or categories of arthritis, as described previously, rather than arthritis that affects either the juvenile or adult population (ie., JIA vs. RA).

Although both diseases appear to have similar genetic susceptibility factors, other predisposing factors, like viral infections, smoking, and periodontitis, may play a role in determining the type of specific disorder and its associated manifestations of disease [Prahalad & Glass, 2002; Nigrovic, Raychaudhuri & Thompson, 2018]. As well, although these diseases may be similar across the age spectrum, management of the disease should not follow the same pattern. This is because disease management needs to carefully consider skeletal growth, drug metabolism and toxicity, exposure and comorbidities, psychosocial development, and locations and methods of patient care [Nigrovic, Raychaudhuri & Thompson, 2018].

1.1.3 *Pathology and Immunology*

Considering the phenotypic and genetic overlap between RA and JIA, it is logical that studying the etiology, pathology and immunology of RA is beneficial in understanding these same processes involved in JIA. Understanding the mechanisms of disease development in RA will help with creating effective preventive strategies, and as well, comprehending the mechanisms of joint

inflammation and disease progression will be beneficial in developing strategies for early treatment.

Prior to the onset of joint inflammation in RA, RA-related autoantibodies have been shown to be elevated in a patient's serum. These levels can be elevated around 3-5 years, and even up to more than 10 years, before clinical RA is presented [Demoruelle, Deane & Holers, 2014; Aho et al., 1985]. This period of elevated autoantibodies is called 'preclinical RA'. RA-related autoantibodies, include, in addition to rheumatoid factor (RF), antibodies to the following: (antibodies to) citrullinated protein antigens (ACPAs), peptidyl arginine deiminase, carbamylated proteins, and mutated citrullinated vimentin. In addition to the elevated levels of autoantibodies, there are also abnormalities of biomarkers that demonstrate systemic inflammation during this preclinical RA period. These include cytokines, chemokines, and variably C-reactive protein [Demoruelle, Deane & Holers, 2014]. Studies have shown that elevated autoantibodies both precede and do not precede cytokine/chemokine elevation, however, it is possible that some degree of local or systemic inflammation that is associated with the early development of autoimmunity of RA may be initially present and then further inflammatory and autoimmune responses expand over time until clinically-apparent RA develops and is identified [Demoruelle, Deane & Holers, 2014; van de Sande et al., 2010; Snir et al., 2010].

In early stages of RA development, the synovium may not show evidence of synovial inflammation even though plasma cells in the synovium of patients with established RA have been shown to generate autoantibodies [van de Sande et al., 2010]. As well, some patients with elevated levels of serum RA-related autoantibodies demonstrate no evidence of synovial inflammation

when analyzed histologically, clinically, or by magnetic resonance imaging (MRI) [van de Sande et al., 2010]. This information may reveal that the initial inflammation and autoimmunity involved in RA begins outside of the joints. These processes may begin at mucosal sites and surfaces like the oral mucosa, the gastrointestinal mucosa, or the respiratory tract that is lined with respiratory epithelium. The predominant antibody of the mucosal immune system is immunoglobulin A (IgA). IgA-ACPAs are elevated and strongly associated with RA in preclinical and early RA subjects. Initially, the host immune system interacts with an environmental antigen at the mucosal surface and a local immune-mediated inflammatory reaction takes place. This action may potentially trigger an autoimmune response that is initially local, but over time, it may develop into a systemic response with circulating RA-related autoantibodies that can be detected in the blood. Complement-mediated immune responses, such as those within a synovial joint (ie. synovitis), may be a direct result from circulating immune complexes that contain citrullinated fibrinogen depositing in the synovium. This type of immune response to these complexes involves immunoglobulin antibodies, such as IgA. Autoimmunity may potentially transition or spread from one inflamed site to another because antigen-specific T cell responses that are initiated at one mucosal surface can traffic to other organs. Blocking this transition between joints may be an interesting mechanism for disease prevention and management. [Demoruelle, Deane & Holers, 2014]

Since RA is an autoimmune disorder, immune cells (mainly B- and T-cells and macrophages) play important roles in RA pathogenesis and can function locally in the synovial tissue within a joint and circulate in the blood. T-cells function by recognizing antigens and activate B-cells. Activated B-cells are responsible for the production and secretion of antibodies,

such as rheumatoid factors (RFs) and (antibodies to) citrullinated protein antigens (ACPAs), and pro-inflammatory cytokines, such as TNF-α, IL-6, IL-12, IL-23 and IL-1α. Similar to B-cells and T-cells, activated macrophages can also produce cytokines and chemokines which further support and promote joint inflammation. [Demoruelle, Deane & Holers, 2014]

As a member of the adaptive immune system, B-cells that are autoreactive identify host antigens and proceed towards the destruction of cells or tissues. Normally, autoreactive B-cells are eliminated by repair mechanisms either during stages of progression from early immature B-cells in the bone marrow, or even prior to B-cells becoming mature naïve B-cells. These processes are regulated at two checkpoints, namely the central and peripheral B-cell tolerance checkpoints. In RA, these checkpoints are typically defective, leading to a large production of autoreactive mature naïve B-cells [Yap et al., 2018]. Interestingly, this defect may potentially be caused by a mutation in the PTPN22 gene. Patients that have this mutated gene may not respond to medications used to reduce inflammation and alleviate other clinical presentations of RA [Yap et al., 2018]. Autoreactive B-cells act as antigen presenting cells (APCs) and stimulate T-cell maturation and differentiation into memory CD4+ T-cells. Normally, CD4+ T-cells interact with HLA and co-stimulating molecules like CD28 which are expressed on the cell surface of APCs. This interaction leads to the activation of intracellular phosphoinositide 3-kinase (PI3K) signaling pathways, ultimately resulting in the maturation of CD4+ T-cells and antigenic activation of naive CD8+ T-cells, which promotes inflammation [Demoruelle, Deane & Holers, 2014].

To further understand autoimmunity in RA, further investigation on how RA-associated autoimmunity is functionally related to bone loss has been initiated. It has been proposed that

antibodies, such as ACPAs, play a role in activating osteoclast differentiation. Although the specific mechanisms of target molecules that reside on the cell surface of osteoclasts and of the downstream signalling remain generally unclear, the mechanisms of how these ACPAs as immune complexes bind and activate these cells has been proposed [Catrina et al., 2017]. Upon osteoclast precursor fusion and osteoclast maturation, citrullinated proteins on the osteoclast cell surface bind to ACPAs. This may stimulate the production and release of pro-inflammatory cytokines involved in enhancing osteoclast activity and therefore increasing bone resorption and bone loss. Additionally, it has been proposed that ACPAs in immune complexes, a complementary mechanism, may further increase osteoclast activation by engaging the Fc receptors on the surface of osteoclasts [Catrina et al., 2017].

T-helper (Th) cells, as previously mentioned, are important T cells involved in both RA and JIA. Th1 cells can also secrete pro-inflammatory cytokines like B-cells. The main cytokines produced by Th1 cells are interferon (IFN)-gamma, IL-2 and TNF-α. Th1 cells can also activate macrophages causing them to act as APCs. Another important type of Th cell involved in RA is the Th17 cell which is a main cell type responsible for secreting IL-17. IL-17 stimulates cell production of pro-inflammatory cytokines (ie. IL-6, IL-8, TNF-α), chemokines (for recruiting immune cells to the synovium [ie. infiltration]), matrix metalloproteinases (MMPs) (ie. MMP-1 and MMP-3), and other important factors like vascular endothelial growth factor (VEGF) (ie. VEGFA). Furthermore, regulatory T-cells (Tregs) are a type of T cell that can function to prevent autoimmunity by suppressing autoreactive lymphocytes, like B-cells. It may be expected that the number of Tregs in RA patients compared to healthy patients is lower, however, the results from studies are controversial on this topic. As demonstrated, multiple types of T-cells (and their

effector pathways) significantly contribute to RA, and likely JIA, by mediating these chronic inflammatory processes. [Demoruelle, Deane & Holers, 2014]

Another cell type that plays a significant role in RA and JIA, and inflammation in general, is the macrophage. Myelomonocytic cells differentiate into monocytes, which migrate into RA synovial membrane. Due to pathophysiological stimuli, such as an imbalance of cytokines or growth factors, these monocytes then differentiate into synovial macrophages [Kinne et al., 2000]. Synovial macrophages act by regulating the secretion of pro-inflammatory cytokines and enzymes that lead to joint destruction. Additionally, they recruit lymphocytes and can also act as APCs to activate T-cells, similarly to how B-cells activate T-cells. Macrophages and B-cells present arthritis-associated antigens to T-cells and activate a signalling cascade to secrete cytokines. This stimulates the activation of chondrocytes and osteoclasts, causing chondrocytes to produce MMPs that degrade the matrix of cartilage and osteoclasts to begin to resorb bone, leading to bone erosion [Demoruelle, Deane & Holers, 2014]. This activation leads to the production of effector T-cells, as well as the expression of pro-inflammatory mediators like IL-1α, IL-1β, and MMPs [Demoruelle, Deane & Holers, 2014]. Activation markers of macrophages include an overexpression of MHC class II molecules, proinflammatory cytokines, such as IL-1, IL-6 and TNF-α [Kinne et al., 2000; Burmester et al., 1997].

1.1.4 *Prevalence and Involvement of the Temporomandibular Joint (TMJ)*

It is estimated that about 150,000 children in North America have JIA. Clinical features of JIA include joint swelling and tenderness, especially in the morning. Using current classification systems, as mentioned previously, JIA includes patients with onset of the disease before the age

of 16 years and where arthritis persists for a minimum of 6 weeks [Carrasco, 2015]. In addition to the more common joints that JIA affects, the temporomandibular joint (TMJ) can be involved, however, it is rarely the first joint to be affected [Carrasco, 2015]. The TMJ is a synovial joint that includes the mandibular condyle and glenoid fossa of the temporal bone. Located between the upper and lower compartments of the joint cavity is an intermediate articular disc made of fibrocartilage. Connective tissue surrounds and encapsulates the joint capsule and attaches to muscles and tendons. The synovium is another lining of tissue inside the joint. This tissue is responsible for secreting synovial fluid to lubricate the joint. The articular surface of the mandibular condyle consists of periosteum with underlying fibrocartilage, however, the periosteal layer is often absent during condylar analysis due to the effect of tissue processing that is required for tissue analysis. Fibrocartilage is distinct from hyaline cartilage in long bones. Although hyaline cartilage has poor healing potential, the secondary growth site of fibrocartilage may have the potential for post-traumatic healing over a lifetime. Mature condylar cartilage has four zones (Fig. 1.1). The first zone is the fibrous tissue on the articulating surface. This zone primarily expresses type I collagen (Col-I). The second zone consists of proliferating cells expressing Col-I. One of the terms for this zone is the prechondroblastic zone. The next zone is the chondroblastic zone. The mature chondrocytes (cartilage cells) in this zone primarily express type II collagen (Col-II). Other proteins expressed in this zone are proteoglycans and aggrecan. The final zone is the hypertrophic zone and this zone is directly adjacent to the underlying bone of the mandibular condyle. This zone mainly expresses type X collagen (Col-X). Some literature collectively expresses these four cell layers as ‘fibrocartilage’ [Stocum & Roberts, 2018].

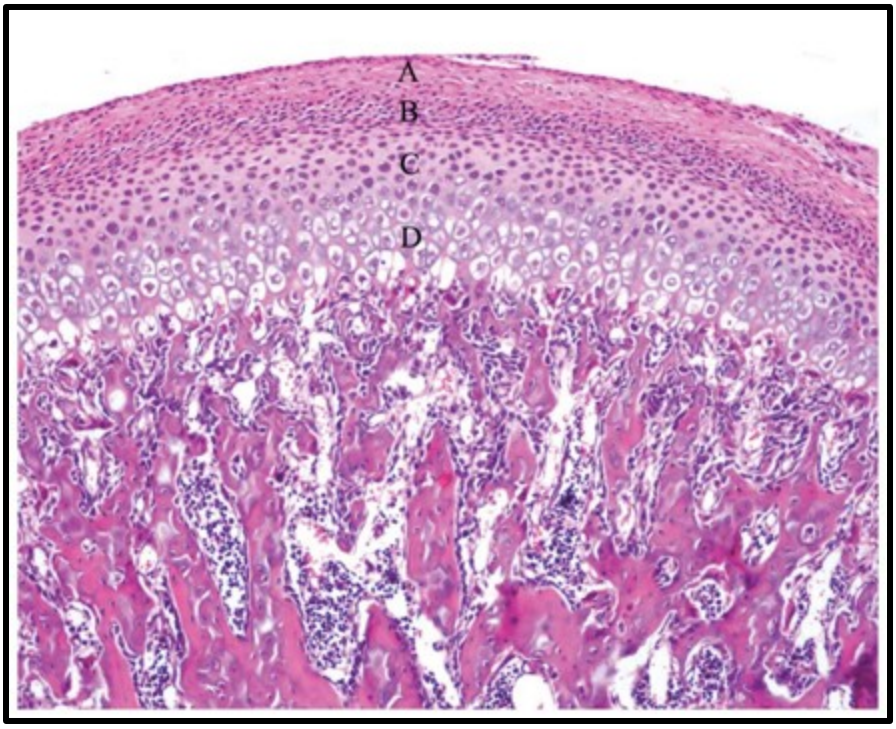

Fig. 1.1: Illustration showing cartilage cell layers of the mandibular condyle. A) Fibrocartilage, B) Proliferating chondrocytes, C) Mature chondrocytes, D) Hypertrophic chondrocytes. [Zhong, Wang & Jian, 2014]

The reported incidence of TMJ involvement in patients with JIA varies extensively which is likely due to the modalities used for evaluation, the subtype of JIA, and how arthritis is classified in medical imaging. One of the largest studies investigating JIA involvement of the TMJ report 62.1% of 169 patients exhibited condylar resorption [Carrasco, 2015; Pedersen et al., 2001]. Studies have investigated the correlation between clinical symptoms and manifestations of TMJ disorders in JIA and the extent of arthritis. There appears to be a lack of clear correlation because healthy children may have similar presentations of TMJ disorders; the TMJs in children may not be easy to palpate to clinically evaluate any pain or swelling; and JIA children have varying levels of pain manifestation. Because of theses issues with clinical evaluation of TMJ involvement in

JIA, imaging modalities can be used in diagnosis. Radiographs, computed tomography (CT), ultrasonography, and magnetic resonance imaging (MRI) help to determine the presence and extent of involvement of the TMJ [Carrasco, 2015]. Imaging techniques have greater importance in investigating TMJ-JIA compared to solely clinical evaluation because it has been reported that up to 69% of JIA patients had asymptomatic TMJ arthritis that was confirmed using orthopantomogram (OPG) imaging [Carrasco, 2015; Ringold & Cron, 2009]. However, OPG imaging does not evaluate any pannus tissue formation, synovial thickening, or if the changes observed are from old/chronic changes or from an active disease. MRIs may be the most advantageous in evaluation of the TMJ in JIA. Since cartilage, bone, ligaments, tendons, and the synovium can be assessed by MRI, it is considered the gold standard of evaluation of inflammatory arthritis. As well, it has been demonstrated to be repeatably sensitive for assessing TMJ-JIA [Carrasco, 2015].

1.1.5 *Management and Treatment of TMJ Arthritis*

From a rheumatologist's viewpoint, the primary goals for the adult and pediatric arthritides are early recognition, prevention of damage, halting any damage if present, suppressing the disease, and ultimately, remission off medications [Carrasco, 2015]. TMJ-JIA, if not recognized early, causes severe pain and affects lower jaw development, resulting in an underdeveloped/smaller lower jaw, dental crowding and incorrect bite, and irreversible damage like TMJ bone resorption [Pederson et al., 2001; Arabshahi & Cron, 2006].

Current clinical treatment of TMJ arthritis and associated growth defects combines medications targeting pro-inflammatory cytokines, orthodontic intervention, and surgery

[Carrasco, 2015]. These medications include anti-inflammatory drugs (ie. non-steroidal anti-inflammatory drugs, NSAIDs), corticosteroids, and biologic disease-modifying antirheumatic drugs (DMARDs). NSAIDs control pain and inflammation but are only effective in one-fourth to one-third of JIA patients. It is also recommended that NSAIDs be considered as adjunctive therapy and not monotherapy [Carrasco, 2015]. Intra-articular steroids (IAS) for the TMJ show some successes but in only 50% or less of patients treated [Carrasco, 2015]. Additionally, a recent pilot study on the long-term effect of these TMJ injections showed that the signs and symptoms of TMJ-JIA worsened at the long-term follow-up compared to the short-term [Stroutstrup et al., 2015]. Also, the long-term effect of these injections on mandibular growth is currently unknown [Carrasco, 2015]. Randomized controlled trials (RCTs) have highlighted concerns regarding the possible malignancy risks, neurologic changes, psoriasis, lupus-like disease, and infections when DMARDs were used [Carrasco, 2015]. Two types of DMARDs approved for clinical use are Tocilizumab and Sarilumab, which both affect IL-6 receptors, and therefore target a specific immune response involved in RA [Yap et al., 2018]. Although DMARDs can help halt and prevent arthritis progression, their efficacy in treating specific TMJ arthritis especially in juvenile arthritic patients is unknown [Cordeiro et al., 2016]. In addition to these shortcomings of the available treatments, these medications and treatments are expensive and may carry substantial financial burden on the patients' families as well as health care systems. Additionally, surgery is risky and painful [Carrasco, 2015]. Because of these reasons, there is significant need to consider other approaches for treating TMJ-JIA. These potential treatment options need to primarily reduce TMJ inflammation and significantly stimulate mandibular growth. Additionally, these options should have predictable outcomes, have no long-

term side effects, be easy to use and non-invasive, and be financially-favourable to prevent any financial burden on these patients and families.

1.2 *Low Intensity Pulsed Ultrasound (LIPUS)*

Ultrasound was developed as both a diagnostic imaging tool and as a therapeutic modality that utilized the deposition of energy in tissue and its induction of various biological events. Exploration of therapeutic ultrasound and its application in medicine began in the 1930s [Miller et al., 2012]. In the 1970s there were advancements in irradiation and focusing the ultrasonic beam, allowing for the treatment of Meniere disease and Parkinson's disease, which also paved the way for therapeutic ultrasound use in physiotherapy, neurosurgery and cancer treatment [Miller et al., 2012; Wells, 1977]. Since potent exposure of ultrasound for therapeutic purposes may pose adverse biological effects, standardization of its application is absolutely required to protect patients and ensure optimal therapeutic outcomes. Therefore, approval from governing authorities, such as the Food and Drug Administration (FDA) and Health Canada, are legally required for marketing suitability and clinical application. A review by Miller et al. (2012) outlines and details many different types of therapeutic ultrasound treatment devices that were approved at that time for clinical use. One of these devices is the low intensity pulsed ultrasound (LIPUS) device that was approved for bone fracture healing in the USA in 1994 [Palanisamy et al., 2021]. In 2000 Canadian authorization included the same approved indications of use as the FDA in the USA for this ultrasound device [Banken, 2004].

To understand how LIPUS exerts biological effects, it is important to have a general understanding of ultrasound, its components, and how its measured. Sound is created by mechanical vibration that transmits energy through a medium, such as an elastic medium.

Ultrasound is a type of mechanical wave in a longitudinal direction that can be transmitted in a straight line or can be focused. As expected, waves obey the laws of reflection and refraction. In ultrasound diagnostics, reflected waves are collected to create data to compose a picture of a target object. However, ultrasound waves cannot be transmitted through a gaseous medium, such as air or lungs. Ultrasound waves vary in power, intensity, and wave continuity or pulse repetition. Power is the rate of energy that is transferred and is measured in Watts. Intensity is a measure of how much power per beam area, therefore, intensity is measured in Watts per area unit (ie. cm^2). Intensity decreases as the ultrasound wave travels through tissue depending on the tissue specific acoustic impedance. Wavelength is the length of a single cycle and has a measurement in units of length. Period is the time it takes to capture one cycle, whereas, frequency is the inverse of period and has the units of 1/second or Hertz (Hz). Frequency is measured as low, medium, or high. High frequency ultrasound has short wavelengths and low frequency ultrasound has long wavelengths. Pulse duration is determined by the number of cycles and the period of each cycle. Pulse repetition period is the amount of time between the beginning of one pulse until the onset of the next pulse. Pulse repetition frequency is related to pulse repetition period, but just like the relationship between period and frequency as mentioned above, pulse repetition period and pulse repetition frequency are reciprocals of each other. Pulse repetition frequency is the number of pulses that occur in 1 second, but this measurement is not related to ultrasound frequency. [Repacholi et al., 1987]

As introduced, LIPUS is one type of therapeutic ultrasound approved for clinical use. A LIPUS device is made of a transducer that is composed of many piezoelectric crystals that are arranged next to each other and that are electronically connected. When a voltage is applied to this piezoelectric element within the transducer, this element's crystals vibrate to generate a

sound wave. The sound wave frequency is dependent upon the thickness of the crystals. To produce an ultrasound pulse, an alternative current is applied to these crystals for a particular time period. As the name 'low intensity pulsed ultrasound' suggests, this type of ultrasound that is approved for clinical use employs a small spatial average-temporal average (termed 'SATA') intensity of 30 mW/cm^2. LIPUS has a frequency of 1.5 MHz (in bursts of 200 μs) that is repeated at 1 kHz (pulse repetition frequency of 1000 cycles per second). [Harrison et al., 2016]

1.2.1 Effect of LIPUS on Fracture Healing

The mode and mechanism of how LIPUS has an effect on hard and soft tissues and on cells have been extensively studied and summarized in recent years. First, LIPUS's effect on bone healing will be explored and condensed. During bone remodelling after fracture, there are phases of fracture healing beginning with the inflammatory phase and this phase involves cell proliferation [Einhorn et al., 1995]. Next, is the chondrogenic phase that consists of cartilage hypertrophy and angiogenesis [Schindeler et al., 2008; Barnes et al., 1999]. Finally, there is the osteogenic phase involving the replacement of cartilage with woven bone followed by remodelling [Schindeler et al., 2008; Mulari et al., 2004]. Cells within the local environment produce factors that are responsible for this conversion (Fig. 1.2).

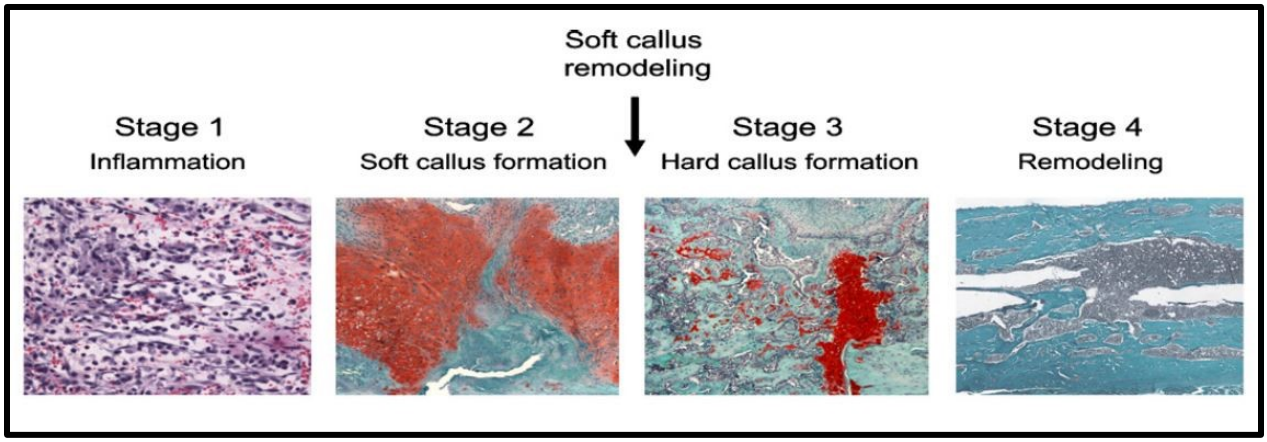

Fig. 1.2: Illustration demonstrating 4 stages of fracture repair: 1) Inflammation, 2) Soft callus, 3) Hard callus, 4) Remodeling. [Schindeler et al., 2008]

During fracture, local soft tissue integrity is disrupted. Bleeding within the fracture site can be contained by the tissues that surrounds the site and a hematoma develops. Cells including macrophages, granulocytes, lymphocytes and monocytes infiltrate the area to combat any infection by secreting cytokines and growth factors and by advancing clotting. Macrophages, giant cells and other types of cells involved in phagocytosis begin to clear any degenerated cells and other types of debris within this fracture area. Some of the cytokines that are secreted by these cells are transforming growth factor-β (TGF-β), vascular endothelial growth factor (VEGF), interleukins -1 and -6 (IL-1 and IL-6), and tumor necrosis factor-α (TNF-α) [Schindeler et al., 2008; Einhorn et al., 1995]. These factors induce the recruitment of additional inflammatory cells, which initiates a positive feedback loop, as well as begins the recruitment of multipotent mesenchymal stem cells that originally reside in bone barrow, in circulation, and in the surrounding soft tissues. These stem cells play a role in bone formation, as well as repair [Schindeler et al., 2008]. After this period of inflammation, other cell types such as chondrocytes

and fibroblasts begin to dominate the process of producing the soft callus. Chondrocytes originate from mesenchymal progenitors. These cells increase in cell number by proliferating and then produce a cartilaginous matrix that replaces fibrinous and granulation tissue, creating cartilage. Specific areas of this cartilage continue to grow until a fibrocartilaginous plug is completed and this plug bridges the gap between fracture fragments [Schindeler et al., 2008; Barnes et al., 1999]. After this, the chondrocytes undergo hypertrophy and begin to mineralize the cartilaginous tissue, and then undergo apoptosis (programmed cell death). Next, this soft callus is converted to a hard callus and then is remodelled into cortical or trabecular bone, whichever was the original type of bone prior to fracture. This conversion, as mentioned, is endochondral ossification and requires increased osteoblast activity and formation of mineralized bone matrix [Schindeler et al., 2008; Mulari et al., 2004]. Through this process and induced neovascularization, this hard callus begins to be remodelled, involving a key cell type called an osteoclast. This cell is a large multinucleated cell that produces and secretes acid and proteinases directly onto a mineralized surface, resulting in the acid demineralizing the cellular matrix and the proteinases degrading the organic components within the hard callus, including collagen [Schindeler et al., 2008; Mulari et al., 2004]. At this point, these mature osteoclasts will either undergo apoptosis or will return to a non-resorbing form. This bone resorption is what creates pits on the bone surface that are termed ‘Howship’s lacuna’. Finally, osteoblasts finalize bone remodelling by laying down new bone on eroded surfaces [Schindeler et al., 2008].

Although most fractures heal normally despite fracture healing complexity, it has been reported that up to 10% of fractures result in either delayed healing or non-union [Harrison et al., 2016]. Exploring the mode and mechanisms involved in how LIPUS stimulates fracture repair contributes to the understanding of how LIPUS biologically affects other tissues and cells. Some

key studies that enhance the understanding of LIPUS on fracture healing are pre-clinical animal studies. Azuma et al. (2001) demonstrated how LIPUS treatment accelerated endochondral ossification. LIPUS was applied for 20 minutes/day for 24 days on closed femoral fractures in rats. LIPUS-treated femurs had smaller mature cartilage, the number of osteoclasts on the trabecular bone surface in the hard callus was higher, and there was increased bone bridging consisting of newly formed cortex and trabecular bone. These results were confirmed by another study that investigated LIPUS's effect on healing rat closed femoral fractures [Freeman et al., 2009].

A further study demonstrated how LIPUS can shorten the process of endochondral ossification. LIPUS was applied for 20 minutes per day for 28 days to femoral fractures in aged mice. Endochondral ossification was reduced by 11 days in wild-type mice. This study also used aged cyclooxygenase (COX)-2 double-knockout (KO) mice [Naruse et al., 2010]. COX-2 is a rate-limiting enzyme that is involved in the arachidonic acid metabolic pathway. COX-2 converts, along with COX-1, arachidonic acid (AA) to prostaglandin H2 (PGH2) via a reduction reaction. Prostaglandin E synthase converts PGH2 prostaglandin E2 (PGE2). Therefore, COX-2 expression regulates PGE2 expression. In the KO mice, LIPUS had no effect, however, when agonists of PGE2 (namely EP-2 and EP-4) were injected after day 5, there was a responsiveness to LIPUS. This study reports that COX-2 was a main factor in delayed endochondral bone healing and its induced production by LIPUS normalized bone healing to a wild-type level. This key finding helps to understand the cellular mechanism by which LIPUS has its biological effect. Murine osteoblastic cell cultures were used to study the mechanism of LIPUS involved in signalling pathways within osteoblasts. A LIPUS transducer was immersed into the cell cultures and was applied for 20 minutes/day and cells were harvested at 1, 3, 6, 12 and 24 hours after

LIPUS stimulation. LIPUS increased the levels of integrin expressed on the cell surface and increased phosphorylation of focal adhesion kinase (FAK). Focal adhesions are groups of integrin molecules that initiate intracellular proteins to translocate inside the cell were intracellular components of integrins are located. These focal adhesions essentially act as mechanoreceptors by detecting mechanical stimuli in the extracellular matrix, including binding components of this matrix, and then converting these stimuli into chemical signalling pathways that can regulate and control cell viability and function. The phosphorylation of FAK then led to subsequent phosphorylation of the p85 sub-unit of phosphoinositol 3 kinase (PI3K) and resulting in the translocation of the p65 subunit of NF-κB into the nucleus of these cells. This study applied specific inhibitors at each stage of this described pathway, and each of these led to an inhibition in the production of COX-2. This demonstrates that this pathway is required for the production of COX-2 in osteoblasts. Additionally, when mutant forms of these cells (e.g., dominant negative mutant forms of FAK, PI3K, etc.) were studied, LIPUS could not stimulate mineralization of osteoblasts, whereas, when LIPUS was applied to non-mutant forms, mineralization occurred in these cells. So, this demonstrates that the LIPUS signal is transduced through this pathway that leads to COX-2 production and ultimately the mineralization of osteoblasts [Tang et al., 2006].

In addition to COX-2's involvement in osteoblastic mineralization, COX-2 is associated with the initiation of inflammatory responses due to its action in producing prostaglandins. PGE2 stimulates osteoclast differentiation by upregulating the expression of RANKL (receptor activator of NF-κB ligand) (via cAMP-PKA [protein kinase A]) and inhibiting the expression of osteoprotegerin (OPG) in osteoblastic cells [Yokoyama et al., 2013]. The effect of LIPUS on PGE2 was demonstrated by Sun et al. (2001). This group exposed osteoblast-osteoclast cell

cultures to LIPUS for 20 minutes per day and tested the media on various days of LIPUS application. LIPUS stimulation significantly increased PGE2 and osteoblast proliferation, but osteoclast formation was inhibited. Prostaglandins, especially PGE2, are important modulators of overall bone metabolism since they can increase bone resorption and bone formation. However, it is apparent from these above studies that the mechanism of how LIPUS affects osteoblasts and osteoclasts is still not fully understood. If LIPUS increases PGE2 production and PGE2 can stimulate osteoclast differentiation (via binding G-protein-coupled receptor subtypes, such as EP1-4), then theoretically, LIPUS should increase osteoclast formation [Lutter et al., 2016]. This was not demonstrated by Sun et al. (2001) because they showed the opposite outcome. It may be possible that the local environment in which these cells are either cultured or reside *in vivo* has a significant effect on how LIPUS affects these cells and how these cells behave in response to stimulation from LIPUS.

1.2.2 Effect of LIPUS on Chondrocytes

The effect of LIPUS has also been investigated in chondrocytes (see Figure 1.1). In one study mandibular chondrocytes were treated with or without IL-1β, changing the environmental conditions in which these cells were cultured. IL-1β induces COX-2 and PGE2, and the production of MMPs is increased through binding PGE2 to its receptor, EP4, in fibroblasts [Iwabuchi et al., 2014]. Therefore, conditioning the chondrocytes with IL-1β would leading to cartilage degradation via an increased production of MMPs. Next, these cells received LIPUS or sham treatment for 20 minutes and then were cultured without IL-1β for 0-24 hours. In cells conditioned with IL-1β with no LIPUS treatment, COX-2 mRNA expression increased, but in these cells treated with LIPUS, this expression decreased. LIPUS did not have an effect on

chondrocytes that were not conditioned with IL-1β (ie. healthy chondrocytes without inflammatory conditions) [Iwabuchi et al., 2014].

To further study how LIPUS affects chondrocytes, Sekino et al. (2018) stimulated differentiation in a chondroprogenitor cell line and then applied LIPUS for 20 minutes/day for up to 7 days. LIPUS increased mRNA expression of phospho-ERK1/2 (activated ERK1/2 – key component in affected cellular pathway), increased aggrecan (main component of cartilage extracellular matrix [ECM] made by mature chondrocytes), Type X collagen (Col-X) and Col-II. As well, LIPUS decreased the expression of MMP-13 which is a marker of chondrocyte hypertrophy. This study demonstrated how LIPUS enhances chondrocyte differentiation (maturation) as shown by increased ECM synthesis by ERK1/2 activation.

1.2.3 Effect of LIPUS on Osteoblasts

To study how LIPUS affects cytokine expression in osteoblasts, Li et al. (2003) isolated osteoblast cells from rat calvaria. They exposed these cultures to LIPUS for only 15 minutes/day for 1, 2, 3 and 4 days. They report that LIPUS increased cell viability, reduced TNF-α production and increased TGF-β production. IL-1β could not be detected in any of their groups. TNF-α plays a role in activating osteoblasts to secrete IL-6 and suppress type I collagen synthesis [Ishimi et al., 1990]. IL-6 is a cytokine that can stimulate osteoclastogenesis [Ishimi et al., 1990]. Since IL-6 was reduced by LIPUS stimulation, as reported in this study, LIPUS may be able to suppress osteoclast formation and prevent bone resorption. As well, TGF-β can be a marker of osteoblast proliferation, and since LIPUS increased TGF-β, this shows that LIPUS stimulated osteoblast proliferation in addition to cell viability. Therefore, this study demonstrates how

LIPUS may be able to suppress osteoclast differentiation via reducing TNF-α production and was able to stimulate osteoblast formation as demonstrated by an increase in TGF-β [Li et al., 2003].

1.2.4 Effect of LIPUS on Synovial Cells

Another important cell type to consider when studying the effect of LIPUS on TMJ arthritis is the synovial cell. Synovial hyperplasia is a main pathophysiologic feature of RA. It is associated with proinflammatory cytokines such as TNF-α and IL-1β. The intimal lining of synovial joints is made up of synovial fibroblasts and these cells are responsible for producing cytokines and proteinases. Sato et al. (2014) demonstrated how LIPUS decreased COX-2 expression in synovial membrane cells that were stimulated with IL-1β. Normally, COX-2 expression increases when these cells are stimulated with IL-1β in the absence of LIPUS treatment. When LIPUS was applied *in vivo* to knee joints in a mouse model of RA, the expression of COX-2 also decreased. This study also investigated how LIPUS affects synovial membrane cells by examining the phosphorylation (activation) of the main intracellular signalling proteins in the integrin-MAPK signalling pathway. LIPUS upregulated the phosphorylation of integrin-β1, FAK, JNK, ERK, and p38. When a FAK phosphorylation inhibitor was added, LIPUS's effect was inhibited. This study demonstrates how LIPUS has a biophysical effect via the integrin/FAK/MAPK pathway and how LIPUS may have an effect on both synovial cell survival and also apoptosis. As well, when considering COX-2 and PGE2 induction by IL-1β, which leads to an increase in the production of MMPs, if LIPUS decreases the expression of COX-2, then LIPUS should decrease the production of MMPs [Iwabuchi et al., 2014]. Therefore, LIPUS should also decrease cartilage degradation by MMP activity.

1.2.5 Effect of LIPUS on Arthritis

As demonstrated in the above study, LIPUS has been considered as a potential anti-inflammatory treatment of inflammatory arthritis, such as RA, by applying LIPUS directly to these affected joints. Another study explored the effectiveness of LIPUS for treating synovitis in the MRL-lpr/lpr mouse, an animal model for studying RA [Nakamura et al., 2011]. In this model, the joint disease that develops is characterized by synovial fibroblast proliferation in early stages of the disease. Additionally, this study investigated how LIPUS affects rabbit synovial membrane cells from the knee joint by studying its effect on cell proliferation and growth *in vitro*. LIPUS was applied to the mice knee joints for 15 minutes per day for 7, 14 and 21 days. LIPUS treatment of 3 weeks resulted in a significant reduction in histological damage when compared to untreated arthritic knee joints as demonstrated by a reduction in hyperplasia, inflammatory cell infiltration, pannus formation, and cartilage destruction. They showed that stimulation of the synovial membrane cells with either IL-1β or TNF-α upregulated the proliferation of these fibroblasts. When LIPUS was applied as a single 15-minute exposure, this proliferation in stimulated cells was significantly suppressed. Interestingly, LIPUS had no effect on cell proliferation in cells that were not stimulated by either IL-1β or TNF-α. LIPUS also significantly decreased cell growth in these stimulated cells. As mentioned previously, LIPUS may have an effect on both synovial cell survival and apoptosis. This study also investigated how LIPUS affects apoptosis to determine if it was apoptosis that increased and resulted in decreased cell growth. LIPUS significantly decreased DNA fragmentation but actually had no effect on caspase-3 activity, showing that LIPUS did not affect apoptosis in this study.

A further study aimed to assess how LIPUS affects the expression of osteoarthritic factors and involved cellular signalling pathways in another animal model of arthritis – the surgically-induced osteoarthritis rabbit [Zhang, 2017]. LIPUS was applied to the surgically-induced OA knee in this animal for 20 minutes/day, 6 days/week for 6 weeks. LIPUS significantly reduced the levels of IL-1β and TNF-α in the articular cartilage, and significantly lowered the expression of integrin-β1, FAK, ERK1/2, JNK, and p38-MAPK, each of these belonging to this intracellular pathway affected by LIPUS. Since LIPUS decreased the expression of these pathway components that lead to the production of these MMPs, LIPUS should theoretically also decrease MMP-1 and -3. This was demonstrated by this study. Because of this, the expression of collagens Type I and Type II were evaluated after LIPUS stimulation. LIPUS significantly increased the expression of these collagens. These described studies help to increase the understanding of how LIPUS affects these intracellular pathways leading to increased or decreased production of pro-inflammatory cytokines and other proteins within these cells and tissues.

Finally, a similar study demonstrated how LIPUS affects cartilage in a surgically-induced OA (knee) rabbit model [Li et al., 2011]. LIPUS treatment was applied to the OA knee for 20 minutes/day, 6 days/week for 6 weeks. LIPUS significantly reduced the expression of MMP-13, another proteinase that degrades collagen, specifically Type II collagen (Col-II). LIPUS significantly decreased the expression of phosphorylated ERK1/2 and p38 proteins in the MAPK signalling pathway and LIPUS had no effect on the phosphorylation of JNK in this pathway. This study's findings support the similar results from the study by Zhang (2017) mentioned above.

In summary, when these above studies and others are considered together to understand how LIPUS affects chondrocytes and synovial cells, there appears to be differences regarding the cellular protein production between healthy chondrocytes or synovial cells and chondrocytes or synovial cells in inflammatory conditions (ie. *in vivo* in arthritis or stimulated by pro-inflammatory cytokines). Figure 1.3 illustrates how LIPUS activates the MAPK and PI3K/Akt pathways in chondrocytes, resulting in increased ECM production and decreased MMP production [Sekino et al., 2018; Takeuchi et al., 2008].

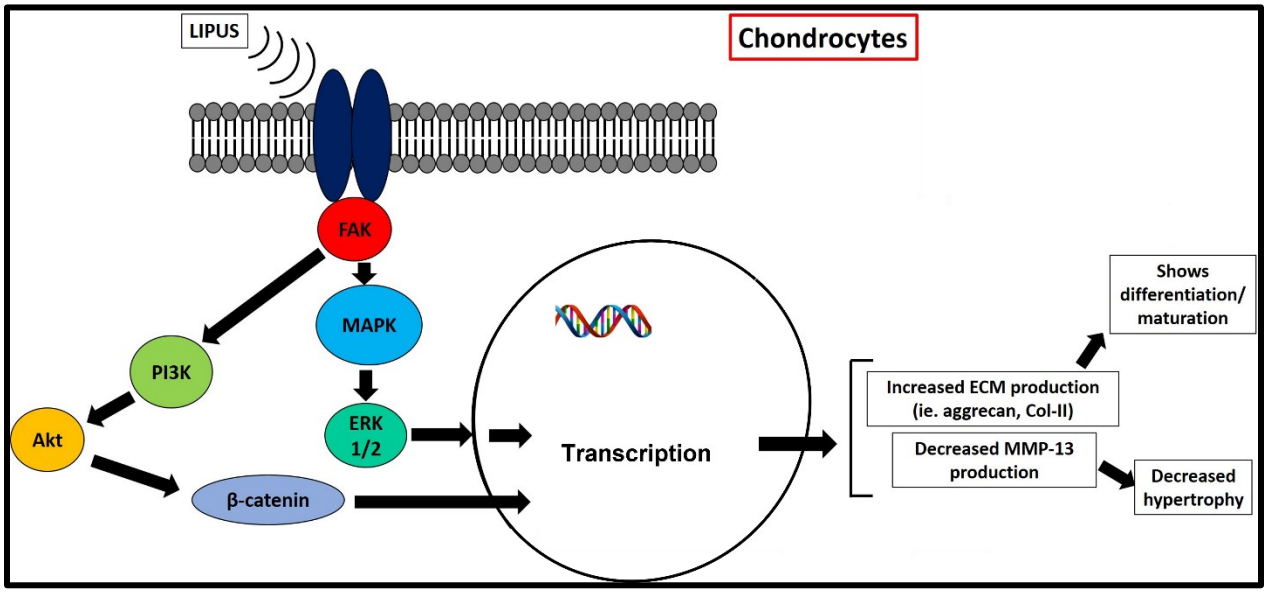

Figure 1.3: Illustration demonstrating how LIPUS affects intracellular signaling pathways in healthy chondrocytes. LIPUS sounds waves stimulate integrin proteins (dark blue) within the cell membrane. This leads to the recruitment and activation of intracellular signalling proteins in these pathways, resulting in the transcription of genes in the nucleus, translation of mRNA to specified protein, and production of protein that is produced by the cell.

In contrast, LIPUS has a different effect on the MAPK pathway in chondrocytes in inflamed joints or stimulated with pro-inflammatory cytokines (Figure 1.4) [Zhang et al., 2017].

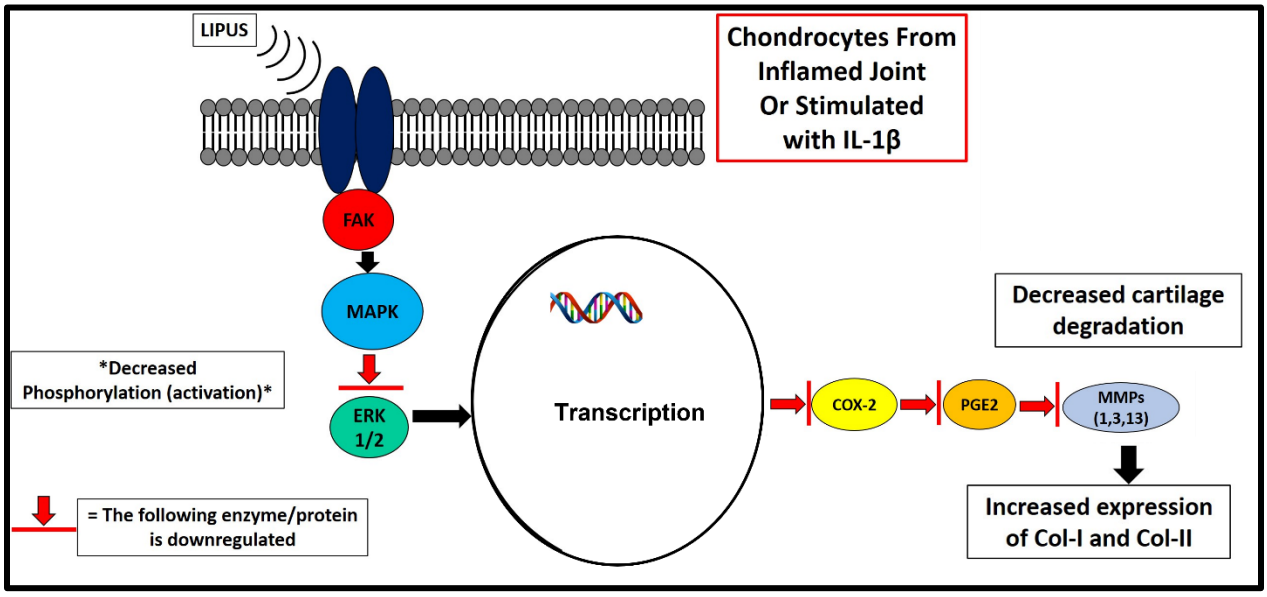

Figure 1.4: Illustration demonstrating how LIPUS affects intracellular signaling pathways in inflamed chondrocytes.

Again, LIPUS affects the MAPK pathway differently in healthy synovial cells compared to inflamed synovial cells (Figures 1.5 and 1.6) [Sato et al., 2014; Nakamura et al., 2010]. LIPUS increased the production of hyaluronan (HA) by synovial cells which is normally decreased in synovial fluid in OA, and LIPUS decreased COX-2 expression, which is normally increased in OA and plays a pathophysiological role in the progression of OA [Nakamura et al., 2010].

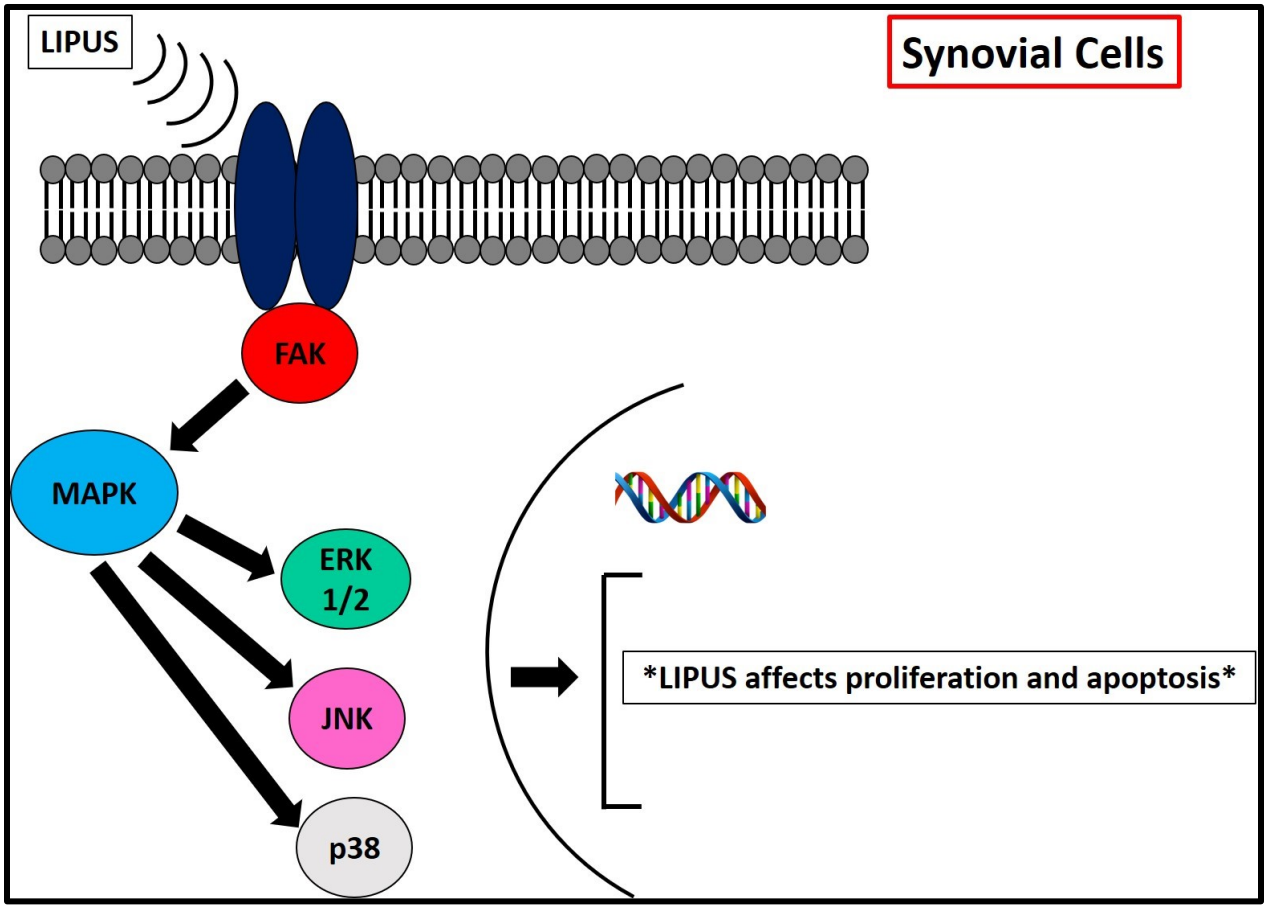

Figure 1.5: Illustration demonstrating how LIPUS affects intracellular signaling pathways in healthy synovial cells.

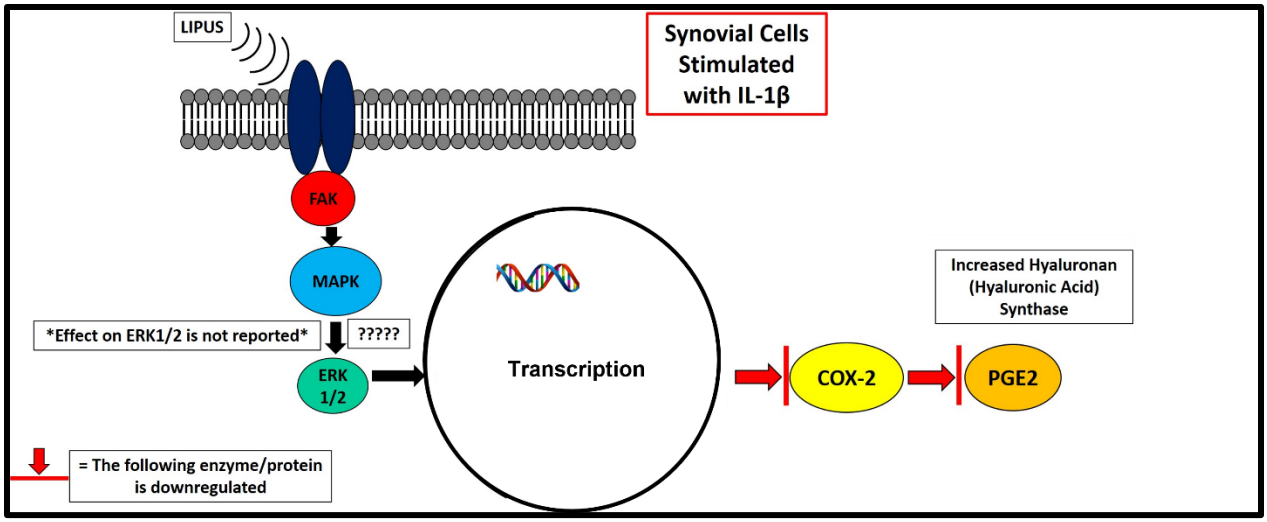

Figure 1.6: Illustration demonstrating how LIPUS affects intracellular signaling pathways in inflamed synovial cells.

1.2.6 Effect of LIPUS on Mandibular Growth

The effect of LIPUS on the TMJ has been previously studied. In healthy 4-week-old rats, LIPUS was applied for either 20 minutes/day or 40 minutes/day for 4 weeks and then the stimulatory effect of LIPUS on mandibular growth was investigated [Kaur et al., 2015]. LIPUS (20 minutes/day) increased proliferation and hypertrophy of chondrocytes by increasing the thicknesses of these cell layers in the mandibular condyle cartilage and by increasing cell number. LIPUS also increased bone volume fraction, trabecular thickness and number, and bone density, and LIPUS decreased trabecular separation. This study's results showing LIPUS's stimulatory effect on mandibular growth was confirmed by Oyonarte et al. (2009) who applied LIPUS to 3-week-old rat TMJs for 20 minutes/day, 5 days/week over a 26-day period. This group found that LIPUS modified mandibular growth patterns in these growing rats.

1.2.7 Effect of LIPUS on TMJ Arthritis

Fewer studies have investigated the effect of LIPUS on TMJ osteoarthritis and no studies have evaluated the effect of LIPUS on TMJ arthritis in a growing model (ie. TMJ-JIA). He et al. (2018) used LIPUS to treat the TMJs of 8-week-old rats with occlusal trauma-induced TMJ OA. They applied LIPUS for 20 minutes/day for 4 weeks. This study did not investigate how LIPUS affected the synovium or cartilage of the TMJ through histological analyses but considered the effect of LIPUS on gene expression only. However, Arita et al. (2017) evaluated how LIPUS may treat TMJ-OA. In this study, they applied LIPUS to 12-week-old rats. Since the mandible in rats ceases growth by 12-14 weeks of age, this study analyzed rats with full-grown, mature mandibles [Zoetis et al., 2003; Losken et al., 1992]. The TMJs were treated with LIPUS for 15 minutes/day for 4 weeks. TMJ-OA decreased the number and thickness of chondrocytes in the cartilage, but when LIPUS was applied, the number of chondrocytes was increased. Additionally, the cartilage in the TMJ-OA rats (no-LIPUS) had an increase in MMP-13 immuno-positive chondrocytes in the proliferative and mature cell layers, but again, when LIPUS was applied, there was less MMP-13-positive chondrocytes.

These studies demonstrate how LIPUS affects osteoblasts, chondrocytes, and synovial cells, suggesting that LIPUS may have a positive effect on treating inflammation in the TMJ which contains these main cell types. Additionally, it has been demonstrated that LIPUS has a stimulatory effect on mandibular growth and may treat negative outcomes involved in TMJ osteoarthritis in mature rats. Since juvenile arthritis can have a detrimental effect on preventing

normal growth and development of mandible in children, it may be possible that LIPUS could treat TMJ inflammation and stimulate mandibular growth in children with TMJ-JIA. So, the aim of this study was to investigate the effect of LIPUS in a juvenile animal model of TMJ arthritis.

1.3 *Animal Models of Rheumatoid Arthritis and Juvenile Idiopathic Arthritis*

Animal models are extensively used to study the pathogenesis of human diseases, as well as to evaluate the potential efficacy of drugs for clinical use. For these animal models to be clinically relevant, they need to be morphologically similar to human tissue and they must be able to predict the efficacy of therapeutic interventions in humans. There are many animal models available to study the etiology of human RA and that have been used by the pharmaceutical industry to test the clinical efficacy of anti-arthritic agents. Animal models of RA are usually easy to perform, the data generated from studying these models are reproducible, and most models are short in duration [Bendele, 2001].

The most common rodent models of arthritis are those that spontaneously develop the disease or require some form of induction such as an injection. These induced models of arthritis include rat and mouse collagen (type II [Col-II]) arthritis, antigen arthritis, and adjuvant arthritis, each representing different degrees of bone resorption and cartilage damage, which is characteristic of RA observed in humans. Adjuvant-induced arthritis in rats results in joint inflammation and bone destruction, but the incidence of arthritis and cartilage damage varies and, therefore, may not be the ideal animal model to study RA-like cartilage damage [[Bendele, 2001; Phadke, Fouts & Parrish, 1984; McNamee, Williams & Seed, 2015]. Antigen-induced arthritis results in rapid development of lesions but may require repeated injections of the antigen

involved [McNamee, Williams & Seed, 2015]. If this type of arthritis progresses past two weeks, a highly destructive pannus within the inflamed joint may destroy most of the articular cartilage [Bendele, 2001]. Finally, lesions observed in type II collagen-induced arthritis in rats have been described as more analogous to those seen in human RA, but there is less published data on the pathological changes seen in this type of induced arthritis than in other models in order to compare this disease to human RA [Bendele, 2001].

1.4 *Collagen-induced Arthritis*

Collagen-induced arthritis (CIA) is one of types of models used to study RA, as described previously, and can be induced in susceptible strains of rats and mice [Holmdahl et al., 2002; Wilson-Gerwing et al., 2013]. Collagen-induced arthritis has been described in Wistar, Lewis, and Sprague-Dawley rats, among other strains [Stuart et al., 1979; Phadke, Fouts & Parrish, 1984; Trentham, Townes & Kang, 1977]. As well, it has been studied in QB, C57BL/6, and DBA/1 mice, as well as in other strains [Nandakumar, Svensson & Holmdahl, 2003]. Typically, CIA is induced after an intradermal immunization (injection) consisting of type II collagen (Col-II) that has been emulsified with an adjuvant, such incomplete Freund's adjuvant (IFA) or complete Freund's adjuvant (CFA) [Holmdahl et al., 2002; Stuart et al., 1979; Phadke, Fouts & Parrish, 1984; Wilson-Gerwing et al., 2013; Trentham, Townes & Kang, 1977; Liu et al., 2015]. Col-II is the main protein component of joint cartilage. This type of immunization invokes an autoimmune response that results in direct attack of the joints. Collagen-induced arthritis depends on activation of Col-II specific T cells. Similar to the previous description of the autoimmune response involved in RA and JIA, the two arms of adaptive immunity that play a role in the immune response in CIA are T and B cells. Collagen molecules introduced by

injection are degraded into peptides and these peptides are presented by antigen presenting cells, most likely macrophages instead of dendritic cells because dendritic cells have poor processing and presenting of collagen [Holmdahl et al., 2002]. These peptides are presented to autoreactive T cells by structural interactions between major histocompatibility complex (MHC) class II with bound peptide on antigen presenting cell and T cell receptors on T cells, along with interactions between co-stimulatory molecules on the surface of both cells [Holmdahl et al., 2002]. Susceptibility to CIA varies greatly in inbred mouse strains because there is a clear association between the disease and the expression of specific class II genes of the MHC [Holmdahl et al., 2002; Brand, Kang & Rosloniec, 2003]. However, rat susceptibility is much less restricted to genetics and the type of the MHC [Griffiths et al., 1992].

Next, T cells are activated to become T helper (Th) cells, specifically Th-1 and Th-17 cells, but Th-17 cells have a predominant pathological role in CIA [McNamee, Williams & Seed, 2015]. Activated T cells play a role in two main ways. They assist B cells (by activating them) in their production of anti-Col-II antibodies and they can activate other cells, such as macrophages, involved in immune responses and by inducing them to produce some pro-inflammatory cytokines, in addition to activated T cells (including Th cells) directly producing pro-inflammatory cytokines and other proteins themselves . To help achieve this immune response that is specific to Col-II, types 1 and 2 immune responses are important. CFA, for example, is composed of mineral oil and heat killed mycobacteria or mycobacteria cell walls [Holmdahl et al., 2002]. The mycobacterium typically used in CFA is *Mycobacterium tuberculosis* [Brand, Latham & Rosloniec, 2007]. This induces the production of IL-12 and IFNγ and secretion of immunoglobulins of different isotypes which is a type 1 immune response. Additionally, there is

a slight type 2 immune response with involvement of primarily the IgG1 isotype in the antibody response [Holmdahl et al., 2002].

After T cells, the second arm of adaptive immunity that plays a role in the immune response is the B cell. The main role of B cells in CIA is to produce anti-Col-II antibodies [Holmdahl et al., 2002]. This has been previously demonstrated as the presence of antibodies that are reactive to Col-II binding to cartilage and inducing arthritis [Terato et al., 1992]. As well, it has been shown that mice that are B cell-deficient are resistant to the development of CIA [Svensson et al., 1998].

After a single immunization, immune priming begins after a few days. This is followed by immune activation in the joints that happens after 1-2 weeks. Then, usually no earlier than 2 weeks but mainly after several weeks or even months after immunization, there is a sudden onset of macroscopic arthritis. After this onset of arthritis, the inflammatory reaction causes severe destruction of the joint that is very similar to what is seen in the histopathology involved in RA in humans. In this type of induced arthritis in rodents, this active, severe inflammation subsides after 3-4 weeks after onset. The joint is left inflammation-free; however, the joint has been destroyed and some remodelling may have occurred. CIA in rodents is typically monophasic, but relapse has been reported and described in certain strains of mice [Holmdahl et al., 2002].

Since CIA produces similar immune responses and histopathology to that are observed in RA/JIA, this study implemented this animal model of arthritis. The aim of this study, as described previously, was to investigate the effect of LIPUS on TMJ arthritis in a growing animal model. Since mice and rats are weaned around 3 weeks of age and require a short period of acclimatization after arriving at weaned age, the minimum age of rodent that can be studied is 4 weeks of age. Due to the shortened juvenile age range of mice, using juvenile rats to study

human JIA is more appropriate in addition to considering the growth of the jaw continues up to age 12-14 weeks in rats, as previously stated above. CIA induced in the TMJ of growing rats resulted in increased osteoclastic activity in TMJ tissues, elevated serum levels of TNF-α and IL-1β, and inflammatory cell infiltration [Liu et al., 2015].

1.5 *Study Aims and Hypotheses*

In this study, we hypothesized that low intensity pulsed ultrasound (LIPUS) would reduce inflammation due to CIA-induced arthritis in the TMJ of juvenile rats and that LIPUS would prevent growth disturbances in the mandible due to TMJ-CIA in this CIA juvenile rat model.

This study had two parts: 1) Validation of the TMJ-CIA juvenile rat model, and 2) The treatment effect of low intensity pulsed ultrasound (LIPUS) on TMJ-CIA in juvenile rats.

In Part 1, we aimed to evaluate arthritic changes in the TMJ due to CIA and any mandibular growth disturbances. In Part 2, we aimed to evaluate how LIPUS affected TMJ inflammation due to CIA in growing rats and how LIPUS may prevent mandibular growth disturbances due to CIA in the TMJ.

The hypotheses for Part 1 were 1) TMJ-CIA would develop arthritic changes in terms of synovitis, increased MMP-13 and pro-inflammatory cytokine expression, and decreased expression of type II collagen and 2) TMJ-CIA would reduce/prevent normal mandibular growth. The hypotheses for Part 2 were 1) LIPUS would: a) reduce synovitis, MMP expression,

and pro-inflammatory cytokine expression and protein levels in the TMJ and blood serum/plasma, b) prevent cartilage thickening, and c) increase TGF-β1 and collagen expression in the cartilage in CIA juvenile rats, and 2) LIPUS would stimulate mandibular growth and increase condylar volume in CIA juvenile rats.

1.6 *References*

Aho K, Palosuo T, Raunio V, Puska P, Aromaa A, Salonen J. When does rheumatoid disease start? *Arthritis and Rheumatism.* 1985; 28 (5): 485-489.

Arabshahi B and Cron R. Temporomandibular joint arthritis in juvenile idiopathic arthritis: the forgotten joint. *Curr Opin Rheumatol*. 2006; 18: 490-495.

Arita A, Yonemitsu I, Ikeda Y Miyazaki M, Ono T. Low-intensity pulsed ultrasound stimulation for mandibular condyle osteoarthritis lesions in rats. *Oral Diseases.* 2018; 24: 600-610.

Azuma Y, Ito Y, Harada Y, Takagi H, Ohta T, Jingushi S. Low-intensity pulsed ultrasound accelerates rat femoral fracture healing by acting on the various cellular reactions in the fracture callus. *Journal of Bone and Mineral Research.* 2001; 16(4): 671-680.

Banken R. Low-intensity ultrasound (Exogen^{TM}) for the treatment of fractures. Technology brief prepared by Reiner Banken (AETMIS 03-05). Montreal: AETMIS. 2004; x-15.

Barnes G, Kostenuik P, Gerstenfeld L, Einhorn T. Growth factor regulation of fracture repair. *Journal of Bone and Mineral Research.* 1999; 14 (11): 1805-1815.

Bendele A. Animal models of rheumatoid arthritis. *J Musculoskel Neuron Interact.* 2001; 1: 377-385.

Brand D, Kang A, Rosloniec E. Immunopathogenesis of collagen arthritis. *Spring Semin Immunopathol*. 2003; 25: 3-18.

Brand D, Latham K, Rosloniec E. Collagen-induced arthritis. *Nature Protocols.* 2007; 2 (5): 1269-1275.

Burmester G, Stuhlmüller B, Keyszer G, Kinne R. Mononuclear phagocytes and rheumatoid arthritis. Mastermind of workhorse in arthritis? *Arthritis & Rheumatism.* 1997; 40 (1): 5-18.

Carrasco R. Juvenile idiopathic arthritis overview and involvement of the temporomandibular joint – prevalence, systemic therapy. *Oral Maxillofacial Surg Clin N Am.* 2015; 27: 1-10.

Catrina A, Svensson C, Malmström V, Schett G, Klareskog L. Mechanisms leading from systemic autoimmunity to joint-specific disease in rheumatoid arthritis. *Nature Review. Rheumatology.* 2017; 13 (2): 79-86.

Cordeiro P, Guimaraes J, de Souza V, Dias I, Silva J, Devito K, Bonato L. Temporomandibular joint involvement in rheumatoid arthritis patients: association between clinical and tomographic data. *Acta Odontol. Latinoam.* 2016; 29 (3): 219-224.

Demoruelle M, Deane K, Holers M. When and where does inflammation begin in rheumatoid arthritis? *Curr Opin Rheumatol.* 2014; 26 (1): 64-71.

Einhorn T, Majeska R, Rush E, Levine P, Horowitz M. The expression of cytokine activity by fracture callus. *Journal of Bone and Mineral Research.* 1995; 10 (8): 1272-1281.

Freeman T, Patel P, Parvizi J, Antoci V, Shapiro I. Micro-CT analysis with multiple thresholds allows detection of bone formation and resorption during ultrasound-treated fracture healing. *Journal of Orthopaedic Research.* 2009; 27: 673-679.

Griffiths M, Cremer M, Harper D, McCall S, Cannon G. Immunogenetics of collagen-induced arthritis in rats. Both MHC and non-MHC gene products determine the epitope specificity of immune response to bovine and chick type II collagens. *The Journal of Immunology*. 1992; 149 (1): 309-316.

Guo Q, Wang Y, Xu D, Nossent J, Pavlos N, Xu J. Rheumatoid arthritis: pathological mechanisms and modern pharmacologic therapies. *Bone Research.* 2018; 6 (15): 1-14.

Harrison A, Lin S, Pounder N, Mikuni-Takagaki Y. Mode & mechanism of low intensity pulsed ultrasound (LIPUS) in fracture repair. *Ultrasonics.* 2016; 7-: 45-52.

He D, An Y, Li Y, Wang J, Wu G, Chen G, Zhu G. RNA sequencing reveals target genes of temporomandibular joint osteoarthritis in rats after the treatment of low-intensity pulsed ultrasound. *Gene.* 2018; 672: 126-136.

Holmdahl R, Bockermann R, Bäcklund J, Yamada H. The molecular pathogenesis of collagen-induced arthritis in mice – a model for rheumatoid arthritis. *Ageing Research Reviews*. 2002; 1: 135-147.

Ishimi Y, Miyaura C, Jin C, Akatsu T, Abe E, Nakamura Y, Yamaguchi A, Yoshiki S, Matsuda T, Hirano T. Il-6 is produced by osteoblasts and induces bone resorption. *J Immunol.* 1990; 145: 3297-3303.

Iwabuchi Y, Tanimoto K, Tanne Y, Inubushi T, Kamiya T, Kunimatsu R, Hirose N, Mitsuyoshi T, Su S. Effects of low-intensity pulsed ultrasound on the expression of cyclooxygenase-2 in mandibular condylar chondrocytes. *J Oral Facial Pain Headache.* 2014; 28: 261-268.

Kaur H, Uludağ H, Dederich D, El-Bialy T. Effect of increasing low-intensity pulsed ultrasound and a functional appliance on the mandibular condyle in growing rats. *J Ultrasound Med.* 2017; 36: 109-120.

Kinne R, Bräuer R, Stuhlmüller B, Palombo-Kinne E, Burmester G. Macrophages in rheumatoid arthritis. *Arthritis Res.* 2000, 2: 189-202.

Kotake S, Udagawa N, Takahashi N, Matsuzaki K, Itoh K, Ishiyama S, Saito S, Inoue K, Kamatani N, Gillespie M, Martin T, Suda T. IL-17 in synovial fluids from patients with rheumatoid arthritis is a potent stimulator of osteoclastogenesis. *J Clin Invest.* 1999; 103: 1345-1352.

Li J, Chang W, Lin J, Ruaan R, Liu H, Sun J. Cytokine release from osteoblasts in response to ultrasound stimulation. *Biomaterials.* 2003; 24: 2379-2385.

Li X, Li J, Cheng K, Lin Q, Wang D, Zhang H, An H, Gao M, Chen A. Effect of low-intensity pulsed ultrasound on MMP-13 and MAPKs signaling pathway in rabbit knee osteoarthritis. *Cell Biochem Biophys.* 2011; 61: 427-434.

Liu J, Dai J, Wang Y, Lai S, Wang S. Significance of new blood vessels in the pathogenesis of temporomandibular joint osteoarthritis. *Experimental and Therapeutic Medicine.* 2017; 13: 2325-2331.

Liu W, Xu A, Li Z, Zhang Y, Han B. RANKL, OPG and CTR mRNA expression in the temporomandibular joint in rheumatoid arthritis. *Experimental and Therapeutic Medicine*. 2015; 10: 895-900.

Losken A, Mooney M, Siegel M. A comparative study of mandibular growth patterns in seven animal models. *J Oral Maxillofac Surg.* 1992; 50: 490-495.

Lutter A, Hempel U, Anderer U, Dieter P. Biphasic influence of PGE_2 on the resorption activity of osteoclast-like cells derived from human peripheral blood monocytes and mouse RAW264.7 cells. *Protaglandins, Leukotrienes and Essential Fatty Acids.* 2016; 111: 1-7.

McNamee K, Williams R, Seed M. Animal models of rheumatoid arthritis: How informative are they? *European Journal of Pharmacology.* 2015; 759: 278-286.

Miller D, Smith N, Bailey M, Czarnota G, Hynynen K, Makin I. Overview of therapeutic ultrasound application and safety considerations. *J Ultrasound Med.* 2012; 31: 623-634.

Mulari M, Qu Q, Härkönen P, Väänänen H. Osteoblast-like cells complete osteoclastic bone resorption and form new mineralized bone matrix in vitro. *Calcif Tissue Int.* 2004; 75: 252-261.

Nakamura T, Fujihara S, Katsura T, Yamamoto K Inubushi T, Tanimoto K, Tanaka E. Effects of low-intensity pulsed ultrasound on the expression and activity of hyaluronan synthase and hyaluronidase in IL-1β-stimulated synovial cells. *Annals of Biomedical Engineering.* 2010; 38 (11): 3363-3370.

Nakamura T, Fujihara S, Yamamoto-Nagata K, Katsura T, Inubushi T, Tanaka E. Low-intensity pulsed ultrasound reduces the inflammatory activity of synovitis. *Annals of Biomedical Engineering.* 2011; 39 (12): 2964-2971.

Nandakumar K, Svensson L, Holmdahl R. Collagen type II-specific monoclonal antibody-induced arthritis in mice. Description of the disease and the influence of age, sex, and genes. *American Journal of Pathology*. 2003; 163 (5): 1827-1837.

Naruse K, Sekya H, Harada Y, Iwabuchi S, Kozai Y, Kawamata R, Kashima I, Uchida K, Urabe K, Seto K, Itoman M, Mikuni-Takagaki Y. Prolonged endochondral bone healing in senescence is shortened by low-intensity pulsed ultrasound in a manner dependent on Cox-2. *Ultrasound in Med. &. Biol.* 2010; 36 (7): 1098-1108.

Nigrovic P, Raychaudhuri S, Thompson S. Genetics and the classification of arthritis in adults and children. *Arthritis Rheumatol.* 2018; 70 (1): 7-17.

Oyonarte R, Zárate M, Rodriguez F. Low-intensity pulsed ultrasound stimulation of condylar growth in rats. *Angle Orthodontist.* 2009; 79 (5): 964-970.

Palanisamy P, Alam M, Li S, Chow S, Zheng Y. Low-intensity pulsed ultrasound stimulation for bone fractures healing. *Journal of Ultrasound in Medicine.* 2021; 9999: 1-17.

Pedersen T, Jensen J, Melsen B, Herlin T. Resorption of the temporomandibular condylar bone according to subtypes of juvenile chronic arthritis. *The Journal of Rheumatology*. 2001; 28 (9): 2109-2115.

Phadke K, Fouts R, Parrish J. Collagen-induced and adjuvant-induced arthritis in rats. *Arthritis and Rheumatism.* 1984; 27: 797-806.

Prahalad S, Glass D. Is juvenile rheumatoid arthritis/juvenile idiopathic arthritis different from rheumatoid arthritis? *Arthritis Res.* 2002; 4 (suppl 3): 303-310.

Repacholi M, Grandolfo M, Rindi A. (1987). Ultrasound: Medical application, biological effects, and hazard potential. Plenum Press.

Ringold S, Cron R. The temporomandibular joint in juvenile idiopathic arthritis: frequently used and frequently arthritic. *Pediatric Rheumatology.* 2009; 7 (11): 1-9.

Sato M, Nagata K, Kuroda S, Horiuchi S, Nakamura T, Karima M, Inubushi T, Tanaka E. Low-intensity pulsed ultrasound activates integrin-mediated mechanotransduction pathway in synovial cells. *Annals of Biomedical Engineering.* 2014; 40 (10): 2156-2163.

Schindeler A, McDonald M, Bokko P, Little D. Bone remodeling during fracture repair: the cellular picture. *Seminars in Cell & Developmental Biology.* 2008; 19: 459-466.

Scott D, Wolfe F, Huizinga T. Rheumatoid arthritis. *Lancet.* 2010; 376: 1094-1108.
Stocum D, Roberts W. Part I: development and physiology of the temporomandibular joint. *Curr Osteoporos Rep.* 2018; 16 (4): 360-368.

Sekino J, Nagao M, Kato S, Sakai M, Abe K, Nakayama E, Sato M, Nagashima Y, Hino H, Tanabe N, Kawato T, Maeno M, Suzuki N, Ueda K. Low-intensity pulsed ultrasound induces cartilage matrix synthesis and reduced MMP13 expression in chondrocytes. *Biochemical and Biophysical Research Communications.* 2018; 506: 290-297.

Snir O, Widhe M, Hermansson M, von Spee C, Lindber J, Hensen S, Lundberg K, Engström Å, Venables P, Toes R, Holmdahl R, Klareskog L, Malmström V. Antibodies to several citrullinated antigens are enriched in the joints of rheumatoid arthritis patients. *Arthritis & Rheumatism.* 2010; 62 (1): 44-52.

Stroustrup P, Kristensen K, Küseler A, Pedersen T, Herlin T. Temporomandibular joint steroid injections in patients with juvenile idiopathic arthritis: an observation study on the long-term effect on signs and symptoms. *Rheumatology.* 2015; 13: 1-6.

Stuart J, Cremer M, Kang A, Townes A. Collagen-induced arthritis in rats. *Arthritis and Rheumatism*. 1979; 22 (12): 1344-1351.

Sun J, Hong R, Chang W, Chen L, Lin F, Liu H. *In vitro* effects of low-intensity ultrasound stimulation on the bone cells. *J Biomed Mater Res.* 2001; 57: 449-456.

Svensson L, Jirholt J, Holmdahl R, Jansson L. B cell-deficient mice do not develop type II collagen-induced arthritis (CIA). *Clin Exp Immunol.* 1998; 111: 521-526.

Takeuchi R, Ryo A, Komitsu N, Mikuni-Takagaki Y, Fukui A, Takagi Y, Shiraishi T, Morishita S, Yamazaki Y, Kumagai K, Aoki I, Saito T. Low-intensity pulsed ultrasound activates the phosphatidylinositol 3 kinase/Akt pathway and stimulates the growth of chondrocytes in three-dimensional cultures: a basic science study. *Arthritis Research & Therapy.* 2008; 10 (4): 1-11.

Tang C, Yang R, Huang T, Lu D, Chuang W, Huang T, Fu W. Ultrasound stimulates cyclooxygenase-2 expression and increases bone formation through integrin, focal adhesion kinase, phosphatidylinositol 3-kinase, and Akt pathway in osteoblasts. *Molecular Pharmacology.* 2006; 69 (6): 2047-2057.

Terato K, Hasty K, Reife R, Cremer M, Kang A, Stuart J. Induction of arthritis with monoclonal antibodies to collagen. *J Immunol.* 1992; 148: 2103-2108.

Trentham D, Townes A, Kang A. Autoimmunity to type II collagen: an experimental model of arthritis. *The Journal of Experimental Medicine*. 1977; 146: 857-868.

Van de Sande M, de Hair M, van der Leij C, Klarenbeek P, Bos W, Smith M, Maas M, de Vries N, van Schaardenburg D, Dijkmans B, Gerlag D, Tak P. Different stages of rheumatoid arthritis: features of the synovium in the preclinical phase. *Ann Rheum Dis.* 2011; 70: 772-777.

Wells P. Ultrasonics in medicine and biology. *Phys. Med. Biol.* 1977; 22 (4): 629-669.

Wilson-Gerwing T, Pratt I, Cooper D, Silver T, Rosenberg A. Age-related differences in collagen-induced arthritis: Clinical and imaging correlations. *Comparative Medicine*. 2013; 63(6): 498-502.

Wojdasiewicz P, Poniatowski L, Szukiewicz D. The role of inflammatory and anti-inflammatory cytokines in the pathogenesis of osteoarthritis. *Mediators of Inflammation.* 2014; 2014: 1-19.

Yap H, Tee S, Wong M, Chow S, Peh S, Teow S. Pathogenic role of immune cells in rheumatoid arthritis: implications in clinical treatment and biomarker development. *Cells.* 2018; 7 (161): 1-19.

Yokoyama U, Iwatsubo K, Umemura M, Fujita T, Ishikawa Y. The prostanoid EP4 receptor and its signaling pathway. *Pharmacol Rev.* 2013; 65: 1010-1052.

Zhang L. Effect of LIPUS on inflammatory factors, cell apoptosis and integrin signaling pathway in osteoarthritis animal models. *Journal of Hainan Medical University.* 2017. 23 (9): 17-20.

Zhong X, Wang H, Jian X. Expression of matrix metalloproteinases-8 and -9 and their tissue inhibitor in the condyles of diabetic rats with mandibular advancement. *Experimental and Therapeutic Medicine.* 2014; 8: 1357-1364.

Zoetis T. Tassinari M, Bagi C, Walthall K, Hurtt M. Species comparison of postnatal bone growth and development. *Birth Defects Research.* 2003; 68: 86-110.

CHAPTER 2: MATERIALS AND METHODS

2.1 *Animal Care and Experimental Design*

This study was approved by the University of Alberta Animal Care and Use Committee (protocol AUP00002169).

2.2 *Part 1: Validation of TMJ arthritis in collagen induced arthritis (CIA) juvenile rats*

2.2.1 *Micro-computed tomography scanning*

Twenty-seven 3-week-old male Wistar rats were obtained from Charles River Canada for this study. Upon arrival into the animal facility, the rats were acclimatized for a period of one week. Then, each rat was weighed using a digital scale and their head width (TMJ area to TMJ area) was measured using manual calipers. Next, each rat was *in vivo* micro-computed tomography (MicroCT) scanned according to the following procedures: 1) Each rat was carefully placed in the isoflurane anesthesia knockdown chamber and then the level of isoflurane was increased slowly up to ~250 mL/minute gas flow. 2) When the rat lost consciousness, the knockdown chamber was flushed with pure oxygen two times before opening the lid and removing the rat.

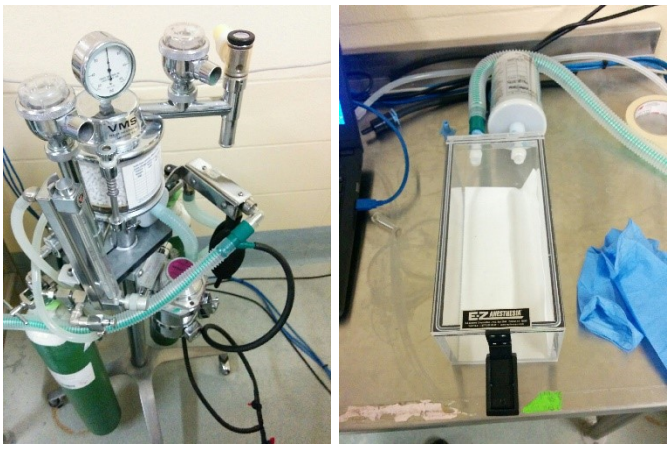

Figure 2.1: Photos of isoflurane anesthesia unit (left) and knockdown chamber (right).

The rat was carefully transferred to a pre-warmed MicroCT scanning bed with an attached nose cone connected to an isoflurane anesthesia unit and oxygen supply. The anesthetic apparatus connected to the scanning bed was adjusted to a gas flow of 300 mL/minute. The rat was fixed to the bed with clear cello wrap to prevent any unwanted and unexpected movements or escaping of the rat during the scan. The rats were visually monitored for a regular respiration rate of 70-180 breaths/minute, the scanning bed was maintained at 36-38 degrees Celsius for the duration of the scan, and a webcam was used to perform a quick, initial webcam scan to set the scanning range. 3) When the scanning range was set to only contain the rat's head, the scan began. The parameters used for the scanning were: magnification = ultra focus, scan angle = full, scan mode = normal, settings = default, energy = single, total scan time = 14 minutes 39 seconds with exposure time of 75 milliseconds, total steps = 960 with 0.3 seconds/step, tube current = 0.19 mA, and tube voltage= 55 kV. 4) Upon completing the MicroCT scan, each rat was placed it is cage for recovery and was monitored to ensure full recovery.

2.2.2 *Collagen-induced arthritis (CIA)*

The rats were divided into 3 equal groups (n=9): CIA group, Saline group, Healthy group. Prior to the TMJ injections, the injection emulsion was prepared for each rat in the CIA group. For each injection (1 injection/TMJ, so 2 injections/rat), 100 μg of bovine type II collagen was dissolved in 50 μL sterile saline (0.09%) and emulsified with 50 μL of complete Freund's adjuvant (CFA) by quick motions of pipetting up and down a pipetting tip. This 100 μL emulsion was transferred into a 1 mL syringe and then a 26 ½ gauge needle was attached. These injections were prepared immediately prior to the scheduled injection time and were kept on ice until use.

Each rat was weighed, and their head width was measured immediately before the TMJ injections. The rat was anesthetized using isoflurane inhalant and surgical plane was confirmed through absent pedal reflex and appropriately reduced breathing rate. Percent isoflurane gas flow was increased when necessary to obtain surgical plane, but most rats were anesthetized and maintained at 2.5% (isoflurane in oxygen). Breathing rate and length of time under anesthesia was recorded for each rat for animal welfare and monitoring purposes. Upon entering surgical plane, the location of the TMJ injection was confirmed by manual palpation of the zygomatic arch and mandible. The needle was guided and angled at 30-40 degrees to the sagittal plane, pointed slightly superiorly-posteriorly and inserted under the zygomatic arch, confirming slight contact with the condyle. The emulsion was slowly injected over 5 seconds, then the needle was immediately removed. Upon completing both right and left TMJ injections, the rat was allowed to return to consciousness prior to returning it to its cage for complete, monitored recovery.

For each rat in the saline group, 100 μL of sterile saline (0.09%) (no type II collagen or CFA) was prepared in 1 mL syringes with 26 ½ gauge needles similarly as the previous description of CIA injection preparation. Identical protocols of anesthesia and injection technique were used for TMJ injections of saline into both right and left TMJs. The rats in the healthy group did not receive any TMJ injections nor anesthesia and remained untreated.

After injections were completed, TMJ-CIA-induced arthritis was allowed to develop for 4 weeks. Rat body weights and head widths were measured, beginning the day after injections, at days 1, 2, 3, 7, 8, 13, 15 and 24. The rats were euthanized with CO_2 at day 28 from the injection day for groups 1, 2 and similar day for group 3.

2.2.3 *Tissue preparation and ex vivo MicroCT scanning*

Rat heads were immediately fixed in 10% buffered formalin for 48 hours, then rinsed in 1X PBS and stored in 1X PBS until *ex vivo* MicroCT scanning which was performed using the same scanning parameters as *in vivo* MicroCT scanning as previously described. After scanning, the TMJs were dissected out. Either right or left TMJs from each rat were randomly allocated to histological analysis and the other TMJ was stored in 1X PBS for any further analysis.

2.2.4 *Histology and Immunohistochemistry*

TMJs allocated to histology were decalcified for about 6 weeks in 10% formic acid that was changed twice per week. Then, the TMJs were processed in an automated series of dehydration and paraffin infiltration steps and embedded in paraffin blocks. These tissue blocks were sectioned at 7-µm thickness in the sagittal plane using a manual microtome, then the tissue samples were placed on charged Superfrost plus microscope slides and dried for 18 hours at 37 degrees Celsius in a drying oven to ensure adhesion of the sample to the glass slide.

Hematoxylin and eosin (H&E) staining was performed by routine staining protocol. In brief, slides were deparaffinized in clearene (2x10 minutes), and rehydrated in 100%, 95%, 70% and 35% ethanol for 20 seconds each. Next, after washing by immersion in TBS washing buffer, Mayer's hematoxylin was applied to each slide and allowed to stain for 1-2 minutes depending on the age of the hematoxylin. After blueing in tris-buffered saline (TBS), 1% acid ethanol was applied to destain slides for 30 seconds, and then the slides were washed by immersion in fresh TBS washing buffer. Eosin working solution was applied to slides for 30 seconds and then the slides were washed again in TBS. Dehydration of the slides was performed by reversing the order of ethanol baths through both clearene baths. Coverslips were mounted onto the slides

using permount (permanent mounting medium) and the slides were allowed to fully dry lying flat in a fume hood overnight.

Toluidine blue (TB) staining was performed in a similar manner as the H&E staining described above. After deparaffinization, rehydration and washing, prepared toluidine blue staining solution was applied to the slides for 2-3 minutes and then the slides were washed in TBS. Again, dehydration was performed as described above prior to mounting the slides.

Immunohistochemistry was performed for detection and observation of Col-II, MMP-13, IL-1β, and TNF-α. After the slides were deparaffinized and rehydrated, antigen retrieval was performed using protease XXV (30 minutes at room temperature) and then bovine testicular hyaluronidase (for Col-II slides only, 30 minutes at 37 degrees Celsius), peroxidase blocking was completed using 3% H_2O_2 solution applied to slides (10 minutes at room temperature), and protein blocking was performed using 5% normal goat serum in 1X PBS with 0.3% Tween-20 (10 minutes at room temperature). Each incubation was performed inside humidity chambers to prevent the slide from drying. After the protein blocking, primary antibodies were applied to the slides for overnight incubation at 4 degrees Celsius (Col-II – 1:500, Abcam, Cambridge, MA; MMP-13 – 1:1500, Abcam; IL-1β – 1:50, Santa Cruz Biotechnology, Dallas TX; TNF-α – 1:10,000, Santa Cruz) (only TBS [diluent] was applied to negative control slides). Appropriate HRP-conjugated secondary antibodies (for Col-II and MMP-13: IgG H + L HRP, 1: 2000, Abcam; for IL-1β and TNF-α: IgG-HRP conjugated, 1:200, Santa Cruz) were applied the next day for 15 minutes, followed by 3,3'-diaminobenzidine (DAB) chromogen and substrate application for 10 minutes. Counterstaining was completed with hematoxylin. Finally, dehydration steps were followed, without immersion into clearene, prior to mounting the slides for analysis.

2.2.5 *Analysis*

Quantitative analysis was performed for TNF-α immunohistochemically-stained slides. Three fields of view, each measuring 80 µm x 40 µm in area, were selected at the chondrogenic cell layer (mature chondrocytes only) at 1) the central axis of the condyle, 2) halfway between the central axis and the anterior edge of the condyle, and 3) halfway between the central axis and the posterior edge of the condyle. These fields of view were parallel to the condyle's articular surface. The percent of immune-positive cells were counted in each area and the averages were used for statistical analysis (Figure 2.2).

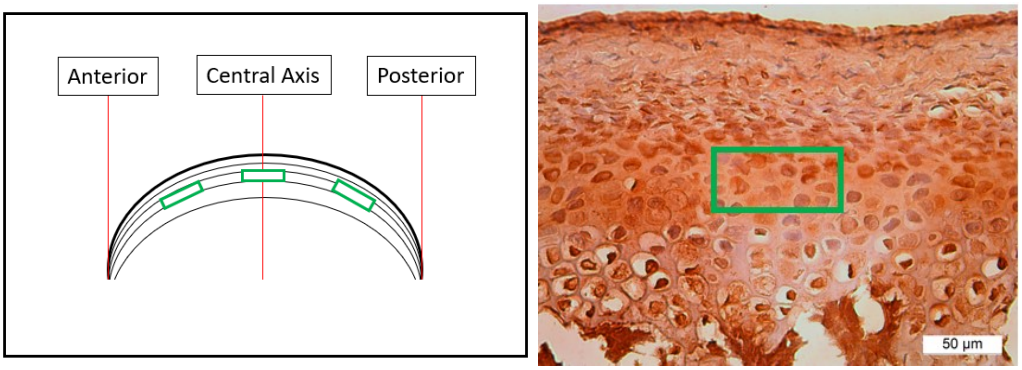

Figure 2.2: Illustration demonstrating TNF-α quantification analysis. Three fields of view (green boxes) on illustrated condyle placed at central axis, midpoint between central axis and anterior edge of condyle, and midpoint between central axis and posterior edge of condyle, as described above. Photomicrograph representing TNF-α-stained cartilage. Scale bar = 50 µm

Cartilage cell layer thickness was measured in each cell layer: fibrocartilage (fibrous articular layer), proliferative cell layer (proliferating pre-chondrocytes), chondrogenic cell layer (mature, differentiated chondrocytes), and hypertrophic cell layer (hypertrophic chondrocytes).

Each layer was defined based on morphology of the cells that it contained. These evaluations were performed by measuring the thickness of each cell layer at 3 equidistant points (83 μm apart) on either side of the central axis of the condyle (3 on the posterior side and 3 on the anterior side), plus one measurement at the central axis. These 7 thickness measurements were averaged and the mean was used in statistical analysis.

Finally, using MicroCT analysis of each rat hemimandible from the *in vivo* and *ex vivo* scans, effective mandibular length was measured as the distance between the condylar point and the menton point (Figure 2.3). Mandibular growth was calculated as the difference between the *in vivo* and *ex vivo* mandibular lengths for each hemimandible.

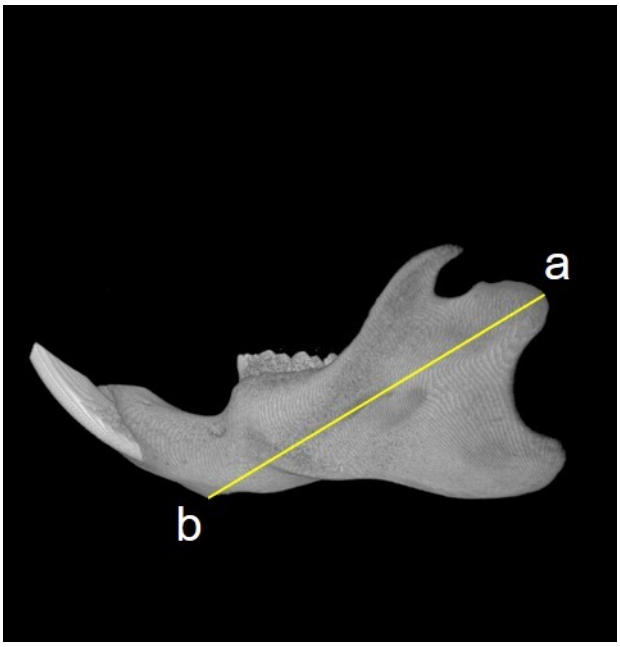

Figure 2.3: Illustration demonstrating mandibular length measurements from condylar point (a) to menton point (b).

Statistical analysis was performed using SPSS 16. Statistical significance was tested using an analysis of variance (ANOVA) with an alpha of 0.05 and *post hoc* analysis was conducted using a Tukey test.

Part 1 of this study as described above was published in the journal Tissue Engineering: Part C in February 2021. This published manuscript is contained with this thesis in Chapter 3.

2.3 *Part 2: The effect of LIPUS on TMJ arthritis in juvenile rats*

2.3.1 *Micro-computed tomography scanning*

Seventy-two 3-week-old male Wistar rats were obtained from Charles River Canada for this part of the study. Upon arrival into the animal facility, the rats were acclimatized for a period of one week. After this, each rat was weighed and their head widths were measured in the same manner as previously described in Part 1. *In vivo* micro-computed tomography (MicroCT) scanning was performed according to similar procedures as previously described.

2.3.2 *Groups*

All rats were divided into 8 equal groups (n=9). The following table describes group allocation:

Table 2.1: Description of group allocation.

Groups (n=9)	**TMJ Injection**	**LIPUS (20 min/day)**
1 *(CIA + immediate LIPUS 4 weeks)*	CIA	Yes
2 *(Saline + immediate LIPUS 4 weeks)*	Saline	Yes
3 *(CIA + immediate isoflurane only 4 weeks)*	CIA	No
4 *(Saline + immediate isoflurane only 4 weeks)*	Saline	No
5 *(CIA + delayed LIPUS 4 weeks)*	CIA	Yes
6 *(Saline + delayed LIPUS 4 weeks)*	Saline	Yes
7 *(CIA + delayed isoflurane only 4 weeks)*	CIA	No
8 *(Saline + delayed isoflurane only 4 weeks)*	Saline	No

The following illustration demonstrates the study design to help further understand group allocation and treatment:

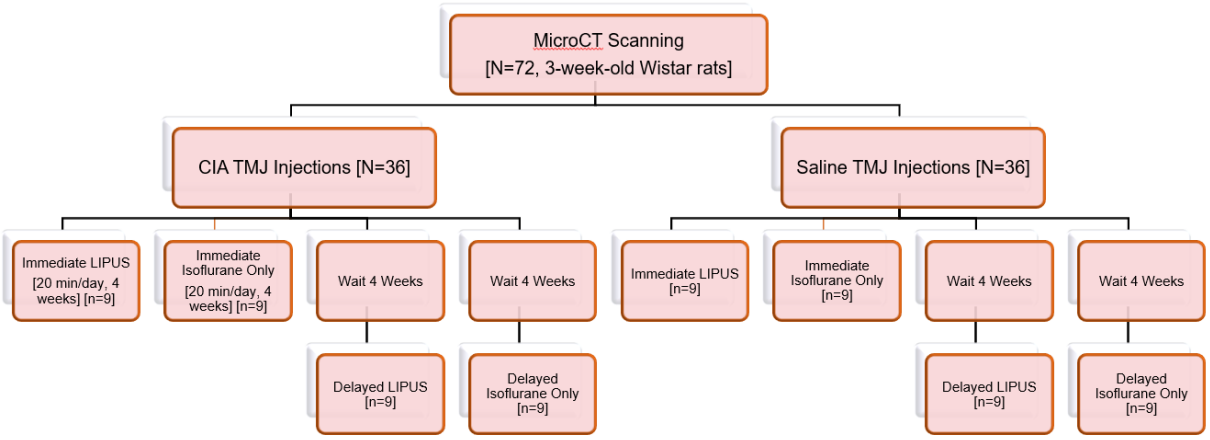

Figure 2.4: Illustration showing study design for Part 2.

The CIA groups received CIA injections into both right and left TMJs in the same manner as previously described in Part 1. The saline groups received saline injections into both TMJs, and the procedures for these injections were identical those previously described for Part 1. Immediate low intensity pulsed ultrasound (LIPUS) treatment was applied to both right and left TMJs (shaved TMJ areas with applied ultrasound coupling gel) as described below in the 'LIPUS treatment' section below. This 'immediate' treatment began at day 1 which was the day after the TMJ injections were performed. LIPUS was applied immediately to evaluate any preventive effect of LIPUS on TMJ arthritis. To control for any potential effect of the isoflurane anesthesia, the groups 'immediate isoflurane' were only exposed to inhalant isoflurane without any LIPUS treatment.

Figures 2.5 and 2.6 demonstrate how LIPUS treatment and isoflurane anesthesia were applied. Both immediate LIPUS treatment or isoflurane only were performed for a total of 20 minutes per day for 28 consecutive days (4 weeks). The groups that had either delayed LIPUS treatment or delayed isoflurane only did not receive any treatment immediately after the TMJ injections. These treatments began exactly 28 days (4 weeks) *after* the TMJ injections were performed for 20 minutes per day, 28 consecutive days (4 weeks). Delayed LIPUS treatment was included in order to evaluate any treatment effect of LIPUS on TMJ arthritis that develops during the first 4 weeks after the TMJ injections were completed. Body weights and head widths (Figure 2.7) were measured on days 1-7, 11, 14 and 21 (day 1 = day after TMJ injections) for groups 1-4 (immediate treatment), and for groups 5-8 (delayed treatment) on days 1-6, 8, 14, 22, 23 (after injections and before delayed treatment) and days 1, 7, 14 and 21 (day 1 = first day of LIPUS/isoflurane).

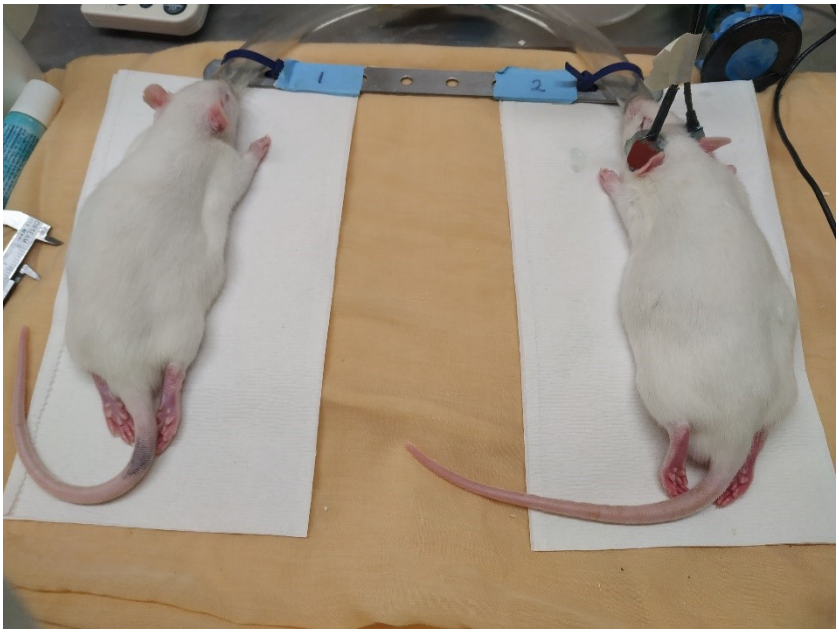

Figure 2.5: Photo of rats receiving LIPUS treatment (right) vs. Isoflurane only (left).

Figure 2.6: Photo of rat receiving LIPUS treatment.

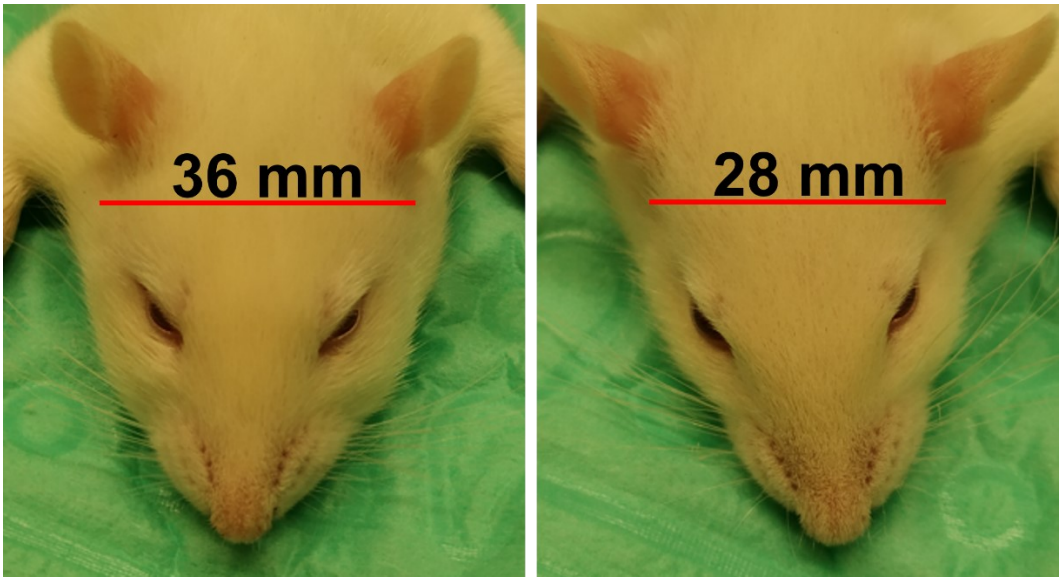

Figure 2.7: Illustrative photo of example head width measurements at day 1 in a CIA (left) and Saline rat (right)

Immediately after completing the 4 weeks of LIPUS (or isoflurane only) treatment, the rats were euthanized by CO_2, and whole blood was collected by cardiac puncture and processed to isolate serum and plasma. Serum and plasma were aliquoted into smaller volumes and kept at

-20 degrees Celsius until analysis. As previously described, the tissues were fixed in preparation for *ex vivo* MicroCT scanning, and then after scanning, TMJs were dissected and right or left TMJs were randomly assigned to either histological analysis or kept in 1X PBS for other analyses. The TMJs destined for histological analysis were decalcified, processed, embedded in paraffin blocks, and sectioned as described in Part 1.

2.3.2 *Histology and Immunohistochemistry*

H&E staining was performed, according to previously described protocol, on histological slides from each available rat. Unfortunately, good histological sections were not able to be obtained from every rat due to sectioning difficulties with some paraffin blocks. Each treatment group contained at least 6 blocks with acceptable sections to be used for analysis. These stained slides were used for general qualitative observation of cartilage cell layer morphology, pannus tissue formation, and synovitis in synovial membrane encapsulating the TMJ. As well, these slides were used for cartilage cell layer thickness measurements that were performed in an identical manner as previously described for Part 1 of the study. Next, toluidine blue (TB) staining was performed, again using the same protocols as previously described.

Immunohistochemistry was completed for immunostaining of the following: Col-II, Col-X, MMP-13, RANKL, TGF-β1, VEGF, IL-1β, IL-17, and TNF-α. In brief, after deparaffinization and rehydration, antigen retrieval was performed using protease XXV (all slides except Col-X, 30 minutes at room temperature, 1 mg/mL) or pepsin (Col-X slides only, 10 minutes at 37 degrees Celsius, 0.25% pepsin in TBS) and then bovine testicular hyaluronidase (for Col-II and Col-X slides only) for 30 minutes at 37 degrees Celsius. Next, peroxidase blocking was completed using 3% H_2O_2 solution applied to slides for 10 minutes at room

temperature, and protein blocking was performed using 1X PBS with 0.3% Tween-20 (10 minutes at room temperature). Primary antibodies were applied to the slides for overnight incubation at 4 degrees Celsius (Col-II – 1:500, Abcam, Cambridge, MA; Col-X – 1:50, Thermo Fisher Scientific, CA; MMP-13 – 1:1000, Abcam; RANKL – 1:50, Santa Cruz Biotechnology, Dallas, TX; TGF-β1 – 1:50, Santa Cruz; VEGF – 1:500, Santa Cruz; IL-1β – 1:25, Santa Cruz; IL-17 – 1:50, Santa Cruz; and TNF-α – 1:1,000, Santa Cruz) (only TBS [diluent] was applied to negative control slides). Appropriate HRP-conjugated secondary antibodies were applied the next day for 15 minutes, followed by DAB chromogen and substrate application for 10 minutes. Counterstaining was completed with hematoxylin. Dehydration steps were followed as previously described.

2.3.3 *Enzyme-linked immunosorbent assays (ELISAs)*

To quantitatively measure the protein levels of IL-1β and TNF-α in blood serum, IL-1β and IL-6 in the articular disc, and TGF-β1 (2 forms: bound to LAP, latency associated peptide [inactive form] and dissociated from LAP [active form]) in blood plasma, we obtained appropriate ELISA kits (Invitrogen, Thermo Fisher Scientific, CA) and performed these assays according to the manufacturer's procedures and protocols. Whole serum and whole plasma were used in these assays. Whole articular discs were dissected from each TMJ that was stored in 1X PBS, representing 1 TMJ/rat. Each disc was homogenized in 1 mL of 1X PBS using a mortar and pestle kept on ice. The articular disc homogenate underwent 2 freeze-thaw cycles in order to further disrupt cell membranes prior to being centrifuged and the supernatant collected for use in the IL-6 ELISA.

2.3.4 *MicroCT Analysis*

MicroCT analysis was used to evaluate mandibular and condylar growth using the software Imalytics Preclincal 2.1 (Gremse-IT GmbH, Acchen, Germany). After correcting the voxel size according to the MicroCT scan reconstruction voxel size, 3D rendering was used to create 3D models to measure mandibular length (Figure 2.3) and condylar volume (Figure 2.8). Threshold adjustments and automatic segmentation was performed to segment each hemimandible. Markers were placed at the condylar point and the menton point, and the distance between these two points were automatically calculated to measure mandibular length.

For condylar volume measurements, a virtual line was drawn from each notch superior and inferior to the condyle and single virtual cut was made along this line on the 3D model of the mandible. The condyle was then automatically segmented from the rest of the mandible, and the volume of this segmentation was automatically calculated with this software. Our lab created this protocol since there was no previously published protocol using this software for segmenting the condyles and measuring the condylar volume.

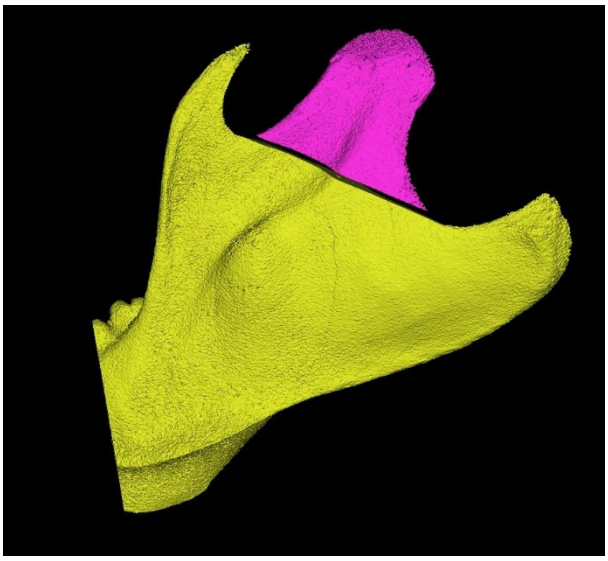

Figure 2.7: Illustration demonstrating segmentation of the mandibular condyle (pink) from mandible (yellow) for calculation of condylar volume.

To calculate the growth of the mandible, mandibular length from the *in vivo* scan was subtracted from the mandibular length from the *ex vivo* scan of each rat and compared between groups. To calculate the growth of the condyle, condylar volume from the *in vivo* scan was subtracted from the condylar volume from the *ex vivo* scan of each rat and compared between groups. These growth calculations were used in statistical analyses.

To evaluate intra-rater reliability of the mandibular length measurements, 10 hemimandibles were randomly chosen for re-evaluation. The evaluator (ie. rater) was blinded to any previous mandibular length values and these re-measurements were performed at least 6 months after the original measurements were completed.

2.3.6 *Statistical Analysis*

Statistical analysis was performed using SPSS 16. Statistical significance was tested using a univariate analysis of variance (ANOVA) with an alpha of 0.05 to determine any significant interaction of 3 factors with 2 levels each [1) CIA vs. Saline, 2) Immediate vs. delayed, 3) LIPUS vs. Isoflurane only]. When there were significant interactions, then a post hoc Tukey test was used to determine which groups were significantly different from another. The data obtained from the TGF-β1 ELISA required conversion from continuous data to ordinal data due to numerous results showing 'zero' protein levels (discussed in discussion section). If TGF-β1 plasma levels were 0-9 ng/mL, then they were categorized as a level of '1'. If the levels were 10-19 ng/mL, then they were categorized as a level of '2'. This continued to encompass and recode all levels of TGF-β1. To statistically analyze this data, we used a Kruskal-Wallis H test to compare between groups.

To evaluate intra-rater reliability, the intra-class correlation coefficient was generated using SPSS using the absolute-agreement, 2-way mixed-effects model.

CHAPTER 3: COLLAGEN-INDUCED TEMPOROMANDIBULAR JOINT ARTHRITIS JUVENILE RAT ANIMAL MODEL

TISSUE ENGINEERING: Part C
Volume 27, Number 2, 2021
[a] Mary Ann Liebert, Inc.
DOI: 10.1089/ten.tec.2020.0294

Collagen-Induced Temporomandibular Joint ArthritisJuvenile Rat Animal Model

Jacqueline Crossman, MSc,[1] Hollis Lai, PhD,[1] Marianna Kulka, PhD,[2] Nadr Jomha, MD, PhD,[3]Patrick Flood, PhD,[1] and Tarek El-Bialy, PhD[1]

Juvenile idiopathic arthritis can affect the temporomandibular joint (TMJ) can cause growth disturbances of the lower jaw (mandible). The collagen-induced arthritis (CIA) juvenile rat model may be an appropriate model forstudying how juvenile arthritis affects this joint during growth. However, studies using this animal model to investigate TMJ arthritis are limited. To validate an animal model for studying TMJ arthritis in growing rats, our study aimed to investigate the changes in mandibular growth and expression of proteins and cytokines in themandibular condyle of CIA juvenile rat TMJs. A total of 27 male Wistar rats (3 weeks old) were scanned with microcomputed tomography (MicroCT) and divided into three groups ($n = 9$); CIA was induced in each TMJ inthe CIA group, the Saline group received saline injections (sham injections) into their TMJs, and the Healthy group remained untreated (no TMJ injections) as negative controls. After 4 weeks, our results show that mandibular growth was significantly reduced in the CIA group compared with the Saline group ($p < 0.01$). There was no difference in mandibular growth between the two control groups (Saline and Healthy). Inflamed synovial tissue, cartilage invaginations, and lipid accumulation were observed in the CIA TMJs. Toluidine bluestaining revealed decreased proteoglycan production in the CIA cartilage. In addition, immunohistochemistry revealed that type II collagen expression decreased, interleukin-1β expression increased, and matrix metalloproteinase-13 expression increased in the CIA TMJs in comparison with the two control groups (Saline and Healthy). Immunostaining of tumor necrosis factor-α (TNF-α) was quantified and we showed that TNF-α expression was significantly greater in the CIA cartilage compared with both control groups ($p < 0.05$), andthere was no difference in TNF-α expression between the Saline and Healthy groups. This CIA juvenile ratmodel of TMJ juvenile arthritis shows that CIA reduced mandibular growth and induced degenerative changes in TMJ condylar cartilage. This new information will help to understand the pathogenesis involved in CIA in juvenile rat TMJs for this animal model to be used in research investigating new therapeutics to treat TMJ juvenile arthritis.

Keywords: collagen-induced arthritis, temporomandibular joint, juvenile arthritis, animal model

Impact Statement

In this study, the effects of collagen-induced arthritis (CIA) on the temporomandibular joint (TMJ) using a juvenile rat model were investigated. Our results showed that local injection of CIA in the TMJ significantly reduced mandibular growthand caused degenerative changes in condylar cartilage. This information helps to validate this animal model for studying theeffect of arthritis in TMJs in growing rats. This model has the potential to be used in future studies to evaluate possible therapies for TMJ arthritis.

[1]Department of Dentistry, Faculty of Medicine and Dentistry, University of Alberta, Edmonton, Canada.
[2]Department of Medical Microbiology & Immunology, Faculty of Medicine and Dentistry, University of Alberta, Edmonton, Canada.
[3]Department of Surgery, Faculty of Medicine and Dentistry, University of Alberta, Edmonton, Canada.

Introduction

Juvenile idiopathic arthritis (JIA) is a chronic inflammatory disease that is similar to rheumatoid arthritis (RA), but affects the growing population. The temporomandibular joint (TMJ) can be affected by JIA. It has been reported that up to 87% of JIA patients have involvement of the TMJ.[1] This is a significant developmental problem since TMJ-JIA severely affects mandibular growth and structure due to joint synovitis, pannus, condylar head flattening, boneerosion, and damage to articular cartilage.[1] The majority of mandibular growth occurs at the mandibular condyle, and growth in length of the condyle is due to cellular changes (proliferation, matrix production, and hypertrophy) within thearticular cartilage.[2] It is necessary to examine the cellular andbiochemical progression of TMJ-JIA and identify potential treatments to block inflammation. If TMJ-JIA is left un- treated, chronic inflammation can cause irreversible damage to the TMJ, resulting in malocclusion, micrognathia, retrognathia, and overjet that may require surgical correction.[3]

Animal models are extensively used in the study of the pathogenesis of human diseases and to evaluate the potential efficacy of drugs for clinical use. For these animal models tobe clinically relevant, they must be morphologically similar to human tissue and they must be able to predict the efficacyof therapeutic interventions in humans. Many animal modelsare available to examine the etiology of human RA, where some of these models have been used by the pharmaceuticalindustry to test the clinical efficacy of antiarthritic agents.[4] RA animal models are usually easy to perform, data generated from studying these models are reproducible, and most models are short in duration.[4]

The most common rodent models of arthritis are based on spontaneous development of the disease or require some form of induction such as an injection. These induced models of arthritis include rat and mouse type II collagen (Col-II) arthritis, antigen arthritis, and adjuvant arthritis, each representing different degrees of bone resorption and cartilage damage, which are characteristic of RA seen in humans. Adjuvant-induced arthritis in rats results in joint inflammation and bone destruction, but the incidence of arthritis and cartilage damage may vary and therefore may notbe the ideal animal model to study RA-like cartilage damage.[4–6] Antigen arthritis results in rapid development of lesions, but may require repeated injections of the antigen involved.[6] If this type of arthritis progresses past 2 weeks, ahighly destructive pannus within the inflamed joint may destroy most of the articular cartilage.[4] Finally, lesions observedin Col-II arthritis in rats are more analogous to those seen inhuman RA, but there is less published data on the pathological changes seen in this type of induced arthritis than inother models to compare this disease with human RA.[4]

Studying the pathogenesis of TMJ arthritis in a juvenile animal model would increase our understanding of the effectof this inflammatory disease on this joint during growth andwould aid in development of potentially new and more effective treatments for TMJ-JIA. Since the type II collagen-induced arthritis rat model is considered to be the most analogous to RA (and JIA), using this induced system in thestudy of juvenile rat TMJs is likely to generate the most relevant data. Collagen-induced arthritis (CIA) is a previously studied juvenile rat model to study TMJ arthritis.[7]

This model resulted in an increased RANKL:OPG expression ratio, which indicates differentiation of osteoclasts, thebone-resorbing cells that cause bone damage. Additionally, serum levels of the proinflammatory cytokines, interleukin (IL)-1β and tumor necrosis factor-α (TNF-α), were in- creased in this animal model, and histological analyses showed evidence of synovitis and cartilage and bone de- struction.[7] Currently, it is not known whether the CIA injection in the TMJ of growing rats has an effect on expression of Col-II and matrix metalloproteinase (MMP)-13 in the articular cartilage, localized expression of IL-1β and TNF-α in the TMJ, and on mandibular growth (mandibular length). In this study, we examined these parametersin the juvenile rat model of CIA to determine whether it is asuitable model of TMJ arthritis in humans. We hypothesizedthat the expression of MMP-13, IL-1β, and TNF-α would be increased in the TMJ condyles in the CIA group, expressionof Col-II would be decreased in the CIA group, and mandibular growth would be decreased in CIA. The data may lead to future studies using this model to study new therapies to treat TMJ arthritis in JIA patients.

Methods

Collagen-induced arthritis

Our research was approved by the animal ethics committee at the University of Alberta [AUP00002169]. The sample size was calculated to be $n = 5$ (5% type I error, 80% power, 1.77 effect size), but to account for any potential mortality before the planned endpoint of the study andnondevelopment of CIA in the TMJ, we used $n = 9$. We acclimatized 27 male Wistar IGS rats (3 weeks old) (Strain Code 003; Charles River Laboratories) and divided them into three equal groups ($n = 9$; CIA, Saline, and Healthy).The rats were allocated to each group by randomly assigningeach cage to a group. Each cage contained 2 rats, therefore cages 1–4 contained 8 rats in the CIA group, cage 5 had 1 rat(tail marking) in the CIA group and 1 rat (no tail marking) inthe Saline group, cages 6–9 contained 8 rats in the Saline group, and cages 10–14 had 9 rats in the Healthy group (cage 14 had only 1 rat). We scanned each rat under anesthesia using *in vivo* microcomputed tomography (MicroCT)(MILabs, 0.19 mA tube current, 55 kV tube voltage, 960 steps, 0.3°/s, 75 ms exposure time, 40 mm reconstruction resolution) before the intervention. For the CIA group, 100 mg of bovine Col-II (Chondrex, Inc.) dissolved in 0.09% sterile saline and an equal volume of complete Freund's adjuvant (Sigma-Aldrich) (contains heat-killed *Myco- bacterium tuberculosis*), totaling 100 mL in volume, were injected into the upper compartment area of the TMJs (both right and left) according to the previously published proto- col.[7,8] The sham injection group (Saline group) received only saline (0.09%) TMJ injections and the Healthy group did not receive any TMJ injections.

Experiment

Experimental design

Body weight and head width. After we performed the TMJ injections, as outlined in the Methods section, wemeasured body weight using a digital weight scale and head

width using manual calipers. We measured these immediately before the initial MicroCT scan, immediately before the TMJ injections, and on days 1, 2, 3, 7, 8, 13, 15, and 24 after the TMJ injections. Four weeks after the TMJ injections (peak inflammatory cytokines described by Liu *et al.*),the rats were euthanized, and the rats underwent a second MicroCT scan.

MicroCT analysis. MicroCT analysis (ImageJ, NIH) was used to measure the mandibular length of each hemimandible (three-dimensional [3D] reconstructions) (Fig. 1A, B)of each rat at baseline and after 4 weeks. From these measurements, mandibular growth was calculated as the difference in values between baseline and after 4 weeks. Additionally, we qualitatively analyzed the 3D reconstruction of segmented mandibular condyles to observe any bonychanges (Fig. 1C).

Histology and immunohistochemistry. Histological samples of H&E-stained slides were used to qualitatively analyze the TMJ, including condylar cartilage, subchondral bone, and synovial tissue. TMJs were also stained with toluidine blue (TB) to determine any proteoglycan changes inthe cartilage matrix. Immunohistochemistry was performedto detect Col-II (Abcam, Cambridge, MA), MMP-13 (Abcam), IL-1β (Santa Cruz Biotechnology, Dallas, TX), and TNF-α (Santa Cruz). In brief, after fixation, decalcification, and sectioning [sagittal plane (Fig. 2A), 7-mm thickness], antigen retrieval (protease XXV, 1 mg/mL, Fisher Scientific, 30 min at room temperature; hyaluronidase, 1 mg/mL, Sigma-Aldrich, 30 min at 37°C/98.6°F) was performed. We completed peroxidase blocking (3% hydrogen peroxide, 10 min) and protein blocking (5% normal goat serum in 1X phosphate-buffered saline [PBS] with 0.3% Tween-20, 10 min) and then applied the primary antibodies for over-night incubation at 4°C/39.2°F (Col-II—1:1500; MMP-13—1:1500; IL-1β—1:50; and TNF-α—1:10,000). Secondary antibodies were applied the next day for 15 min (for Col-II and MMP-13 samples: IgG H+L HRP, 1:2000, Abcam; and for IL-1β and TNF-α samples: IgG-HRP conjugated, 1:200, Santa Cruz Biotechnology). Finally, 3,3℄-diaminobenzidine chromogen and substrate were applied for 10 min, followed by Mayer's hematoxylin counterstaining. For negative controls, the primary antibody was omitted and only tris-buffered saline (diluent in primary antibody solutions) was applied to tissues. Quantitative analysis of TNF-α expression in each sample was performed by counting the total number of TNF-α-positive cells in an 80 - 40 μm area. In total, three fields ofview were chosen: one at the central axis, one halfway be-tween the anterior edge of the condyle and the central axis,and one halfway between the posterior edge and the centralaxis. These three areas were placed at these locations so thateach area's upper edge was parallel to the condylar surfaceand contained only mature chondrocytes located within the chondrogenic cell layer. The total number of cells (onlyentire cells that were contained in the selected area) withinthese areas and the total number of immunopositive cellswere counted. A cell was counted as immunopositive if the intensity of staining was observed to be greater than the background staining of nearby cells. The total immunopositive cell count was divided by the total number of cells within each area to determine the percentage of cells positive for TNF-α, and the percentage was averaged for each group.[9] Calculating the percentage of cells—within the selected area—that were positive for TNF-α was chosen instead of simply counting the number of positive cells because cell size may vary between samples.

Each cartilage cell layer (fibrocartilage, proliferative cell layer, chondrogenic [mature] cell layer, and hypertrophic cell layer) was measured. To perform these measurements, the central axis of the condyle was located, and three equidistant length measurements of each cell layer were

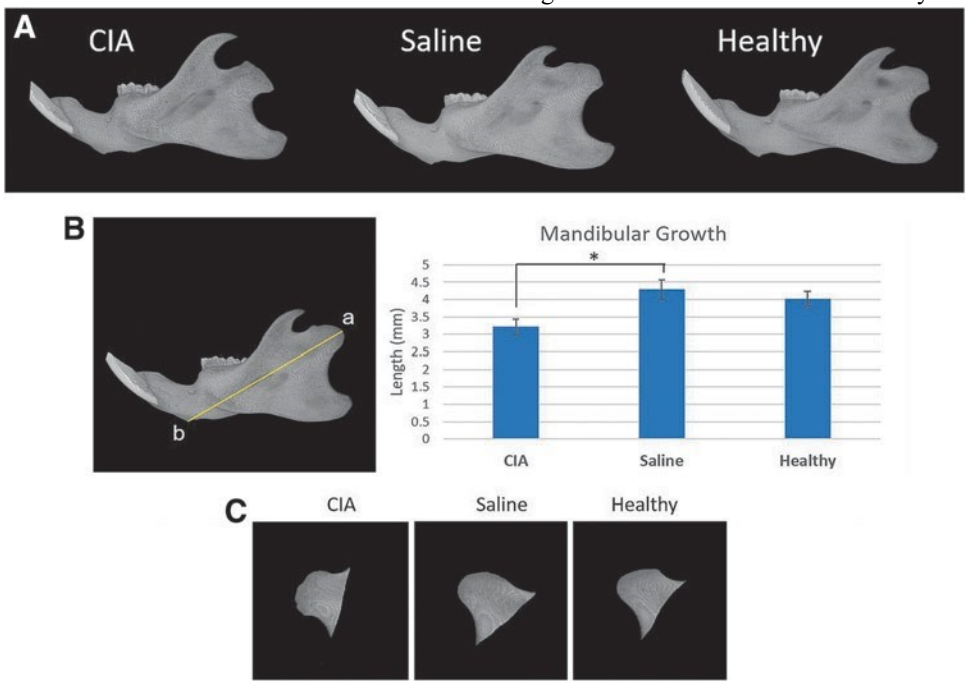

FIG. 1. (A) 3D Reconstruction. Representative hemimandibles from each group (CIA, Saline, and Healthy). (B) Mandibular length. Illustration showingmandibular length; a—condylar point, b—menton point. Average mandibular growth (mm) in each group. $^{**}p < 0.01$. (C) TMJ condyles. Representative bony changes between TMJ condyles (only condyle shown) in each group. 3D,three-dimensional; CIA, collagen-induced arthritis; TMJ, temporomandibular joint.

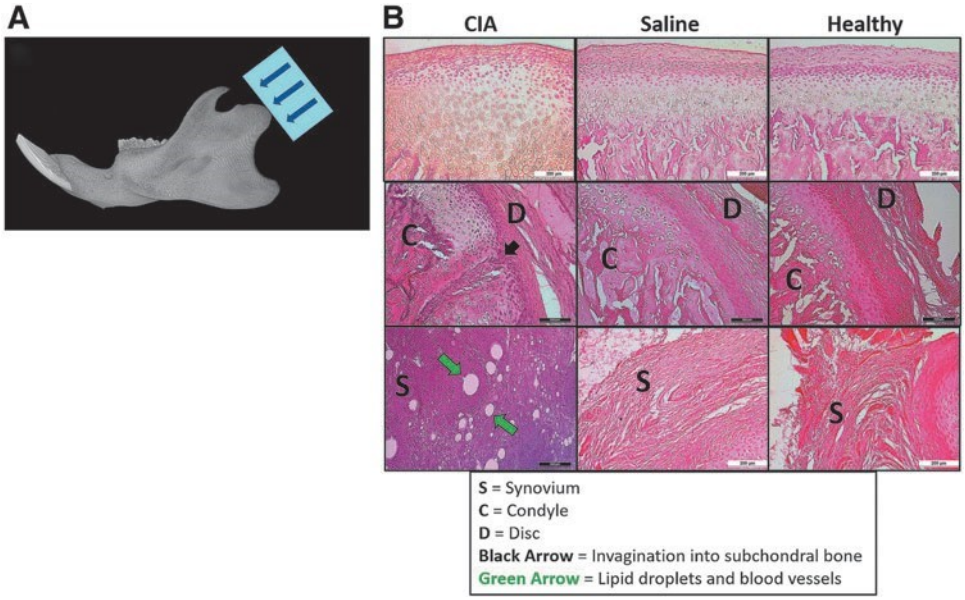

FIG. 2. (A) Schematic illustration showing direction of histological sectioning (sagittal plane). (B) Representative H&E-stained TMJs from CIA, Saline, and Healthy groups. Articular cartilage and synovial tissue. *White* scale bar = 200 mm and *black* scale bar = 100 mm.

completed (Fig. 3A). These were performed perpendicular to the condylar surface on both the anterior and posterior sides of the central axis. One measurement at the central axis was performed. Each condyle, therefore, had seven measurements that were averaged to obtain a mean thickness for each cell layer of each condyle.

Statistical analyses

All statistical analyses were conducted using SPSS 16. Significant differences were tested using an analysis of variance (ANOVA) with an alpha of 0.05. *Post hoc* analysis was conducted using the Tukey test.

Experimental results

Body weight and head width. Although the rats were randomized into three groups, the rats in the CIA group weighed more than those in the Healthy group before MicroCT scanning and after MicroCT scanning (Fig. 4A and Table 1). However, all rats had similar increases in body weight throughout the study (Fig. 4A). The rat head width in the CIA group was significantly greater than the head widths in both the Saline and Healthy groups on day 1 postinjection as well as on day 2 postinjection (Fig. 4B and Table 1). The head widths returned to normal at day 3, as shown in Figure 4B.

MicroCT analysis. Observation only of bony changes of the mandibular condyle suggests that CIA induction in growing rat TMJs may result in more condylar erosion on the articular surfaces (Fig. 2). These changes were only described and were not measured; therefore, no statistical analysis could be performed. MicroCT analysis revealed that there was a significant decrease in mandibular growth in the CIA group [$F(2, 51) = 5.120$, $p = 0.009$, Fig. 1B].

Histology and immunohistochemistry. Figure 2B shows representative photomicrographs of the TMJ (including articulating cartilage) in each group. Inflamed synovial tissue, invaginations in the cartilage toward the subchondral bone, and lipid accumulation and blood vessel development in synovial tissue were qualitatively observed. TB staining was generally greater in the Saline and Healthy cartilage compared with the CIA cartilage (Fig. 5A).

Immunostaining of Col-II showed that the expression of Col-II was mainly in the chondrogenic (mature chondrocytes) and hypertrophic cell layers in the cartilage. Col-II expression was decreased in the CIA cartilage. These photomicrographs also demonstrate generally less uniformity and organizational patterns within each cell layer within the cartilage (Fig. 5A). The distribution of MMP-13 staining revealed that in addition to MMP-13 expression in hyper- trophic cells undergoing endochondral ossification, there was greater expression of MMP-13 in chondrogenic and (pre-) hypertrophic cells in the CIA group compared with the expression of MMP-13 in the other groups. IL-1β expression was higher in the chondrogenic and hypertrophic cartilage compared with the other two control groups. There were significantly more TNF-α-positive chondrocytes in CIA tissues compared with the other groups [$F(2, 24) = 4.382$, $p = 0.024$, Fig. 5B].

The thickness of each cartilage cell layer was measured and showed that the hypertrophic cell layer was significantly thicker in the CIA group compared with the Saline group (Fig. 3B).

Discussion

Our study using the juvenile rat model for CIA in the TMJ demonstrated the inflammatory effects that this type of induced arthritis has on protein expression within the condylar cartilage. The inflammatory responses that are induced in this method of CIA are both T helper (Th) 1 and Th17 responses, which are elucidated by antigen-presenting cells presenting antigens to T cells. B and T cell responses lead to antibody production,[6] autoreaction to Col-II,[10] and production of proinflammatory cytokines such as IL-1β.[6] These cytokines further induce responses in other cells, including

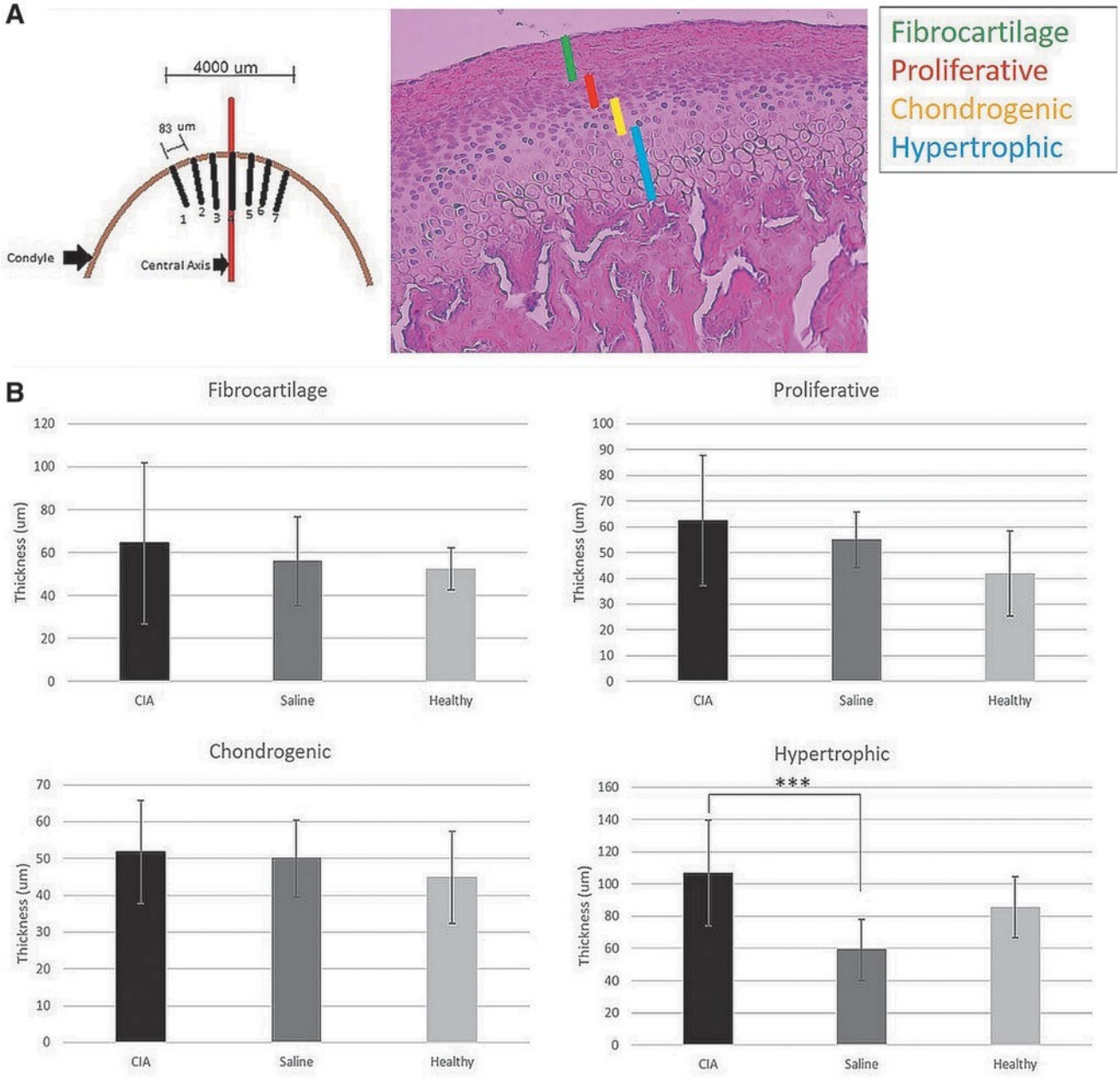

FIG. 3. (A) Illustration representing the seven condylar cartilage measurements performed for each cartilage cell layer of the mandibular condyle. (B) TMJ condylar cartilage cell layer thicknesses (mm) (fibrocartilage, proliferative, chondrogenic,and hypertrophic cell layers) for CIA, Saline, and Healthy groups. ***$p < 0.005$.

chondrocytes. Upregulation of IL-1b has also been demonstrated in cartilage harvested from knee or hip joints in patients with osteoarthritis.[11] Increased expression of IL-1βin cartilage has downstream effects on chondrocytes. An- other group investigated the relationship between IL-1β and transforming growth factor (TGF) β in cartilage in arthritic TMJs in mice. They report that IL-1β downregulated the expression of TGFβ.[12] TGFβ (specifically, TGF-β1) is one factor that regulates mandibular growth by reducing the rate of hypertrophy in chondrocytes.[13] If IL-1β is upregulated, as demonstrated in our study, then this may have down-regulated TGFβ (not analyzed in our study), which may have resulted in a decrease in mandibular growth. Mandibular growth results from proliferation of progenitor cells, production of cartilaginous matrix (such as proteoglycans), and hypertrophy of chondrocytes in the mandibular condylar cartilage. The hypertrophic cells express Col-X and Col-II. Since the immune response induced by CIA consists of autoreactive T cells to Col-II, it would be expected that the expression of Col-II would be down- regulated in CIA chondrocytes in the TMJ. Additionally, proinflammatory cytokines, such as IL-1β, induce proteoglycan degradation and production of collagenases, such as MMP-13, which degrades Col-II.[14] MMP-13 is the most prominent MMP involved in osteoarthritis and other types of arthritis such as RA.[15–17]

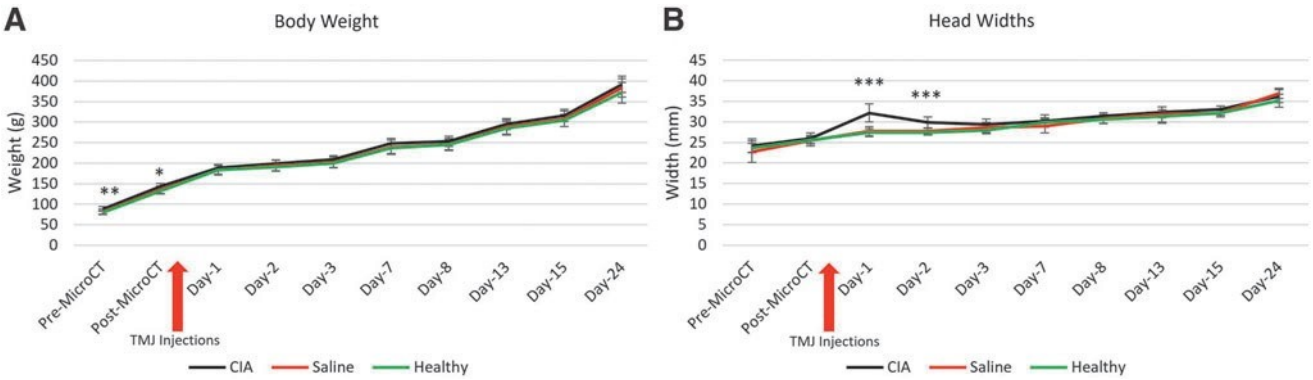

FIG. 4. Rat body weight and head widths. Average body weight (g) (A) and head widths (mm) (B) measured at each time point before and after TMJ injections. *$p < 0.05$, **$p < 0.01$, ***$p < 0.005$.

TNF-α is a key proinflammatory cytokine and central mediator of pathophysiological changes in arthritis. In the TMJ, TNF-α is synthesized by chondrocytes, osteoblasts, cells in the synovial membrane, and mononuclear cells that reside either in the joint or that infiltrate into the joint during an inflammatory response. This leads to an increase in TNF-α concentration in the synovial fluid, synovial membrane, cartilage, and subchondral bone layer. TNF-α binds membrane receptors (mainly TNF-R1) expressed on chondrocytes, among other cells, and decreases their synthesis of proteoglycan components and Col-II, but increases production of MMP-13.[18] The results of our study suggest that this process could have been activated in the CIA tissues. Inhuman TMJ RA, TNF-α levels in synovial fluid are directly correlated with the degree of TMJ condylar erosion, and thissuggests that TNF-α in TMJ synovial fluid mediates TMJcartilage and bone damage in RA.[19]

Invaginations in articular cartilage were observed in our CIA cartilage and also in TMJ cartilage in an osteoarthritic rabbit model in another study.[20] The presence of such observations potentially demonstrates decreased cartilage in- tegrity.[20] Lipid bodies and blood vessels were noted in our CIA synovial tissue and observed in the synovial tissue of inflamed rat TMJs in another study using a different TMJ arthritis rat model.[21] Lipid body accumulation can occur within inflammatory cells. It has been reported that *M. tuberculosis* induces foamy macrophages to compartmentalizelipid bodies. Since our CIA injections contained *M. tuberculosis* in the complete Freund's adjuvant, this likely induced macrophages, as well as other inflammatory cells such as leukocytes, to form lipid bodies. Additionally, lipid bodies formed in activated leukocytes may also contain cytokines such as TNF-α.[22] Lipid body biogenesis has been observed inleukocytes from joints of patients with arthritis.[22]

Table 1. Mean, Standard Deviation, *F*-Values, and *P*-Values (*Post Hoc*) for Body Weight (g)(Before and After MicroCT Scanning) and Head Width (mm) at Days 1 and 2 Postinjection in Each Group (CIA, Saline, and Healthy)

Mean		*SD*	F-*Value*	P-*Value (*post hoc*)*
Body weight (g)				
Before MicroCT				
CIA	88.68	5.90	$F(2, 24) = 5.976$	0.008[a]
Saline	82.10	6.09		NS
Healthy	79.89	4.74		0.008[a]
After MicroCT (before TMJ injections)				
CIA	143.28	7.72	$F(2, 24) = 4.296$	0.024[a]
Saline	135.26	9.44		NS
Healthy	132.27	7.42		0.024[a]
Head width (mm)				
Day 1 postinjection				
CIA	32.18	2.18	$F(2, 26) = 27.714$	0.005[a], 0.005[b]
Saline	27.73	1.13		0.005[b]
Healthy	27.38	0.96		0.005[a]
Day 2 postinjection				
CIA	29.87	1.39	$F(2, 24) = 17.200$	0.005[a], 0.005[b]
Saline	27.73	0.80		0.005[b]
Healthy	27.38	0.53		0.005[a]

[a]Between CIA and Healthy groups.
[b]Between CIA and Saline groups.
CIA, collagen-induced arthritis; MicroCT, microcomputed tomography; NS, not significant; SD, standard deviation; TMJ, temporomandibular joint.

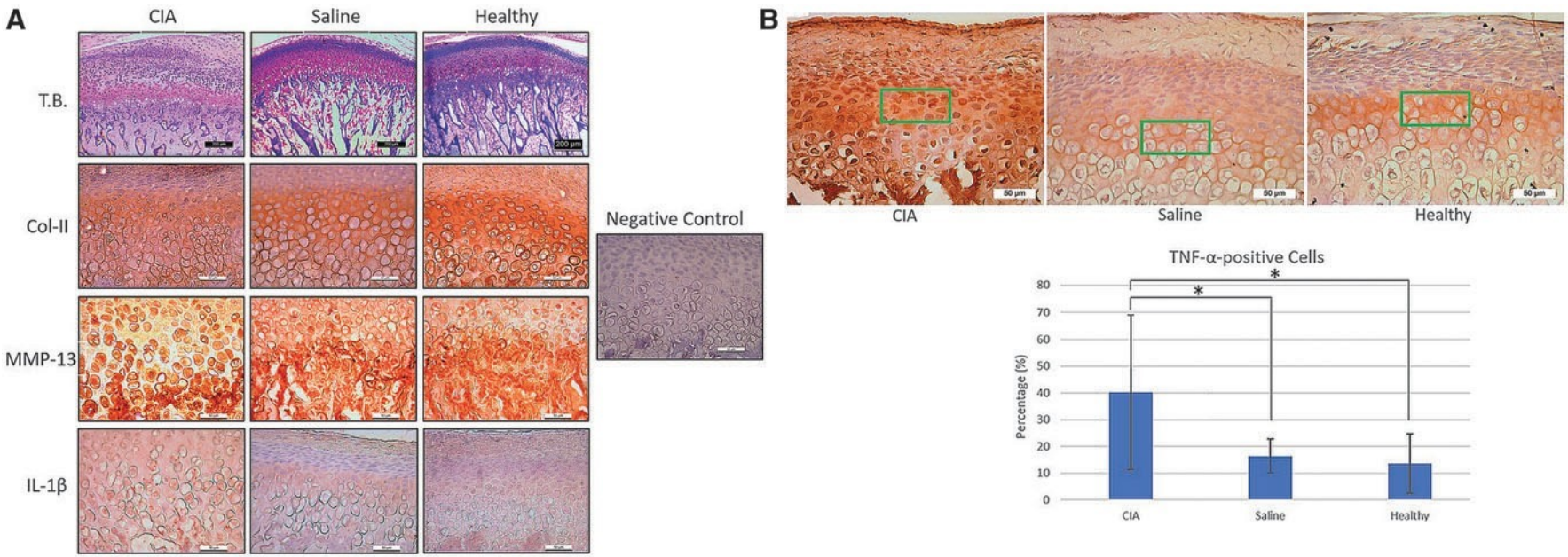

FIG. 5. (A) TB-stained TMJ condyles and immunohistochemical staining for Col-II, MMP-13, and IL-1β. Immunohistochemistry photomicrographs from each group (CIA, Saline, and Healthy groups). Negative control involved the absence of primary antibody. Representative photomicrographs for the negative control and from each group are shown for each immunostain. Scale bars = 200 mm (TB only) and 50 mm. (B) Representative images for CIA, Saline, and Healthy groups for TNF-α immunohistochemicalstaining. Quantification of chondrocytes positive for TNF-α in articular cartilage. Means − SDs are shown. Scale bar = 50 mm. *$p < 0.05$. Col-II, type II collagen; IL-1β, interleukin-1β; MMP-13, matrix metalloproteinase 13; SD, standard deviation; TB, Toluidine blue; TNF-α, tumor necrosis factor-α.

Finally, an imbalance between anabolism and catabolism causes cartilage degeneration due to an increase in proteases degrading the matrix and a decrease in matrix synthesis.[21] Interestingly, while MMP-13 is involved in cartilage degradation, there were no significant decreases in chondrogenic cell layer thickness and therefore little to no cartilage degradation. Potentially, CIA may have an effect on premature chondrogenic hypertrophy since MMP-13 induces hypertrophy in chondrocytes.[23] However, the expression of MMP-13 under normal and pathological conditions needs further investigation. Another study analyzed the effect of a complete Freund's adjuvant (CFA) injection into the TMJsof growing rats. Although they did not measure mandibular length, they looked at changes in ramus height, among other measures of bone growth and quality. They report that the CFA injection into the TMJ resulted in a decrease in ramus height after 4 weeks when compared with no TMJ injection. Their study also did not observe any condylar resorption, but rather an overall decrease in the size of the mandibles.[24] This could potentially be due to the short-term inflammationin this model and our model, and possibly more chronic inflammation is needed to observe any surface resorption and additional cartilage degradation. However, additional research is needed to understand how CIA increases the expression of MMP-13, resulting in an increase in chondrocyte hypertrophy, but a decrease in mandibular growth.In this study, we included one experimental group and two control groups. We did not expect to observe any differences between our control groups, but we did anticipate significant differences between our experimental group (CIA) and eitheror both control groups. As mentioned above, there were no differences in mandibular growth between the Saline group and Healthy group. This was expected because saline alone would not increase or decrease mandibular growth. Histologically, the CIA group showed evidence of an inflammatory response in the synovium, as well as multiple invaginations of the cartilage into the subchondral bone of the condyle, potentially demonstrating decreased integrity of the CIA cartilage. In addition, we observed increased hypertrophy of chondrocytes in the CIA group, and this was statistically significantly greater than that in the Saline control group. We did not observe much difference between the condylar cartilage in the Saline group and the Healthy group, which is expected. Immunohistochemically, we also observed differences between the CIA group and the two control groups, but there was not much difference to be demonstrated between the control groups.

The use of two control groups in this study was importantto determine any differences between these two types of control groups and to establish which group can be considered optimal for future studies with the CIA animal model. The Healthy group was maintained as a clean control group with no intervention (injection). The Saline group was our sham injection group and, as mentioned, only received saline injections. We included these two control groups to determine if there were any significant differences between a control group receiving no interventions and a control group receiving an injection of only the vehicle (saline) since the CIA group received TMJ injections of an emulsion of CFA and Col-II (which was dissolved in 0.09% saline). Our study demonstrates that there were no statistically significant differences between our control groups. However, we do recommend using a sham injection group (vehicle only) as a control group for studying TMJ CIA to account for any potential effect of slight tissue damage from the needle and introduction of a foreign substance (sterile saline).

Limitations

This study was constrained by some limitations that are important to highlight and discuss. Mandibular growth was considered to be only a one-way linear measurement of mandibular length when, in reality, the mandible does grow in all directions. However, the majority of such growth is due to increases in mandibular length, so we only included this measurement in this study. In addition, since it was anticipated that induced inflammation in the TMJ would likely only affect the condyle and therefore mandibular length, we did not consider other measures of growth, such as changes in mandibular ramus length/height and mandibular plane. Additionally, this study's analyses were completed by a single observer, therefore it is important to keep subjectivity in mind while determining the strength of such evidence in this study and other published studies.

Conclusion

In conclusion, our study has investigated part of the pathogenesis involved with CIA in juvenile rat TMJs. The CIA juvenile rat had significantly less growth of the lower jaw, increased proinflammatory cytokine expression in TMJ condylar cartilage, degenerative changes in cartilage, and evidence of TMJ inflammation. This animal model has the potential to be used in future studies investigating therapeutic effects of a drug/treatment on TMJ cartilage degeneration, TMJ inflammation, or mandibular growth disturbances. Understanding how a therapy may affect production of proinflammatory cytokines, individual cartilage components, or cartilage cell proliferation/maintenance/hypertrophy may provide new information. This new information could potentially be used for developing studiesfor either preventing damage or developmental disturbancesof the lower jaw caused by TMJ arthritis or for treating inflammation in the TMJ or stimulating any lower jawgrowth.

Authors' Contributions

J.C. designed and performed the experiments, collected and analyzed the data, and wrote the article. H.L. helped design the experiments, performed statistical analysis, and edited the article. M.K. helped analyze the data and edited the article. N.J. helped analyze the data and edited the article. P.F. helped design the experiments, helped analyze thedata, and edited the article. T.E.-B. helped design the experiments, analyzed data, edited the article, and supervised the project.

Disclosure Statement

No competing financial interests exist.

Funding Information

This research was supported by a Women and Children's Health Research Institute Innovation Grant and the School of Dentistry (University of Alberta) Fund for Dentistry.

References

1. Carrasco, R. Juvenile idiopathic arthritis overview and involvement of the temporomandibular joint—prevalence, systemic therapy. Oral Maxillofac Surg Clin North Am 27,1, 2015.
2. Mizoguchi, I., Toriya, N., and Nakao, Y. Growth of the mandible and biological characteristics of the mandibular condylar cartilage. Jpn Dent Sci Rev 49, 150, 2013.
3. Arabshahi, B., and Cron, R. Temporomandibular joint arthritis in juvenile idiopathic arthritis: the forgotten joint. Curr Opin Rheumatol 18, 490, 2006.
4. Bendele, A. Animal models of rheumatoid arthritis. J Musculoskelet Neuronal Interact 1, 377, 2001.
5. Phadke, K., Fouts, R., and Parrish, J. Collagen-induced andadjuvant-induced arthritis in rats. Arthritis Rheum 27, 797,1984.
6. McNamee, K., Williams, R., and Seed, M. Animal models of rheumatoid arthritis: how informative are they? Eur J Pharmacol 759, 278, 2015.
7. Liu, W., Xu, Z., Li, Z., Zhang, Y., and Han, B. RANKL, OPG and CTR mRNA expression in the temporomandibular joint in rheumatoid arthritis. Exp Ther Med 10, 895, 2015.
8. Brand, D., Latham, K., and Rosloniec, E. Collagen-induced arthritis. Nat Protoc 2, 1269, 2007.
9. Kartha, S., Zhou, T., Granquist, E., and Winkelstein, B. Development of a rat model of mechanically induced tunable pain and associated temporomandibular joint responses. J Oral Maxillofac Surg 74, 54e1, 2016.
10. Holmdahl, R., Bockermann, R., Bäcklund, J., and Yamada, H. The molecular pathogenesis of collagen-induced arthritis in mice—a model for rheumatoid arthritis. Ageing Res Rev 1, 135, 2002.
11. Moos, V., Fickert, S., Müller, B., Weber, U., and Sieper, J. Immunohistological analysis of cytokine expression in human osteoarthritic and healthy cartilage. J Rheumatol 26,870, 1999.
12. Lim, W., Toothman, J., Miller, J., *et al.* IL-1b inhibits TGFb in the temporomandibular joint. J Dent Res 88, 557, 2009.
13. Delatte, M., Von den Hoff, J., van Rheden, R., and Kuijpers-Jagtman, A. Primary and secondary cartilages of the neonatal rat: the femoral head and the mandibular condyle. Eur J Oral Sci 112, 156, 2004.
14. Kinne, R., Bräuer, R., Stuhlmüller, B., Palombo-Kinne, E., and Burmester, G. Macrophages in rheumatoid arthritis. Arthritis Res 2, 189, 2000.
15. Rose, B., and Kooyman, D. A tale of two joint: the role of matrix metalloproteases in cartilage biology. Dis Markers 2016, 1, 2016.
16. Aref-Eshghi, E., Liu, M., Harper, P., *et al.* Overexpression of MMP13 in human osteoarthritic cartilage is associated with the SMAd-independent TGF-b signalling pathway. Arthritis Res Ther 17, 1, 2015.
17. Li, H., Wang, D., Yuan, Y., and Min, J. New insights on the MMP-13 regulatory network in the pathogenesis of early osteoarthritis. Arthritis Res Ther 19, 1, 2017.
18. Wojdasiewicz, P., Poniatowski, Ł., and Szukiewicz, D. The role of inflammatory and anti-inflammatory cytokines in the pathogenesis of osteoarthritis. Mediators Inflamm 2014,1, 2014.
19. Ahmed, N., Ptersson, A., Irinel Catrina, A., Mustafa, H., and Alstergren, P. Tumor necrosis factor mediates tempo- romandibular joint bone tissue resorption in rheumatoid arthritis. Acta Odontol Scand 73, 232, 2015.
20. Wu, G., Zhu, S., Sun, X., and Hu, J. Subchondral bone changes and chondrogenic capacity of progenitor cells fromsubchondral bone in the collagenase-induced temporo- mandibular joints osteoarthritis rabbit model. Int J Clin ExpPathol 8, 9782, 2015.
21. Wang, X., Kou, X., He, D., *et al.* Progression of cartilage degradation, bone resorption and pain in rat temporoman- dibular joint osteoarthritis induced by injection of iodoa- cetate. PLoS One 7, 1, 2012.
22. Melo, R., D'Avila, H., Wan, H., Bozza, P., Dvorak, A., and Weller, P. Lipid bodies in inflammatory cells: structure, function, and current imaging techniques. J HistochemCytochem 59, 540, 2011.
23. D'Angelo, M., Yan, Z., Nooreyazdan, M., *et al.* MMP-13 is induced during chondrocyte hypertrophy. J Cell Biochem 77, 678, 2000.
24. Holwegner, C., Reinhardt, A., Schmid, M., Marx, D., and Reinhardt, R. Impact of local steroid or statin treatment of experimental temporomandibular joint arthritis on bone growth in young rats. Am J Orthod Dentofacial Orthop 147,80, 2015.

Address correspondence to:
Jacqueline Crossman, MSc7-020 Katz Centre for Pharmacy and Health Research
University of AlbertaEdmonton T6G 2E1
AlbertaCanada

E-mail: jcrossma@ualberta.ca

Received: October 1, 2020
Accepted: December 17, 2020
Online Publication Date: February 9, 2021

CHAPTER 4: THE EFFECT OF LOW INTENSITY PULSED ULTRASOUND ON TMJ ARTHRITIS IN JUVENILE RATS

4.1 Abstract

Juvenile idiopathic arthritis (JIA) is an inflammatory disease that can affect the temporomandibular joint (TMJ), causing growth disturbances of the lower jaw (mandible). Current treatment options for TMJ-JIA and the associated growth defects involve a combined use of medications that target inflammation, orthodontic intervention, and surgeries. These medications are unsatisfactory due their ineffectiveness in many patients, there are no options that have been shown to stimulate mandibular growth, and surgery is risky, painful, and costly. Our study considered investigating the effect of low intensity pulsed ultrasound (LIPUS), a type of therapeutic ultrasound, on TMJ arthritis. LIPUS has been studied for its effect on osteoblasts, chondrocytes, and synovial cells which are the main cell types of the TMJ. LIPUS has been demonstrated to have an anti-inflammatory effect on arthritis in animal models of rheumatoid arthritis and can stimulate mandibular growth.

To study the effect of LIPUS on TMJ arthritis we used the collagen-induced arthritis (CIA) juvenile rat model. Seventy-two 3-week old male Wistar rats were obtained for this study. All rats were micro-computed tomography (MicroCT) scanned and divided into 8 groups (n=9). Four groups received CIA injections into their TMJs, and 4 groups received saline (sham) injections into their TMJs. LIPUS groups received LIPUS treatment (under isoflurane anesthesia) to their TMJs either immediately after the TMJ injections, or after 4 weeks after the TMJ injections were completed. LIPUS treatment was applied for 20 minutes/day for 4 weeks. Saline groups were used as a control to the CIA and these groups received only TMJ injections saline. To control for LIPUS treatment, groups that received only isoflurane anesthesia were included. After the 4-week treatments were finished, all rats were euthanized and whole blood

was collected for serum and plasma analysis. *Ex vivo* MicroCT scanning was completed and tissues were prepared for histological and immunohistochemical analyses.

Using H&E-stained histological sections, we observed synovitis in the CIA TMJs but the severity of the synovitis appeared to be greater in the TMJs that did not received any LIPUS treatment. Next, we used histomorphometric analysis to measure cartilage thickness. The thickness of the fibrocartilage and hypertrophic cell layer in the CIA group that had immediate isoflurane only was significantly thicker ($p < 0.05$). Toluidine blue staining was used to stain proteoglycans in the cartilage and this staining appeared greater in the groups that received LIPUS treatment. We observed various results in our immunohistochemical staining. Immediate LIPUS increased the expression of type II collagen, type X collagen, and TGF-β1, and CIA (no LIPUS) increased MMP-13, VEGF and IL-1β immunostaining. LIPUS treatment prevented growth disturbances that were observed in the CIA groups without LIPUS treatment ($p < 0.005$). Our results have provided additional information for understanding this animal model of arthritis, its uses and limitations, as well as providing more understanding of LIPUS and its effects on the TMJ and mandibular growth. This study's results will help in designing additional studies to further investigate LIPUS and TMJ arthritis, toward potentially developing a new treatment option for children with juvenile arthritis in their TMJs.

4.2 *Introduction*

Juvenile idiopathic arthritis (JIA) is an autoimmune, inflammatory disease that has similarities to rheumatoid arthritis (RA), but JIA affects the juvenile population [Prahalad & Glass, 2002]. In 2015, it was estimated that JIA affected about 150,000 children in North America [Carrasco,

2015]. According to Statistics Canada, as of 2017, approximately 6,200 children (ages 15 years and younger) had JIA. JIA can involve multiple joints of the body, including the temporomandibular joint (TMJ) [Carrasco, 2015]. Although the TMJ is less affected by JIA than other joints, it was reported that 62% of 169 patient with JIA had TMJ involvement [Pedersen et al., 2001]. Studying the involvement of and the effect on the TMJ by JIA is important because inflammation in this joint during growth and development can have a significant impact on preventing normal mandibular growth, causing micrognathia, dental malocclusion, and irreversible damage like condylar resorption and erosion [Pedersen et al., 2001]. This happens due to joint synovitis, pannus tissue, condylar head flattening, bone erosions, and damage to articular cartilage, where the majority of mandibular growth occurs [Carrasco, 2015; Mizoguchi, Toriya & Nakao, 2013]. Cellular changes, such as chondrocyte proliferation, extracellular matrix (ECM) production, and chondrocyte hypertrophy occur within this articular cartilage on the mandibular condyle, resulting in mandibular growth lengthwise [Mizoguchi, Toriya & Nakao, 2013]. Since inflamed joint tissues contain activated macrophages that are involved in the progression of joint destruction in arthritis due to their increased production of pro-inflammatory cytokines such as TNF-α, IL-1β, and IL-17, treatments that can decrease inflammation due to these factors could have a positive effect on managing this inflammatory disease in children [Kinne et al., 2000]. Additionally, a treatment that could not only mitigate TMJ inflammation but also stimulate normal mandibular growth, since this growth can be compromised during TMJ-JIA, is especially needed to effectively treat these patients. Current clinical treatment of TMJ-JIA and the associated growth defects combine a variety of medications used to target these pro-inflammatory cytokines, as well as orthodontic intervention and surgeries. However, these medications are unsatisfactory because they are generally ineffective, either immediately or in

the long-term, for many JIA patients, and none of these treatments have been shown to stimulate mandibular growth in order to rescue it to normalcy. As well, surgery is risky and painful, and can be costly to both the patients and their families, as well as the healthcare system [Carrasco, 2015].

To study human diseases, like RA and JIA, and to evaluate the efficacy of drugs to be used clinically, animal models of those specific diseases are utilized. Choosing appropriate models of disease can be challenging since the animal tissue must be morphologically and physiologically similar to human tissue, and similar pathology of the disease, either many aspects or at least one aspect of it, must be present and characterized. When this occurs, the animal model may be clinically relevant to predict the efficacy of therapeutic interventions in humans [Bendele, 2001]. The collagen-induced arthritis (CIA) juvenile rat model of TMJ arthritis has been previously studied by other groups as well as our own lab [Liu et al., 2015; Crossman et al., 2021]. This CIA rat model has been reported to have an increased RANKL:OPG (osteoprotegerin) expression ratio which indicates the differentiation of osteoclasts, the bone-resorbing cells that cause bone damage. Additionally, serum levels of the pro-inflammatory cytokines IL-1β and TNF-α, were increased in this animal model, and histological analyses showed evidence of synovitis, inflammatory cell infiltration, and cartilage and bone destruction [Liu et al., 2015]. Our previous study demonstrated how this CIA rat model had significantly less mandibular growth, increased expression of pro-inflammatory cytokines in the TMJ condylar cartilage, degenerative changes in the cartilage, and evidence of TMJ inflammation [Crossman et al., 2021].

Using this juvenile animal model of TMJ arthritis, our study aimed to investigate the effect of a type of therapeutic ultrasound on TMJ arthritis. This therapeutic ultrasound is called

low intensity pulsed ultrasound (LIPUS). LIPUS has been extensively studied for its effect on osteoblasts, chondrocytes and synovial cells, as well as its effect on their intracellular signaling pathways, helping to understand the mechanism how LIPUS affects these cells [Tang et al., 2006; Li et al., 2003; Iwabuchi et al., 2014; Sekino et al., 2018; Sato et al., 2014; Nakamura et al., 2011]. LIPUS has been demonstrated to have a treatment effect on synovitis in a mouse model of RA and on arthritis in a rabbit model of osteoarthritis (OA) [Nakamura et al., 2011; Li et al., 2011]. Additionally, LIPUS has been shown to stimulate mandibular growth in growing rats [Kaur et al., 2015; Oyonarte et al., 2009]. The effect of LIPUS has been investigated in growing rats in TMJ-OA but this study only evaluated the gene expression profile [He et al., 2018]. Another study evaluated how LIPUS may treat TMJ-OA in adult (non-growing) rats and reported that LIPUS increased chondrocyte cell number and decreased the expression of matrix metalloproteinase (MMP)-13, a collagenase that degrades collagen in the articular cartilage, which is characteristic of OA [Arita et al., 2017]. As well, our lab's pilot study using an adult mouse model of RA showed how LIPUS significantly increased mandibular height in this RA mouse model and upregulated the expression of type II collagen (Col-II) and vascular endothelial growth factor (VEGF), demonstrating how LIPUS can positively affect mandibular growth during arthritis by potentially preventing these growth disturbances due to joint inflammation [Crossman et al., 2019]. Although these studies may indicate that LIPUS has potential in treating TMJ arthritis and stimulating mandibular growth, none of them investigated the effect of LIPUS on TMJ arthritis in a growing, juvenile rat model of arthritis, such the CIA juvenile rat. Therefore, this study aimed to evaluate this effect. We hypothesized that LIPUS would have an anti-inflammatory effect on TMJ-CIA and that LIPUS would stimulate mandibular growth.

4.3 *Materials and Methods*

4.3.1 *Animals and Study Design*

Our research was approved by the animal ethics committee at the University of Alberta [AUP00002169]. The sample size was calculated to be n=7 (5% type I error, 80% power, 1.77 effect size), but to account for any potential mortality prior to the planned endpoint of the study and non-development of CIA in the TMJ, we used n=9. We calculated this sample size based on the data from our previous study [Crossman et al., 2021]. First, we acclimatized 72 three-week old male Wistar IGS rats (Strain Code 003, Charles River Laboratories). These rats were divided into 8 equal groups as described in Table 1 (below).

Table 4.1: Group allocation including 8 described groups (n=9) receiving either CIA or Saline TMJ injections and LIPUS or no LIPUS treatment (isoflurane only) for 20 minutes/day.

Groups (n=9)	**TMJ Injection**	**LIPUS (20 min/day)**
1 *(CIA + immediate LIPUS 4 weeks)*	CIA	Yes
2 *(Saline + immediate LIPUS 4 weeks)*	Saline	Yes
3 *(CIA + immediate isoflurane only 4 weeks)*	CIA	No
4 *(Saline + immediate isoflurane only 4 weeks)*	Saline	No
5 *(CIA + delayed LIPUS 4 weeks)*	CIA	Yes
6 *(Saline + delayed LIPUS 4 weeks)*	Saline	Yes
7 *(CIA + delayed isoflurane only 4 weeks)*	CIA	No
8 *(Saline + delayed isoflurane only 4 weeks)*	Saline	No

4.3.2 *Body Weights, Head Widths and MicroCT Scanning*

We weighed each rat and measured each rat's head width prior to performing *in vivo* micro-computed tomography (MicroCT) scanning of each rat under anesthesia (isoflurane) (MILabs, 0.19 mA tube current, 55 kV tube voltage, 960 steps, 0.3 degrees/second, 75 milliseconds

exposure time, 40 μm or 18 μm reconstruction resolution) before intervention. For the CIA groups, 100 μg of bovine type II collagen (Col-II) (Chondrex, Inc.) dissolved in 50 μL of 0.09% sterile saline and emulsified with equal volume Complete Freund's Adjuvant (Sigma Aldrich) (contains heat-killed *Mycobacterium tuberculosis*), totalling 100 μL in volume, was injected into the TMJ area (both right and left) according to previously published protocol [Liu et al., 2015; Brand Latham & Rosloniec, 2007]. For the Saline groups, 100 μL of 0.09% saline only was injected into the TMJ area (right and left).

Body weights and head widths were measured on days 1-7, 11, 14 and 21 (day 1 = day after TMJ injections) for groups 1-4 (immediate treatment), and for groups 5-8 (delayed treatment), on days 1-6, 8, 14, and 22 (after injections [day 1 = day after TMJ injections] and before delayed treatment) and days 1, 7, 14 and 21 (day 1 = first day of LIPUS/isoflurane). The rats in the immediate LIPUS/isoflurane groups received either LIPUS (under isoflurane inhalant anesthesia) or isoflurane only for 20 minutes/day for 28 consecutive days (4 weeks) with Day 1 of treatment beginning the next day after TMJ injections were administered (Figure 4.1). The rats in the delayed LIPUS/isoflurane groups received either LIPUS or isoflurane only for 20 minutes/day for 4 weeks as well, however, their treatment began exactly 28 days after the TMJ injections were administered.

Figure 4.1: Photographic example of a rat receiving LIPUS treatment to right and left TMJs under isoflurane anesthesia. LIPUS transducers with ultrasound coupling gel were applied to shaved TMJ areas.

4.3.3 *Histology and Immunohistochemistry*

After LIPUS or isoflurane treatments for 4 weeks, the rats were euthanized with CO_2. Whole blood was collected for serum/plasma analysis, *ex vivo* MicroCT scanning was performed, and then the TMJ tissues (randomly chosen right or left TMJs) were prepared for histological and immunohistochemical analyses. The remaining TMJs not used for these analyses were stored in 1X PBS to be used in articular disc analysis. TMJs were sectioned at a 7-μm thickness in the sagittal plane.

H&E staining was performed for qualitative observation of cartilage cell layer morphology, any pannus tissue formation and synovitis in the synovial membrane. These stained sections were also used to measure cartilage cell layer thicknesses. The thickness of each cartilage cell layer (fibrocartilage, proliferative cell layer, chondrogenic [mature] cell layer, and

hypertrophic cell layer) was measured. To accomplish this, three equidistant length measurements of each cell layer were completed. These were performed perpendicular to the condylar surface on both the anterior and posterior sides of the central axis. One measurement at the central axis was performed. A total of seven measurements were taken per condyle which were then averaged to obtain a mean thickness for each cell layer of each condyle [Crossman et al., 2021] (Figure 4.2).

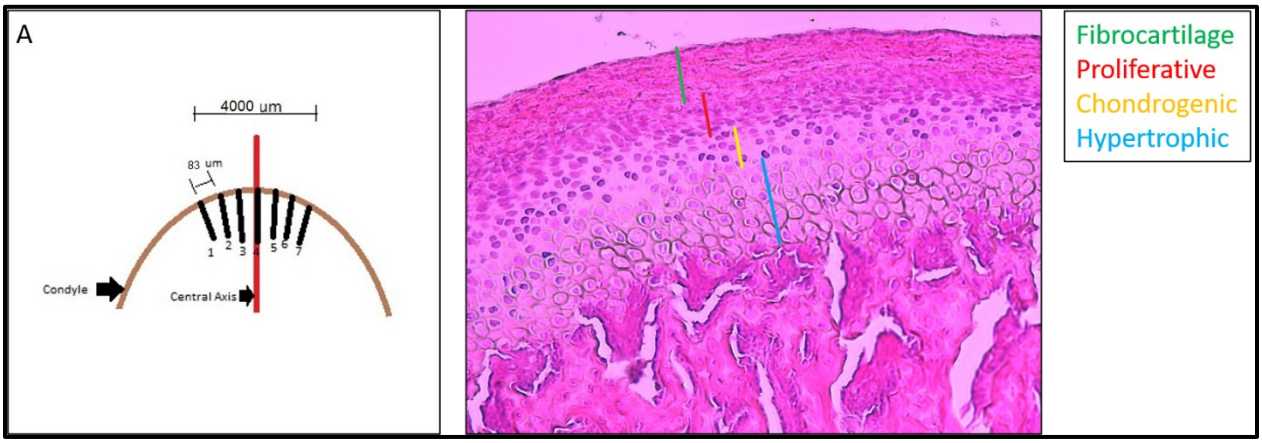

Figure 4.2: Illustration demonstrating how the thickness of fibrocartilage, proliferative, chondrogenic and hypertrophic cell layers were measured at 7 points on the mandibular condylar cartilage [Crossman et al., 2021].

Next, the TMJs were stained with toluidine blue (T.B.) to determine any proteoglycan changes in the cartilage matrix. Immunohistochemistry was performed for immunostaining of the following: Col-II, Col-X, MMP-13, receptor activator of NF-κB ligand (RANKL), VEGF, transforming growth factor (TGF)-β1, IL-1β, IL-17, and TNF-α. In brief, after deparaffinization and rehydration, antigen retrieval was performed using protease XXV (all slides except Col-X,

30 minutes at room temperature, 1 mg/mL) or pepsin (Col-X slides only, 10 minutes at 37 degrees Celsius, 0.25% pepsin in TBS) and then bovine testicular hyaluronidase (for Col-II and Col-X slides only) for 30 minutes at 37 degrees Celsius. Next, peroxidase blocking was completed using 3% H_2O_2 solution applied to slides for 10 minutes at room temperature, and protein blocking was performed using 5% normal goat serum in 1X PBS with 0.3% Tween-20 (10 minutes at room temperature). Primary antibodies were applied to the slides for overnight incubation at 4 degrees Celsius (Col-II – 1:500, Abcam, Cambridge, Massachusetts, USA; Col-X – 1:50, Thermo Fisher Scientific, California, USA; MMP-13 – 1:1000, Abcam; RANKL – 1:50, Santa Cruz Biotechnology, Dallas, Texas, USA; VEGF – 1:500, Santa Cruz; TGF-β1 – 1:50, Santa Cruz; IL-1β – 1:25, Santa Cruz; IL-17 – 1:50, Santa Cruz; and TNF-α – 1:1,000, Santa Cruz) (only TBS [diluent] was applied to negative control slides). Appropriate HRP-conjugated secondary antibodies were applied the next day for 15 minutes, followed by DAB chromogen and substrate application for 10 minutes. Counterstaining was completed with hematoxylin. Dehydration was performed by immersion into ethanol baths increasing in percent ethanol up to 100%, and then the slides were cover-slipped in preparation for analysis.

4.3.4 *Enzyme-linked Immunosorbent Assays (ELISAs)*

To quantitatively measure the protein levels of IL-1β and TNF-α in blood serum, IL-1β and IL-6 in the articular disc, and TGF-β1 (2 forms: bound to LAP [latency associated peptide] [inactive form] and dissociated from LAP [active form]) in blood plasma, we obtained appropriate ELISA kits (Invitrogen, Thermo Fisher Scientific, California, USA] and performed these assays according to the manufacturer's procedures and protocols. Whole articular discs were dissected from each TMJ that was stored in 1X PBS, representing 1 TMJ/rat. Each disc was homogenized

in 1 mL of 1X PBS using a mortar and pestle kept on ice. The articular disc homogenate underwent 2 freeze-thaw cycles in order to further disrupt cell membranes prior to being centrifuged and the supernatant collect to be used in the IL-1β and IL-6 ELISAs.

4.3.5 *MicroCT Analysis*

MicroCT analysis was used to evaluate mandibular and condylar growth using the software Imalytics Preclinical 2.1 (Gremse-IT GmbH, Acchen, Germany). After correcting the voxel size according to the MicroCT scan reconstruction voxel size, 3D rendering was used to create 3D models to measure mandibular length and condylar volume (Figure 4.3). Threshold adjustments and automatic segmentation were performed to segment each hemimandible. Markers were placed at the condylar point and the menton point, and the distance between these two points were automatically calculated to measure mandibular length. Mandibular growth per hemimandible was calculated by subtracting the measured mandibular length in the *in vivo* scan from that in the *ex vivo* scan. To measure condylar volume, a virtual line was drawn on the 3D model from each notch superior and inferior to the condyle and single, straight virtual cut was made along this line. Automatic segmentation was used to automatically segregate the condyle from the rest of the mandible [Figure 4.3] and the volume of the condyle was automatically calculated with this software. Condylar growth in volume per hemimandible was calculated by subtracting the calculated condylar volume in the *in vivo* scan from that in the *ex vivo* scan.

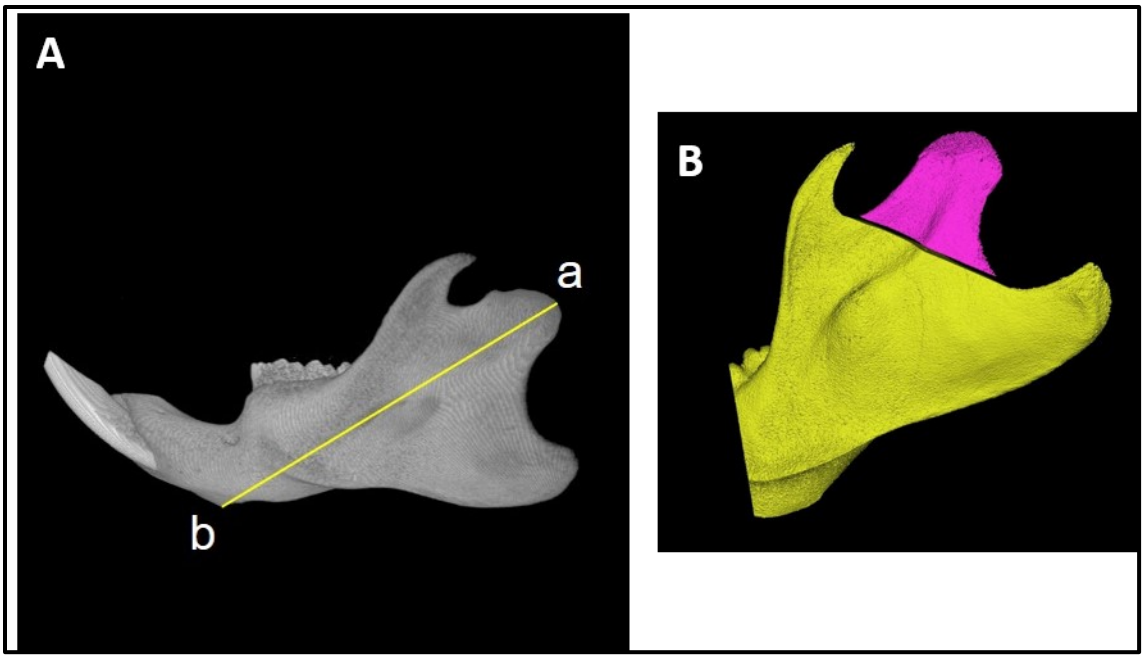

Figure 4.3: Illustration demonstrating how mandibular length (A) was performed and how the mandibular condyle (pink) was segmented from the mandible (yellow) to calculate condylar volume [B]. a = condylar point, b = menton point.

4.3.6 *Statistical Analysis*

Statistical analysis was performed using SPSS 16. Statistical significance was tested using a univariate analysis of variance (ANOVA) with an alpha of 0.05 to first determine any significant interaction of 3 factors with 2 levels each [1) CIA vs. Saline, 2) Immediate vs. delayed, 3) LIPUS vs. Isoflurane only]. When there were significant interactions, then a post hoc Tukey test was used to determine which groups were significantly different from another. The data obtained from the TGF-β1 ELISA required conversion from continuous data to ordinal data due to numerous results showing 'zero' protein levels (discussed in discussion section). If TGF-β1 plasma levels were 0-9 ng/mL, then they were categorized as a level of '1'. If the levels were 10-

19 ng/mL, then they were categorized as a level of '2'. This continued to encompass and recode all measured levels of TGF-β1. To statistically analyze this data, we used a Kruskal-Wallis H test to compare between groups.

4.4 *Results*

In this study we measured head width changes (Figure 4.4) and changes in body weight (Figure 4.5) throughout the duration of the study, decreasing the frequency of these measurements as time from initial injections increased. We performed these measurements for multiple reasons. Observing an initial increase in head width immediately after TMJ injections, especially those in the CIA groups, helped to confirm an initial response in the TMJ to these injections. The increase in head width in the Saline+Immediate LIPUS/isoflurane groups were generally less compared the CIA+Immediate LIPUS/isoflurane groups as observed in the pattern of head width increases in Figure 4.4. The increase in head width remained elevated in the CIA+Immediate isoflurane group, and the increase in head width in the CIA+Immediate LIPUS group appeared to begin following the pattern of the Saline groups after the first week after the TMJ injections. The head width increases in the groups that received delayed LIPUS/isoflurane generally followed a similar pattern to each other throughout the duration of the study.

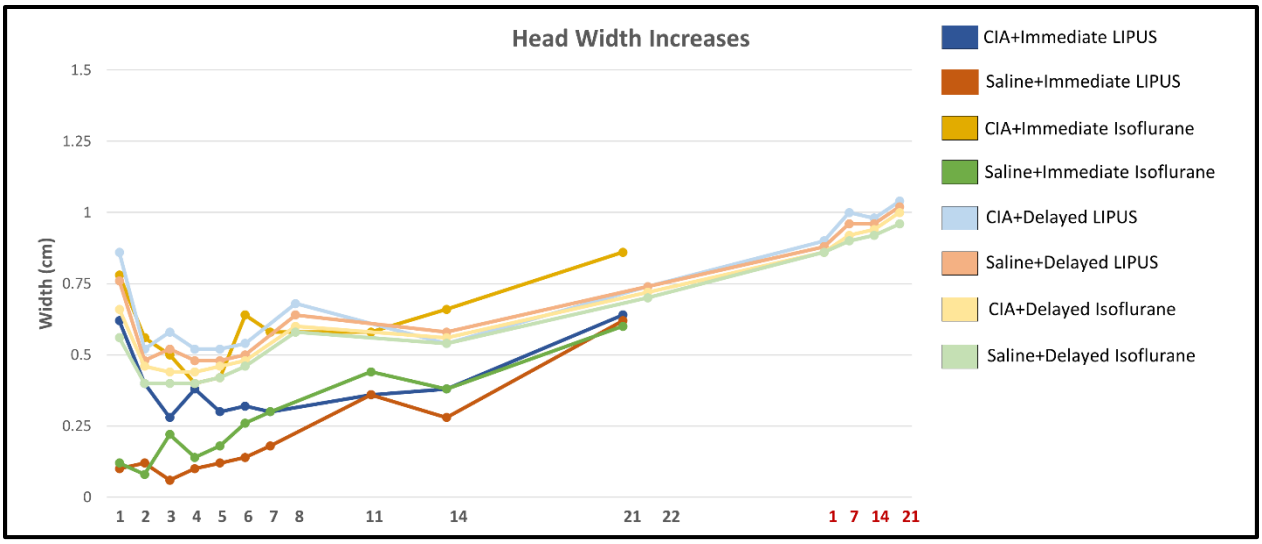

Figure 4.4: Head width increases compared to baseline (pre-injection) head widths in each group through the study at the indicated days. Days 1-22 (black) began the day after TMJ inections. Days 1-21 (red) were days 1-21 of delayed LIPUS/isoflurane treatment.

Body weights were measured throughout the study in order to monitor animal welfare and health, as well as to monitor whether or not any discomfort caused by CIA TMJ injections would result in decreased food consumption in the rats, which would be evident as a decrease in body weight or a slower progression of body weight increases. The body weight increases in each group were very similar to one another [Figure 4.5].

Figure 4.5: Body weight increases from each group throughout the study and are shown as a percent increase from their weights pre-injection.

Histological slides were H&E stained in order to qualitatively observe any inflammatory evidence within the TMJ. Figure 4.6 shows representative TMJ sections from each group. Comparing tissue sections to those in the Saline+Immediate/delayed isoflurane groups aids in observing any histological changes due to CIA and/or LIPUS interventions because the Saline+Immediate/delayed isoflurane groups can be representative of 'negative controls' since there are no expected effects of saline or isoflurane only on the TMJ. In all of the TMJ sections in groups with the CIA injections, synovitis was observed, as indicated by the red arrows in Figure 4.6. Synovitis appeared to decrease over time as shown in the groups with delayed treatment, but synovitis was greatest in the CIA groups that did not receive any LIPUS treatment, especially in the CIA+Immediate Isoflurane group as shown.

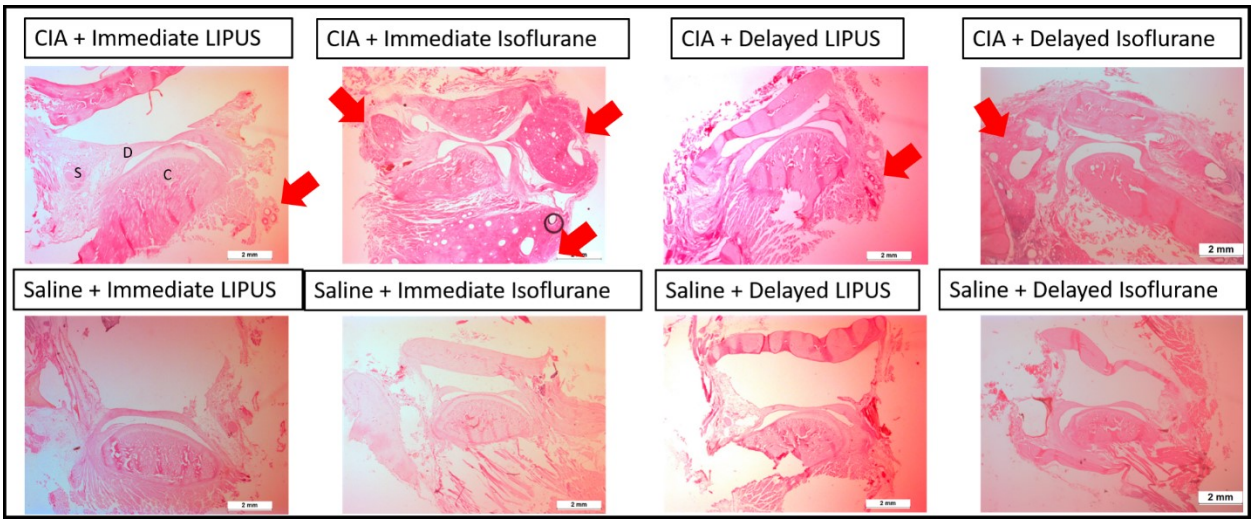

Figure 4.6: Representative photomicrographs of H&E-stained histological sections of the TMJ from each group. Scale bar = 2 mm.

Next in Figure 4.7, we can observe any cartilage changes in representative sections at a high magnification. The layers of chondrocytes in the CIA+Immediate Isoflurane group have a more disorganized appearance, with less obvious stratification, and appear to have an increased thickness. The thinnest cartilage appears to be represented in the older rats (delayed treatment), especially in the groups without any LIPUS treatment.

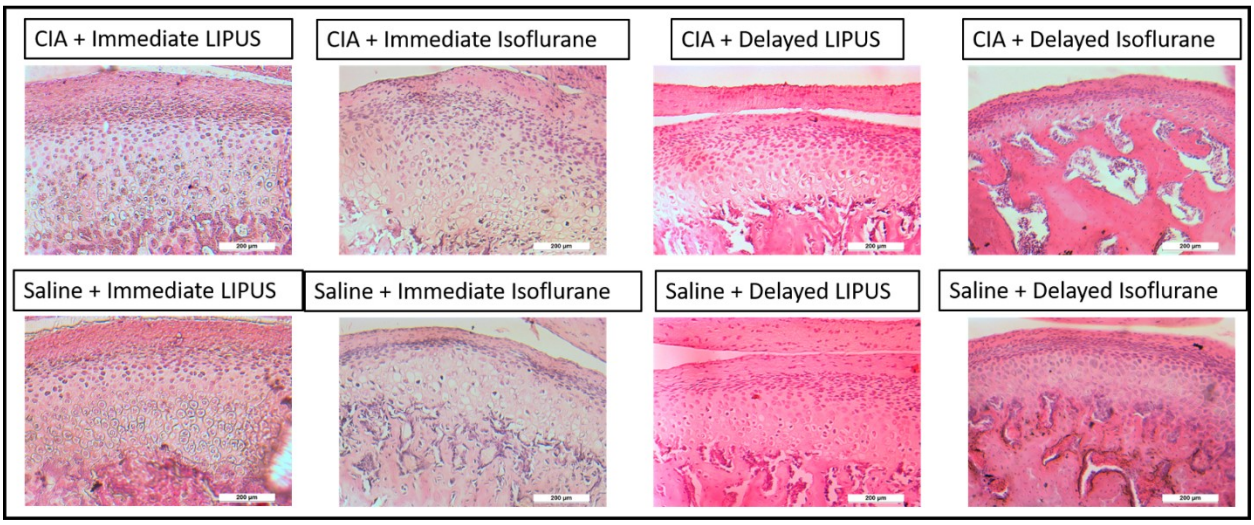

Figure 4.7: Representative photomicrographs of H&E-stained histological sections of TMJ condylar cartilage from each group. Scale bar = 200 μm.

Using the H&E-stained TMJ sections, the thickness of each cartilage cell layer (fibrocartilage, proliferative, chondrogenic, hypertrophic) was measured (Figure 4.8). The fibrocartilage in the CIA+Immediate Isoflurane group was significantly thicker compared the Saline+Immediate Isoflurane group [$F(7,51) = 3.170$, $p = 0.007$]. As well, the hypertrophic cell layer in the CIA+Immediate Isoflurane group was significantly thicker compared to each of the other groups that received immediate treatment [$F(7,51) = 8.726$, $p < 0.005$].

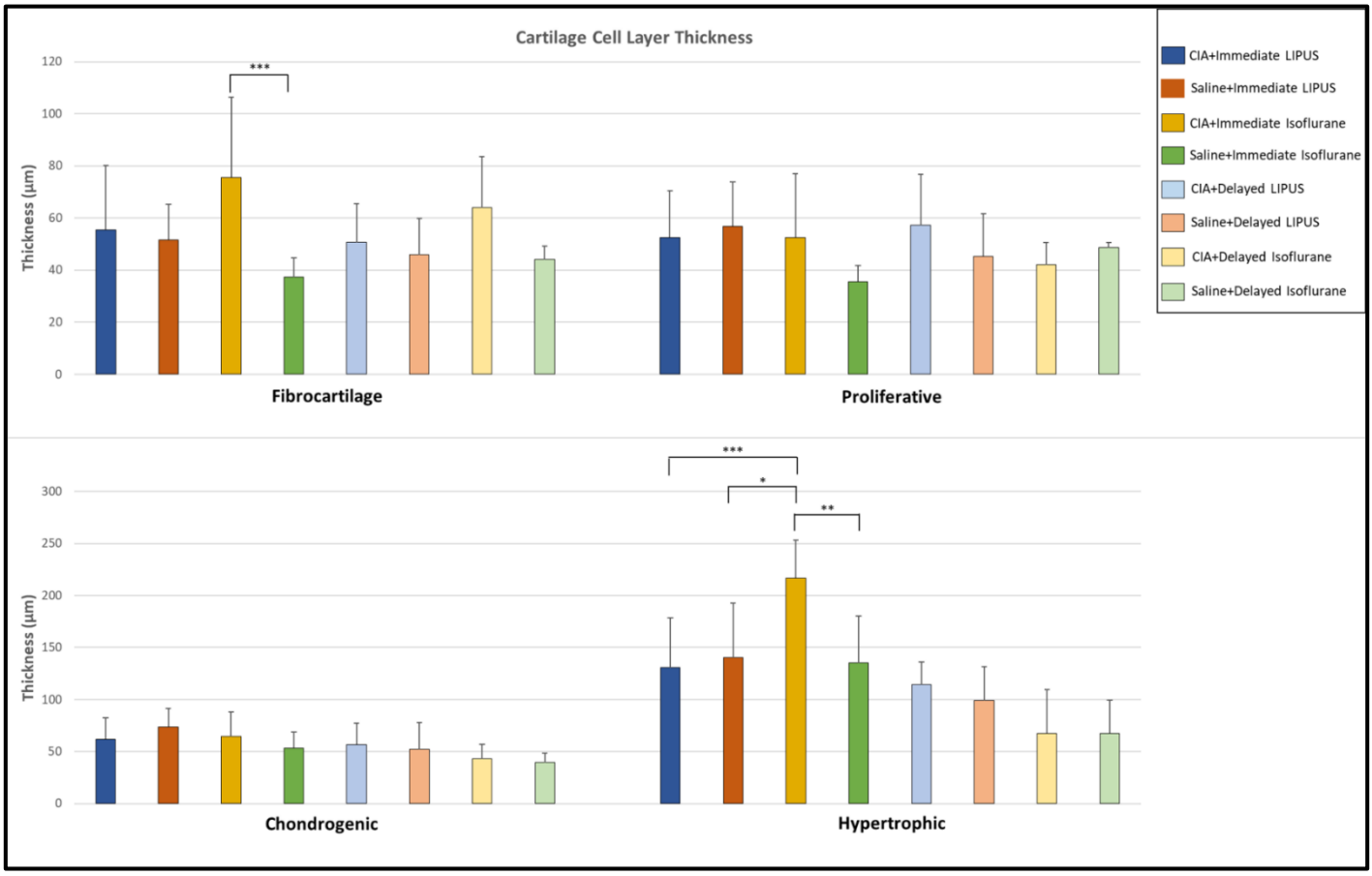

Figure 4.8: The cartilage cell layer (fibrocartilage, proliferative, chondrogenic, hypertrophic) thicknesses in each group. Data is represented as the mean ± S.D. * = $p < 0.05$, ** = $p < 0.01$, *** = $p < 0.005$

Toluidine blue (T.B.) staining, as shown in Figure 4.9, is used to observe proteoglycan production in the ECM in the cartilage. The amount of T.B. staining is directly proportional to the amount of proteoglycan present in the tissue. In these representative photomicrographs there may be an increase in proteoglycans in the ECM in the immediate LIPUS groups compared to the immediate isoflurane groups. Proteoglycan production appears to decrease over time in the delayed treatment groups, but still appears to remain increased in the delayed LIPUS groups compared to the delayed isoflurane groups.

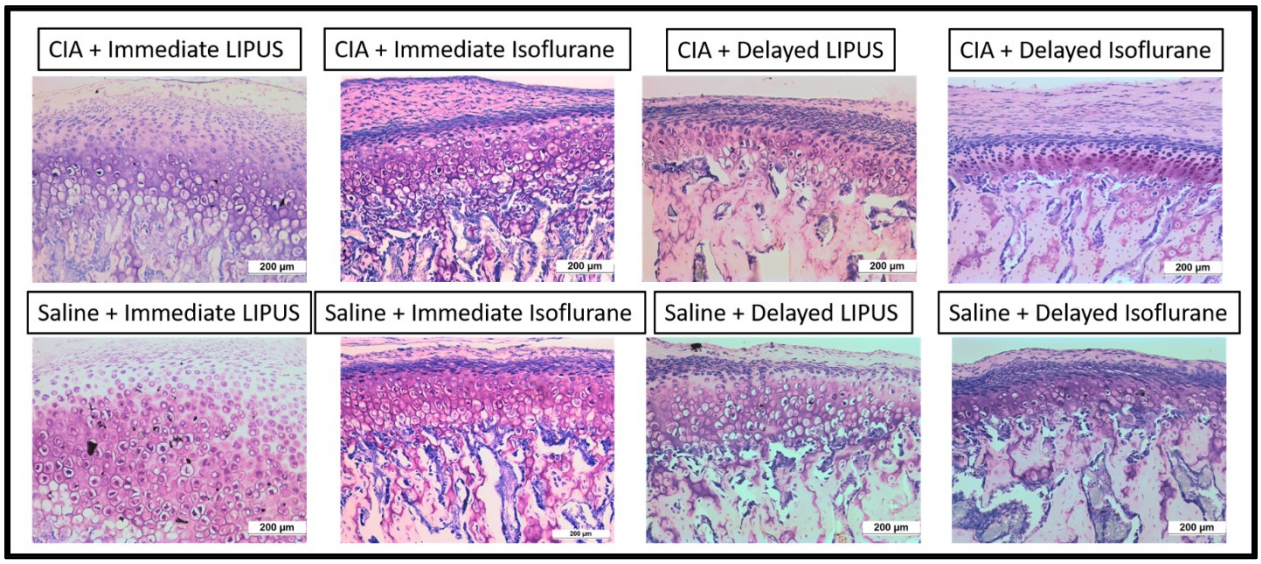

Figure 4.9: Representative photomicrographs of T.B.-stained histological sections of TMJ cartilage from each group. Scale bar = 200 µm.

Next, immunohistochemistry was performed for Col-II, Col-X, and MMP-13. Col-II is a main type of collagen for immunostaining in TMJ cartilage and is produced by mature chondrocytes in the chondrogenic layer. The expression of Col-II appears to be greater in the LIPUS groups compared to the isoflurane groups and in the CIA groups compared to the Saline groups (Figure 4.10A). The expression of Col-X was minimal in these cartilage sections and was almost absent in the TMJ sections in the delayed treatment groups (Figure 4.10B). Col-X is mainly expressed by hypertrophic chondrocytes, especially during growth. Groups that received immediate LIPUS treatment had greater Col-X expression compared to the other groups. Figure 4.10C shows representative immunostaining for MMP-13 which is a collagenase that degrades

collagen, especially Col-II. The expression of MMP-13 appears to be greater in the CIA groups, and greatest in CIA groups without LIPUS treatment.

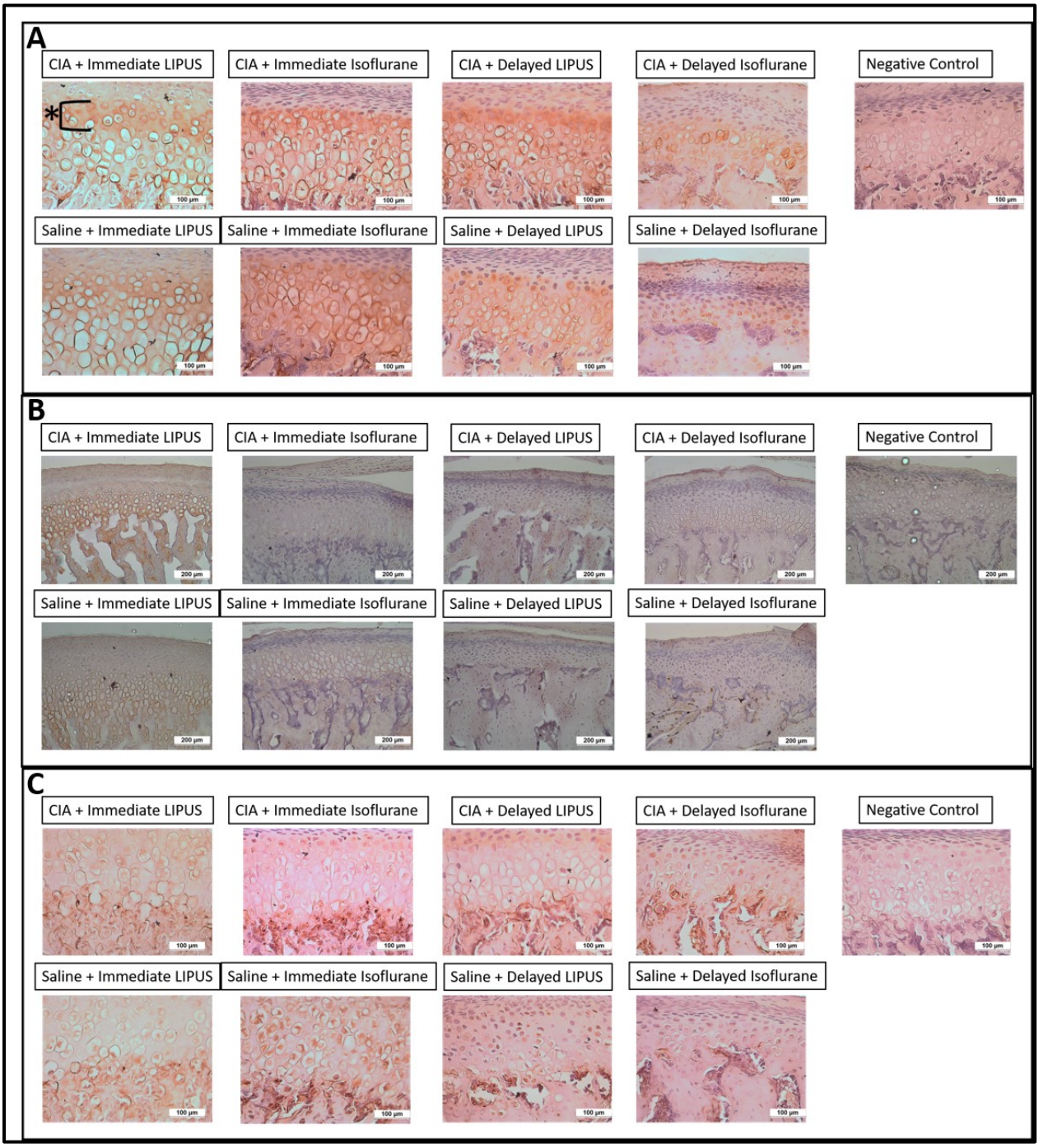

Figure 4.10: Photomicrographs representing immunohistochemically-stained TMJ cartilage from each group. A) Col-II, B) Col-X, C) MMP-13. Scale bar = 100 µm (A, C), 200 µm (B).

Next, we immunohistochemically stained the TMJ cartilage for RANKL, VEGF, and TGF-β1. The expression of RANKL was minimal across each group (Figure 4.11A). VEGF expression was increased in the immediate isoflurane groups compared to the immediate LIPUS groups, and this expression remained increased in the CIA groups with delayed treatment (Figure 4.11B). TGF-β1 expression appears to be greatest in the CIA and Saline groups with immediate LIPUS treatment and appeared to be decreased in the CIA group with immediate isoflurane (Figure 4.11C). Again, groups with delayed LIPUS treatment appeared to have increased TGF-β1 expression compared to those with delayed isoflurane.

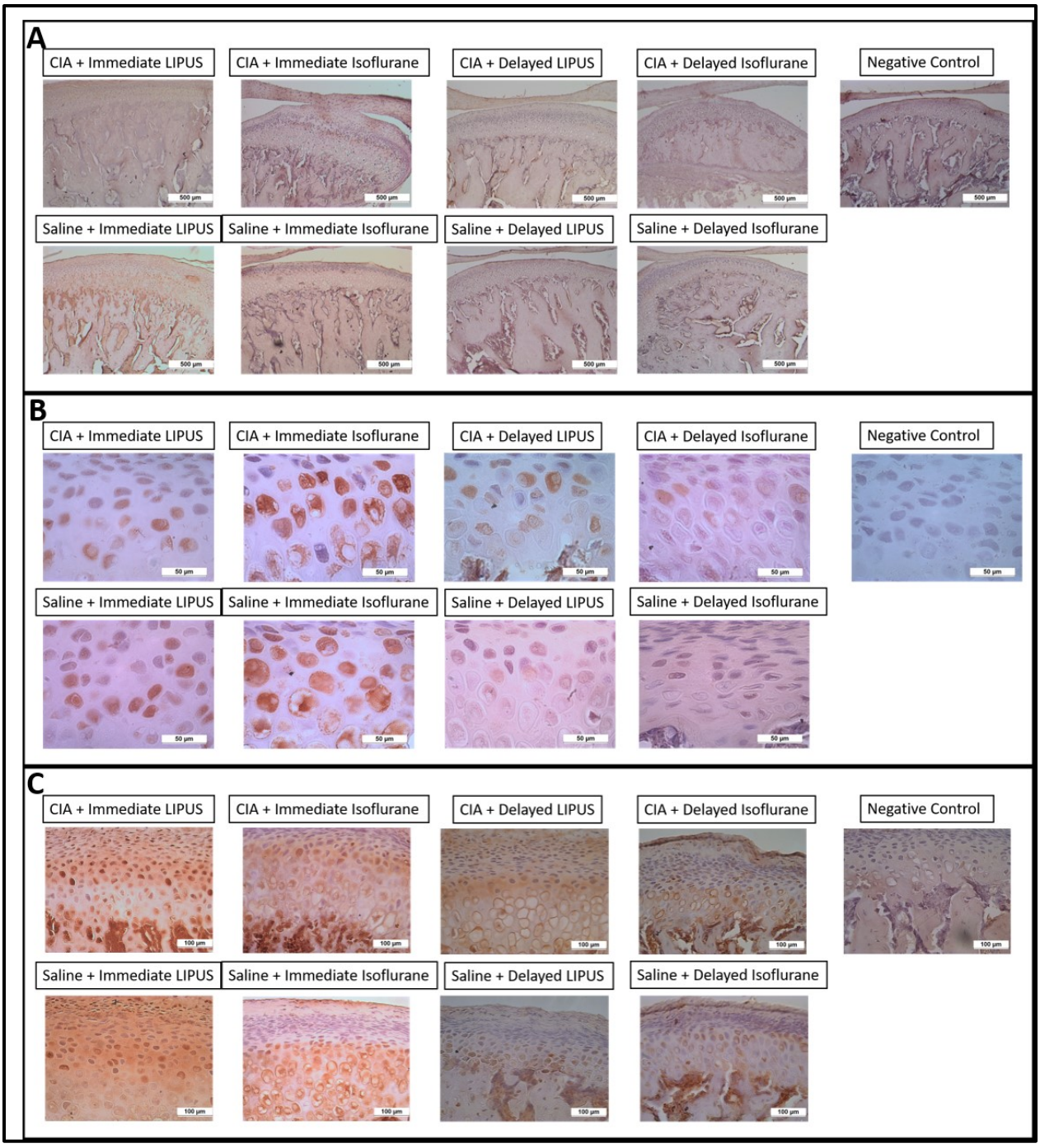

Figure 4.11: Photomicrographs representing immunohistochemically-stained TMJ cartilage from each group. A) RANKL, B) VEGF, C) TGF-β1. Scale bar = 500 µm (A), 50 µm (B), 100 µm (C).

Finally, we immunostained for IL-1β, IL-17, and TNF-α. We analyzed the local expression of IL-β and IL-17 in the synovium and articular disc, and TNF-α in the cartilage and synovium using histology tissue sections of the TMJ (approximately 3 sections/TMJ, 6 to 9 TMJs/group). The expression of IL-1β appeared to be increased in the CIA groups, with the greatest expression in the CIA+Immediate isoflurane group (Figure 4.12A). There was no evident IL-1β expression in the articular disc (Figure 4.12B). Interestingly, IL-17 expression appeared to be greatest in the groups with LIPUS treatment, especially those with CIA+LIPUS (immediate or delayed) (Figure 4.12C), while there was no obvious expression of IL-17 in the articular disc (Figure 4.12D). TNF-α expression was greatest in the cartilage of those groups that received immediate LIPUS treatment, and this expression was generally absent in the cartilage in the other Saline groups with either immediate isoflurane or any delayed treatment (Figure 4.12E). Finally, TNF-α expression appeared to be greatest in the synovium in groups that received LIPUS treatment (immediate or delayed) (Figure 4.12F).

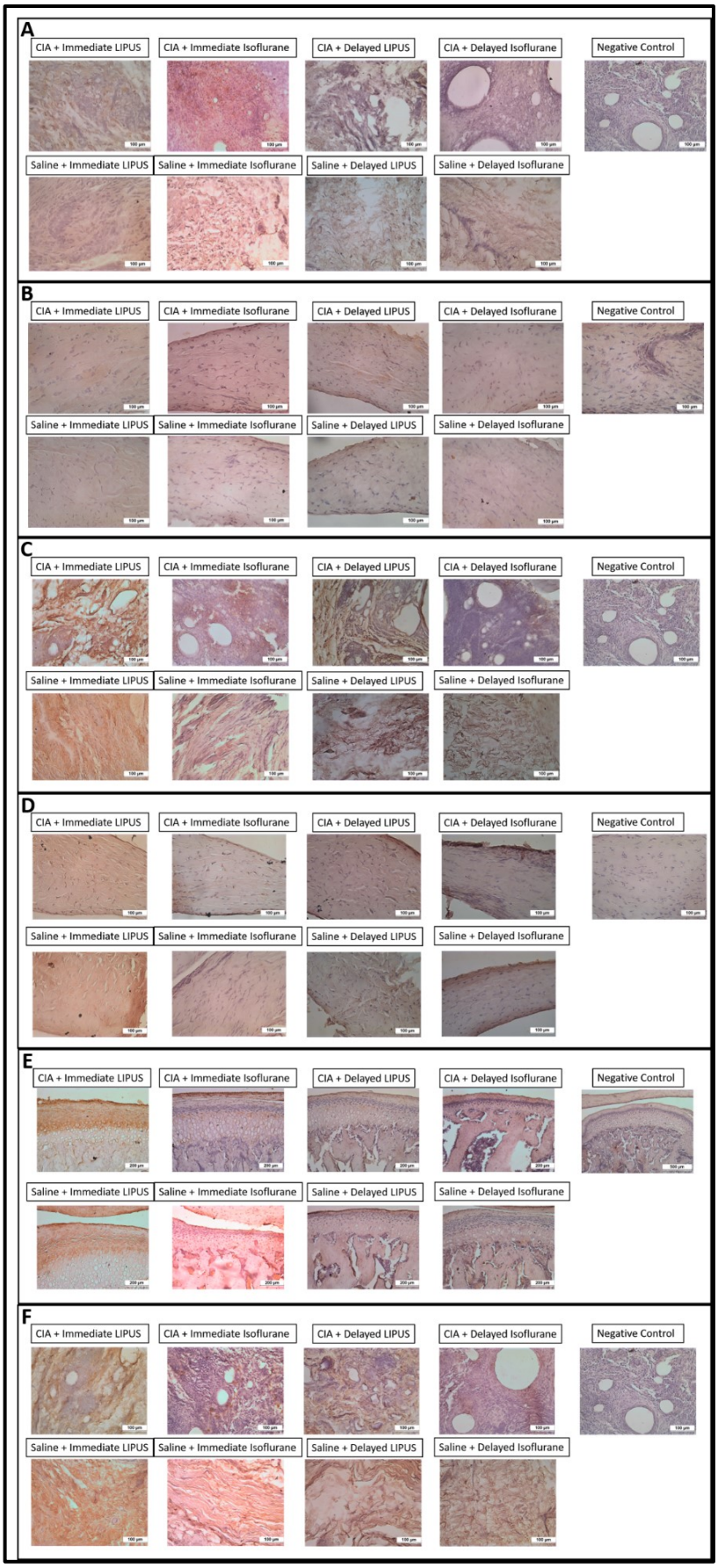
A
CIA + Immediate LIPUS
CIA + Immediate Isoflurane
CIA + Delayed LIPUS
CIA + Delayed Isoflurane
Negative Control
Saline + Immediate LIPUS
Saline + Immediate Isoflurane
Saline + Delayed LIPUS
Saline + Delayed Isoflurane
B
CIA + Immediate LIPUS
CIA + Immediate Isoflurane
CIA + Delayed LIPUS
CIA + Delayed Isoflurane
Negative Control
Saline + Immediate LIPUS
Saline + Immediate Isoflurane
Saline + Delayed LIPUS
Saline + Delayed Isoflurane
C
CIA + Immediate LIPUS
CIA + Immediate Isoflurane
CIA + Delayed LIPUS
CIA + Delayed Isoflurane
Negative Control
Saline + Immediate LIPUS
Saline + Immediate Isoflurane
Saline + Delayed LIPUS
Saline + Delayed Isoflurane
D
CIA + Immediate LIPUS
CIA + Immediate Isoflurane
CIA + Delayed LIPUS
CIA + Delayed Isoflurane
Negative Control
Saline + Immediate LIPUS
Saline + Immediate Isoflurane
Saline + Delayed LIPUS
Saline + Delayed Isoflurane
E
CIA + Immediate LIPUS
CIA + Immediate Isoflurane
CIA + Delayed LIPUS
CIA + Delayed Isoflurane
Negative Control
Saline + Immediate LIPUS
Saline + Immediate Isoflurane
Saline + Delayed LIPUS
Saline + Delayed Isoflurane
F
CIA + Immediate LIPUS
CIA + Immediate Isoflurane
CIA + Delayed LIPUS
CIA + Delayed Isoflurane
Negative Control
Saline + Immediate LIPUS
Saline + Immediate Isoflurane
Saline + Delayed LIPUS
Saline + Delayed Isoflurane

Figure 4.12: Representative photomicrographs of immunohistochemically-stained TMJ cartilage from each group. A) IL-1β (synovium), B) IL-1β (articular disc), C) IL-17 (synovium), D) IL-17 (articular disc), E) TNF-α (cartilage), F) TNF-α (synovium). Scale bar = 100 μm (A-D, F), 20 μm (D).

Next, we measured the level of TNF-α in the serum of rats in each of the 8 groups. Our results show that serum TNF-α was significantly higher in the Saline+Dealyed LIPUS group compared to the Saline+Delayed Isoflurane group (Figure 4.13) [$F(7,60) = 7.625$, $p < 0.005$].

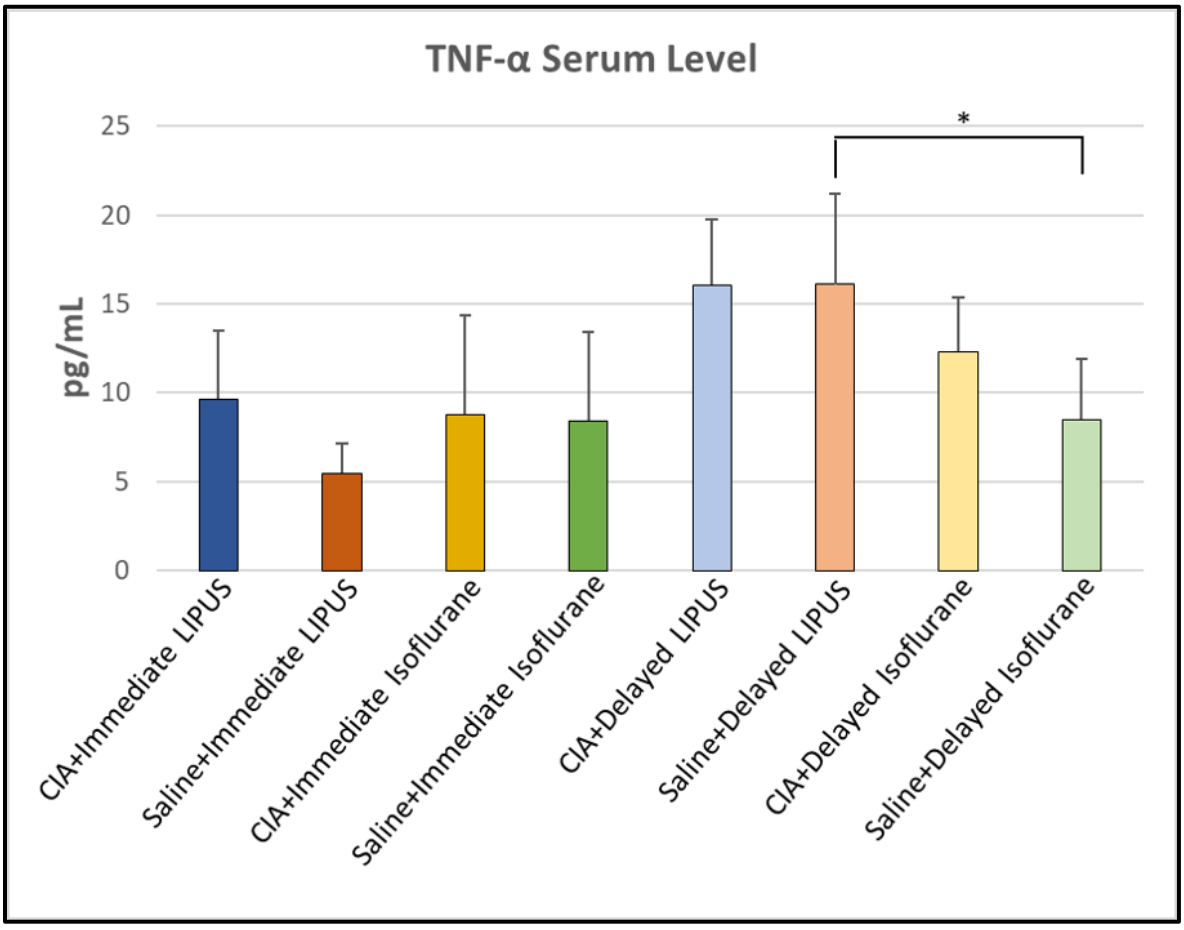

Figure 4.13: Level of TNF-α (pg/mL) in blood serum. Data is represented as the mean ± S.D. * = $p < 0.05$

A Kruskal-Wallis test was chosen to analyze TGF-β1 in the blood plasma of rats in each group. This test was selected because the obtained data was transformed from continuous data to ordinal data in order to appropriately deal with numerous zeroed data points. Because the data was no longer normally distributed because of this transformation, a Kruskal-Wallis test was chosen because it is the non-parametric test compared to ANOVA. This test revealed non-statistically significant differences across the 8 groups, χ^2 (7, N=72) = 5.942, p = 0.547. TGF-β1 levels were ranked lowest in the Saline+Immediate Isoflurane group (median [Md] = 1.00) in comparison to the CIA+Immediate LIPUS (Md = 2.00), Saline+Immediate LIPUS (Md = 4.00), CIA+Immediate Isoflurane (Md = 5.00), CIA+Delayed LIPUS (Md = 5.00), Saline+Delayed LIPUS (Md = 3.00), CIA+Delayed Isoflurane (Md = 2.00), and Saline+Delayed Isoflurane (Md = 2.00) groups.

Our results demonstrate that there were no significant differences in TGF-β1-LAP (bound to LAP in inactive form) plasma levels between groups (Figure 4.14).

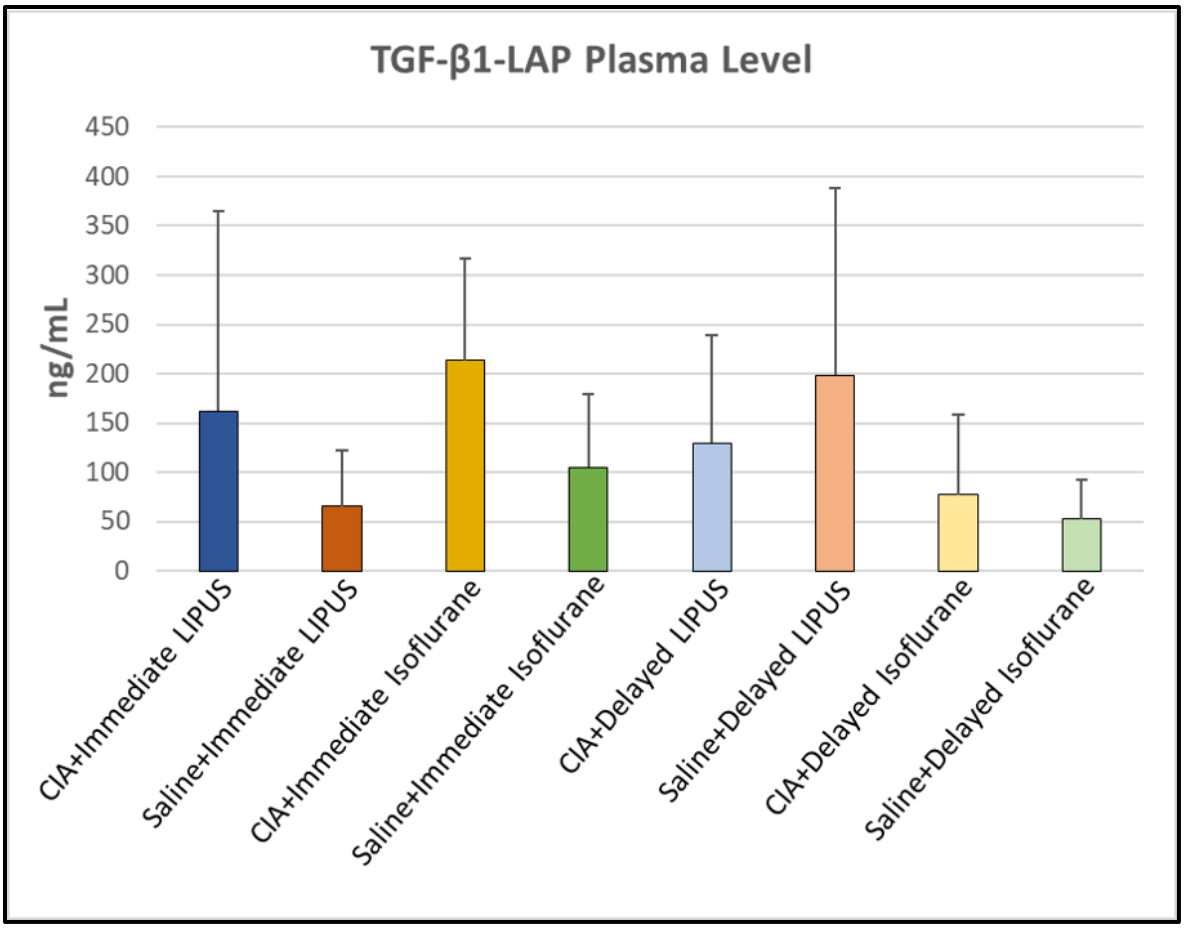

Figure 4.14: Level of TGF-β1-LAP (ng/mL) in blood plasma. Data is represented as the mean ± S.D.

Our results revealed that the level of IL-1β in the blood serum and IL-6 and IL-1β in the articular disc homogenate were below the detectable levels of the proteins in these ELISA kits, therefore all levels were represented as less than 0 (<0.00). Because of these results, graphs containing these results were not created and the results are only declared in this text.

Three-dimensional reconstructions of each hemimandible were used to first observe any bony changes of the condyle. Figure 4.15 shows representative models from each group. Each hemimandible in the CIA groups that did not receive any LIPUS treatment (immediate or

delayed) appeared to show condylar erosion, whereas the CIA groups that received LIPUS treatment appeared to have little or no bone erosion.

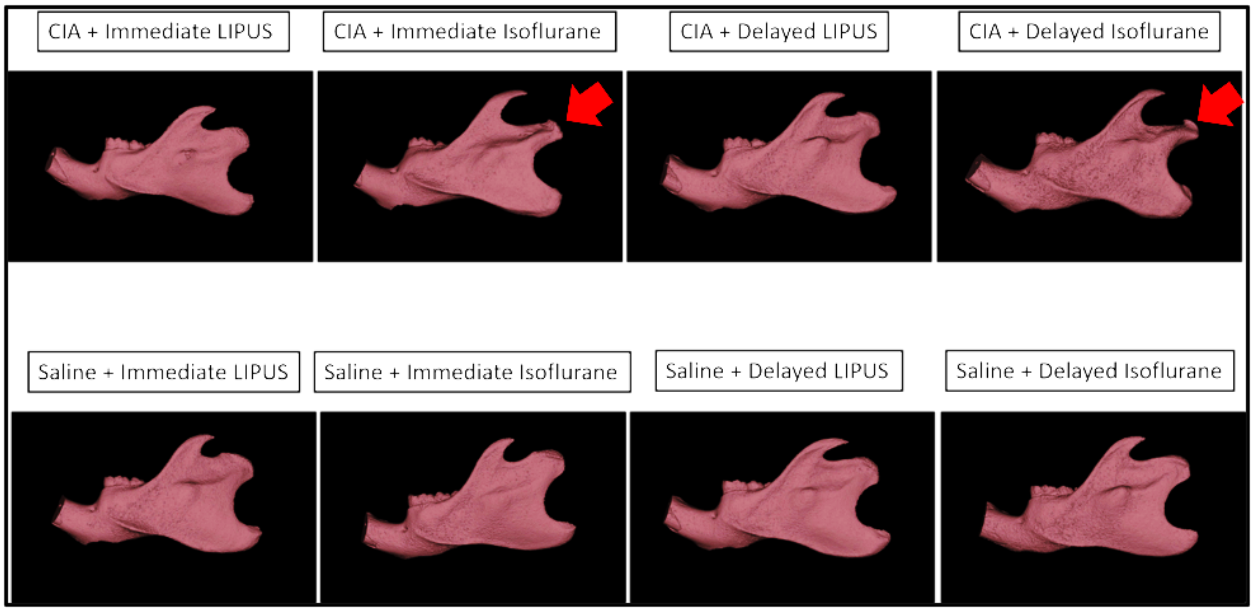

Figure 4.15: 3D reconstructions of hemimandibles from each group. Condylar erosion is indicated by the red arrows.

The MicroCT analysis of mandibular length of each hemimandible (n = 18/group since 2 hemimandibles/rat) in each scan used to calculate how much each hemimandible grew over the length of the study reveals that mandibular growth in the CIA+Immediate Isoflurane group was significantly less compared to the CIA+Immediate LIPUS and Saline+Isoflurane groups (Figure 4.16). As well, mandibular growth in the CIA+Delayed Isoflurane group was significantly less compared to the CIA+Delayed LIPUS group (Figure 4.16) [$F(7,136) = 13.459$, $p < 0.005$]. The

intraclass correlation coefficient (average measures) used to evaluate intra-rater reliability was calculated to be 0.967, indicating excellent reliability.

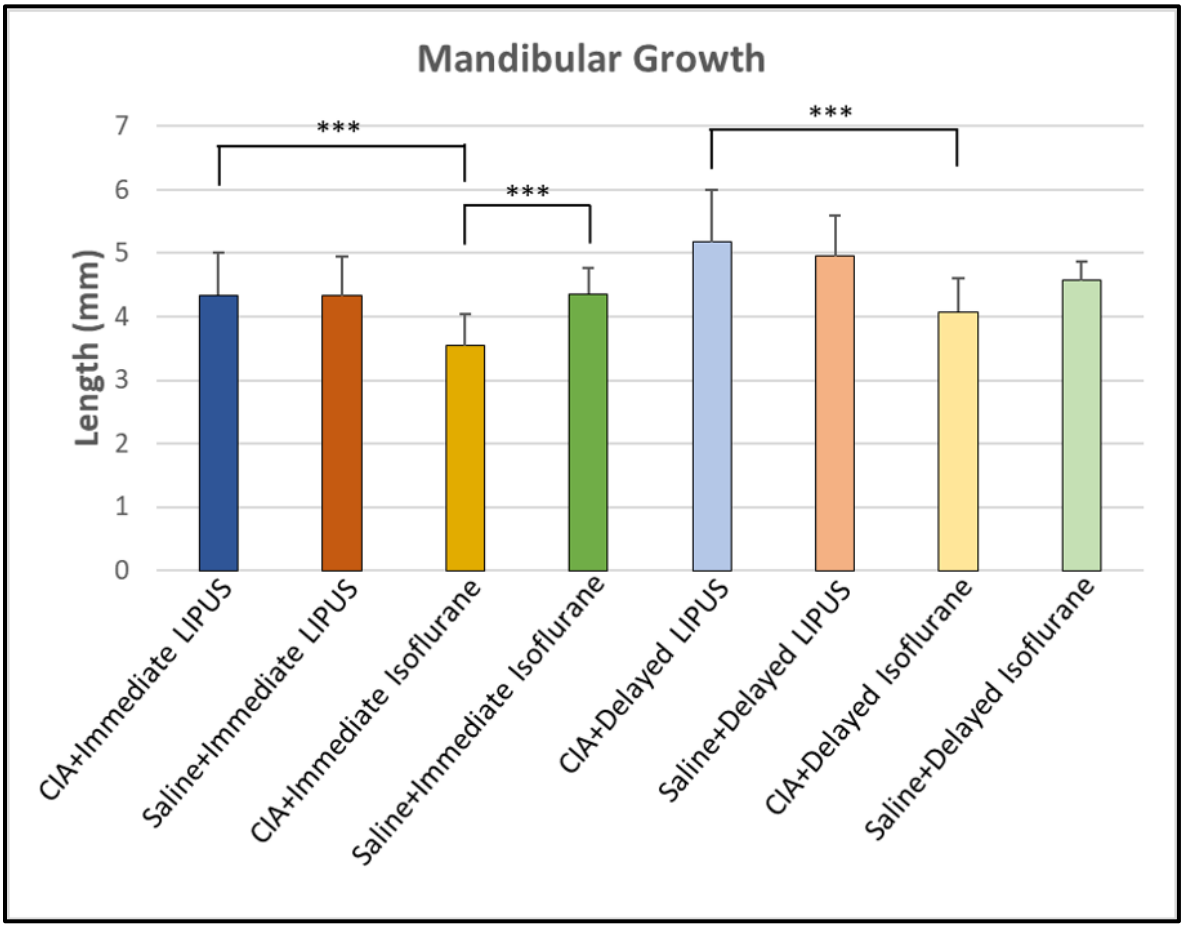

Figure 4.16: Mandibular growth (lengthwise) (mm) in each group. *** = $p < 0.005$

Next, we used MicroCT analysis to calculate how much the condyles grow in volume over the length of the study. The condyles grew significantly less in the Saline+Immediate LIPUS group compared to the CIA+Immediate LIPUS and Saline+Immediate Isoflurane groups (Figure 4.17). Our results also show that the condyles grew significantly less in the

CIA+Immediate LIPUS group compared to the CIA+Immediate Isoflurane group, and in the CIA+Delayed LIPUS group compared to the Saline+Delayed LIPUS group (Figure 4.16) [$F(7,135) = 35.719$, $p < 0.005$].

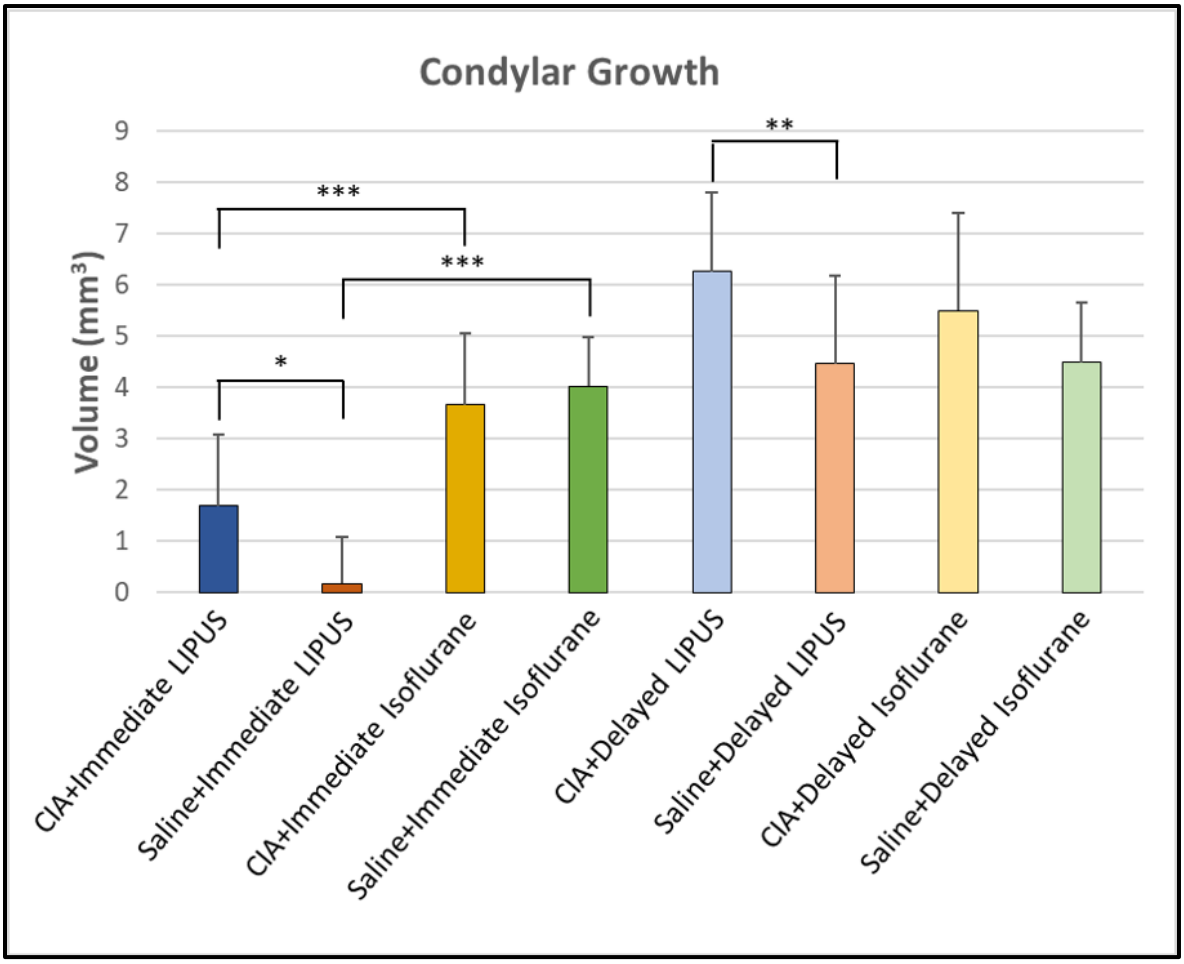

Figure 4.17: Condylar growth (volume-wise) (mm^3) in each group. * = $p < 0.05$, ** = $p < 0.01$, *** = $p < 0.005$

4.5 *Discussion*

This study demonstrated the effects of low intensity pulsed ultrasound (LIPUS) on TMJ arthritis and mandibular growth in the CIA-induced arthritis juvenile rat, a growing rat model of JIA. Our study investigated how LIPUS and CIA affected TMJ cartilage, synovium and articular disc; blood serum/plasma and articular disc cytokine levels; and mandibular and condylar growth. RA and JIA are inflammatory joint diseases that primarily include type 1 T helper (Th1) immune responses involving pro-inflammatory cytokines like TNF-α and IL-1β and the activation of macrophages [Prahalad & Glass, 2002; Demoruelle, Deane & Holers, 2014]. These immune responses involved in TMJ-JIA support and promote TMJ inflammation, resulting in synovial inflammation, cartilage damage, bone erosion, and a detrimental effect on normal mandibular growth.

Our study considered exploring the use of LIPUS because of the extensive research on its effect on synovial cells, osteoblasts, and chondrocytes, helping to understand the cellular mechanisms involved in these cells when LIPUS is used to stimulate them. As well, many studies have reported its effect on reducing pro-inflammatory cytokines and the inflammatory effects of these involved cytokines [Li et al., 2003; Sato et al., 2014, Nakamura et al., 2011; Zhang et al., 2017; Li et al., 2011; Arita et al., 2017], as well as its stimulatory effect on mandibular growth [Kaur et al, 2015; Oyonarte et al., 2009; Crossman et al., 2019].

In this study we first aimed to analyze the potential preventive/protective effect of LIPUS on TMJ-CIA in juvenile rats. Immediately after TMJ injections, we applied LIPUS to the TMJs for 20 minutes/day for 4 weeks. Since our previous study [Crossman et al., 2021] showed that CIA negatively affects normal mandibular growth and increases TMJ inflammation, we wanted to demonstrate if LIPUS could prevent these growth disturbances and inflammatory effects.

Figure 4.4 represents the pattern of average increases in head width from baseline (pre-injection) measures. Since the group that received only saline TMJ injections and only isoflurane, we expect that this group would represent normal head width increases. By observing this graph, it is obvious that the head width in the group that received CIA TMJ injections and no immediate LIPUS treatment remained greater, whereas the group that also had CIA TMJ injections and received daily LIPUS treatment appeared to have normal head width increases, following a similar pattern to those with only saline TMJ injections. Application of LIPUS may have reduced some external swelling of the TMJ areas that was caused by an initial inflammatory response to the CIA TMJ injections.

After this we also aimed to analyze if LIPUS could treat or reduce the effect of CIA in the TMJ in these rats by applying the LIPUS 4 weeks after the TMJ injections were completed. Again, LIPUS was applied for 20 minutes/day for 4 weeks. In general, the increases in head width in each group that received delayed treatment followed a similar pattern to each other throughout the study.

Next, we qualitatively observed our histological TMJ sections (Figures 4.6 and 4.7) for any changes in synovial tissue and cartilage. We observed that in each TMJ section from groups that received CIA injections, there were clear indications of synovitis as shown as lipid droplets and new blood vessels forming within the synovium. Although synovitis was present in all CIA TMJs, there appeared to be less synovitis present within the CIA joints that also received LIPUS treatment. In our previous study analyzing the effect of CIA on the TMJ in juvenile rats, we also observed similar synovitis. Lipid bodies can accumulate within inflammatory cells present within inflamed tissues. One possible reason causing this lipid accumulation could be that the *M. tuberculosis* contained within the CFA in our CIA injections induces foamy macrophages to

compartmentalize lipid bodies. Other inflammatory cells such as leukocytes can also function in a similar manner. Another explanation could be that activated leukocytes within the inflamed synovial tissue may have formed lipid bodies that contain cytokines like TNF-α which is similar to what is observed as lipid body biogenesis in leukocytes obtained from human arthritic joints [Crossman et al., 2021; Wang et al., 2012; Melo et al., 2011]. We did not observe any differences in the synovial tissue between the groups that received saline injections. Next, we observed characteristic patterns within condylar cartilage and each cell layer. The cartilage in the CIA group that only received immediate isoflurane appeared thicker and had a more disorganized appearance with less obvious cellular stratification. Similar patterns of chondrocyte disorganization and disturbances to normal columnar arrangement have been reported in mouse models of TMJ OA [Nejad et al., 2017]. The cartilage in the groups that received delayed treatment appears to be thinner especially in the group that had CIA injections and did not receive LIPUS treatment. Many published studies that measure any changes in cartilage thickness typically do not include a similar study length (ie. 4-8 weeks) like our study, so any reported changes in cartilage thickness in those studies cannot be related to our current study. However, Maldonado & Nam (2003) explain that although an initial increase in cartilage thickness in an experimental animal model of OA, this cartilage may become thinner over time due to a combined loss of aggrecan, a major proteoglycan and important protein component of cartilage ECM. Interestingly, the cartilage in the CIA group that had delayed LIPUS treatment has a thicker appearance. If inflammation over time has a detrimental effect on ECM components, such as aggrecan, and causes a decrease in ECM production, which leads to decreased cartilage thickness, then it may be possible that LIPUS treatment may prevent these inflammatory effects or may increase ECM production by chondrocytes. To observe changes in

ECM, we performed toluidine blue (T.B.) staining of the cartilage. This staining is specific to proteoglycans, which includes aggrecan, and the amount of T.B. staining is directly proportional to the amount of proteoglycans that have been produced in the ECM of the cartilage. In Figure 4.8 the cartilage with the greatest amount of proteoglycan staining is in the groups with immediate LIPUS treatment. This staining appears to decrease in the older rat cartilage in the groups that had delayed treatment. The least of amount T.B. staining appears to be in the CIA group with only delayed isoflurane (no LIPUS). Sekino et al. (2018) demonstrated how LIPUS can increase the expression of aggrecan in chondrocytes. Again, since we observed that the cartilage in this CIA group with delayed isoflurane only had thinner cartilage and we know that inflammation due to CIA may result in the loss of aggrecan, a type of proteoglycan, then we would expect to see decreased proteoglycan staining, which we have observed.

Next, to quantitatively evaluate each specific cartilage cell layer to further understand how CIA and LIPUS affect the superficial, articulating fibrocartilage and the three layers of chondrocytes within the cartilage, we systematically measured the thicknesses of these four cell layers. Our results reveal that the fibrocartilage layer and the hypertrophic chondrocyte layer are significantly thicker in the CIA group that did not receive LIPUS treatment and only immediate isoflurane. In another study that evaluated the effect of CFA on cartilage thickness, both TMJ mandibular condyle explants and TMJs *in vivo* were included [Morel et al., 2019]. In the explants treated with a lower dose of CFA for 48 hours, cartilage thickness significantly increased due to cellular expansion in cartilage cell zones, including a superficial zone (similar to our fibrocartilage) and a chondrocyte zone that encompassed mature and hypertrophic cells. However, in their *in vivo* TMJs, the cartilage thickness was not significantly different from their controls. So, it may be possible that, as discussed by Morel et al. (2019), acute changes due to

inflammation in this joint include cartilage thickening, but then overtime in a later stage of disease, this cartilage thickening lessens possibly due to a loss of proteoglycans, as discussed above.

To continue to analyze how LIPUS and CIA can affect cartilage and chondrocyte phenotype and activity, we performed immunohistochemistry to study chondrocyte production of collagens, a collagenase, growth factors, cytokines and other proteins. Additionally, we included some analysis of cytokines in the synovium as well as the articular disc. In general, immunostaining for Col-II was increased in the CIA groups, but especially in those that received LIPUS treatment when compared to those that did not. If we consider how chondrocytes responded to TMJ inflammation, in reference to the above discussion regarding increased cartilage thickening and chondrocyte production of ECM components, then it may be possible that an acute response to this type of induced arthritis in the TMJ may include an initial increase of Col-II production by chondrocytes. However, over time, theoretically this expression of Col-II should decrease due to increased production of MMPs, including MMP-13, which are collagenases that degrade collagen [Arita et al., 2017; Demoruelle, Deane & Holers, 2014). This is demonstrated in the CIA+Delayed Isoflurane group's cartilage. But the expression of Col-II in the CIA groups that received LIPUS treatment, either immediately or after 4 weeks (delayed), is increased. Sekino et al. (2018) also demonstrated that LIPUS applied for 20 minutes per day for up to 7 days increased the production of Col-II in chondrocytes. Our group also showed that LIPUS increased the expression of Col-II in the TMJ cartilage in a mouse model of RA [Crossman et al., 2019].

Next, we analyzed the expression of Col-X and our results show that immunostaining of this type of collagen was fairly minimal in our sections. However, as demonstrated by our

representative photomicrographs in Figure 4.10B, the expression of Col-X appears to be greater in the groups that received immediate LIPUS treatment compared to their controls. Col-X is normally expressed in hypertrophic chondrocytes, extending into the mineralized cartilage, separating the soft cartilage from the underlying subchondral bone [Utreja et al., 2016]. This type of collagen is present during the growth stage of the mandible and condyle and its expression decreases as growth also decreases during maturation [Ohashi N et al., 1997]. LIPUS has been shown to increase the expression of Col-X in chondrocytes [Sekino et al., 2018]. Our results support these findings. However, interestingly the CIA group with immediate isoflurane (no LIPUS) had a significantly thicker hypertrophic chondrocyte cell layer but this layer also did not express greater Col-X. Although the CIA group that receive immediate LIPUS treatment did have greater Col-X expression, its thickness of hypertrophic chondrocytes was not greater than other groups. During the process of endochondral ossification within the growth plate, the synthesis of Col-X starts when chondrocytes become hypertrophic, but exactly how the Col-X plays a functional role in cartilage is poorly understood. It is suggested that Col-X may play a role in calcification, it may be connected to chondrocyte hypertrophy and endochondral bone formation, and it may be involved in the pathogenesis of OA. If Col-X plays a role in stimulating mineralization, then it would be expected that mandibular growth would be increased [Ohashi et al., 1997].

Another factor that we studied was MMP-13, which is involved in hypertrophy and mandibular growth and is produced by chondrocytes [Wang, Rigueur & Lyons, 2014]. To immunostain for MMP-13 in cartilage, we used an anti-MMP13 antibody that does recognize not only the active form of this enzyme but also the proenzyme as well. Our results reveal that MMP-13 expression in hypertrophic cells undergoing mineralization and endochondral

ossification was greatest in the CIA group with immediate isoflurane only. There is no observed difference between the CIA and Saline groups that received immediate LIPUS treatment. Hypertrophic cells produce mineralized ECM that contains MMP-13, which is involved in its active form of the enzyme in modifying the ECM to increase vascular invasion. Neovascularization allows access of progenitor cells, such as osteoprogenitors, into the tissue. Osteoprogenitors will then differentiate into osteoblasts that lay down bone matrix that will eventually replace the cartilage [Wang, Rigueur & Lyons, 2014]. However, the overexpression of MMP-13 in cartilage may play a role progressing OA [Aref-Eshghi et al., 2015]. This may explain why we observe increased MMP-13 expression in our CIA group with immediate isoflurane only. In the CIA with delayed isoflurane only, there appears to be increased MMP-13 expression compared to the CIA group that received delayed LIPUS treatment and especially to the Saline group with delayed isoflurane. MMP-13 expression is not only more prevalent in the mineralized chondrocytes just beneath the hypertrophic cells, but also in the hypertrophic cells themselves. Again, LIPUS has been demonstrated to decrease the expression of MMP-13 in chondrocytes [Sekino et al., 2018] and potentially through the MAPK signalling in chondrocytes as demonstrated by Zhang (2017).

Next, we immunostained for RANKL, TGF-β1, and VEGF in the condylar cartilage. Although we did not observe much difference in expression of RANKL, we observed clear differences in the amount and intensity of staining of VEGF since the groups with immediate LIPUS treatment had reduced VEGF expression in its appearance. VEGF is a growth factor that is expressed in synovial cells and chondrocytes during mandibular growth, and this expression is low in mature articular cartilage. VEGF influences chondrocyte proliferation, apoptosis, and metabolism. This results in a production of MMPs and other factors involved in cartilage matrix

degradation. Finally, it is suggested that VEGF plays a significant role in the development of TMJ arthritis [Shen et al., 2015]. Our results demonstrate that the groups with immediate isoflurane only had greater VEGF expression compared the groups with immediate LIPUS treatment. Increased expression of VEGF could be interpreted differently depending on the condition of the cartilage. In cartilage that is not expected to have any inflammation, such as in the Saline group with immediate isoflurane only, higher VEGF expression would not play a role in the development of arthritis but may actually show a representative example of normal VEGF expression in hypertrophic chondrocytes in healthy cartilage in a normal growing mandible. However, when observing increased VEGF expression in CIA cartilage, such as that from the CIA group with immediate isoflurane (no LIPUS), it may show either normal, comparative expression to healthy cartilage or it may show the initiation if cartilage matrix degradation and development of TMJ arthritis. Because of these possibilities, it is important to consider the other factors that are differently expressed in that particular CIA cartilage and to not consider VEGF expression alone. Since the expression of MMP-13 is also increased in this group and MMP-13 is also produced by hypertrophic cells and plays a role in its active form in the development of arthritis, then it is likely that this increased expression in this CIA cartilage is due to CIA. Although the effect of LIPUS on the expression of VEGF in cartilage is less studied, LIPUS may have an effect on reducing VEGF expression in chondrocytes. However, when we observe the expression of VEGF in the groups that received delayed treatment, we find that the CIA cartilage has increased expression, particularly in the group that received delayed LIPUS treatment. It may be possible that since VEGF expression decreases as mandibular growth decreases during maturation, as mentioned above, then potentially there is less inflammation due to CIA in these older rats. If LIPUS stimulates mandibular growth as shown in previous studies mentioned

above, and since VEGF is expressed in chondrocytes during mandibular growth, then it may be expected that LIPUS increases VEGF expression. This may explain why there is increased VEGF expression in the CIA group with delayed LIPUS treatment. However, this does not explain the decreased expression in the younger rats that should be growing more. Further studies need to address this issue to help explain these discrepancies and to determine whether or not LIPUS has a different effect during inflammation, such as in the groups with immediate treatment, compared with those with less inflammation, as potentially shown in the CIA rats with delayed treatment.

Prior to exploring how and if LIPUS affects pro-inflammatory cytokines involved in CIA in the TMJ, we first analyzed how CIA and LIPUS affected the expression of TGF-β1. TGF-β1 is included in the TGFβ superfamily. These growth factors play important roles in the regulation of chondrocyte proliferation and differentiation during growth and development [Wang, Rigueur & Lyons, 2014; Mukai et al., 2005]. This factor regulates integrin expression on the cell surface of chondrocytes, therefore affecting which integrins are available to serve as receptors for ligands like cytokines, collagens and peptides [Mukai et al., 2005]. Our results show that the expression of TGF-β1 was increased in the CIA group with immediate LIPUS treatment compared to all other groups, and there is less expression in groups that did not receive LIPUS treatment. Mukai et al. (2005) report that LIPUS also increased the mRNA expression and protein production of TGF-β1 in chondrocytes. As well, Li et al. (2003) also report that LIPUS increased TGF-β production in osteoblasts. TGF-β1 also plays a role in decreasing the rate on chondrocyte hypertrophy. In the CIA group that only received immediate isoflurane, there is much less TGF-β1 expression in the chondrocytes, which should result in increased hypertrophy and this is what our results showed concerning this group and the thickness of the hypertrophic

cell layer. Another study investigated how exogenous TGF-β1 affected the expression of Col-II and Col-X in chondrocytes, and it demonstrated how TGF-β1 increased Col-II expression but decreased Col-X expression (Mukai et al. (2005). In our study, TGF-β1 and Col-II appear to be increased by LIPUS, and Col-X may have only been slightly increased, instead the expected decrease in its expression according to this previous study by Mukai et al. (2005). It may be possible that there are different cartilage responses to LIPUS between *in vitro* and *in vivo*, as previously seen above in the discussion regarding cartilage thickness and acute responses.

To explore if and how LIPUS affects inflammation, we immunostained for IL-1β, IL-17, and TNF-α. These 3 pro-inflammatory cytokines as associated with RA and JIA [Demoruelle, Dean & Holers, 2014]. Li et al. (2003) demonstrated how LIPUS could decrease the production of TNF-α in healthy osteoblasts from rats. However, they could not detect any IL-1β in any groups in their study. Furthermore, Zhang et al. (2017) showed how LIPUS could significantly reduce IL-1β and TNF-α in articular cartilage in a surgically-induced rabbit model of OA. However, there are no studies that have evaluated the effect of LIPUS on IL-17 involved in any type of arthritis. Our study suggested that CIA would increase the production of these pro-inflammatory cytokines in the synovium, articular disc, or cartilage. Our results show that there was slightly more IL-1β expression in the synovial tissues in the CIA groups that received immediate treatment, and the CIA group that received immediate isoflurane (no LIPUS) may have slightly more expression compared to the CIA group that received LIPUS treatment. However, as we observe the older rat cartilage in the groups that received delayed treatment, there is very little expression of IL-1β. When we analyze the articular discs, we find that there is no expression of IL-1β in these tissues. Next, we immunostained for IL-17 in the synovium and articular disc. Interestingly, the groups that received LIPUS treatment appear to have increased

expression, whereas there is very little difference in expression of IL-17 in the articular discs between each group. Finally, the expression of TNF-α in the cartilage and synovium appeared to be increased in the CIA and Saline groups that received immediate LIPUS treatment. Because of these results, we can reject our hypothesis regarding an anti-inflammatory effect of LIPUS on TMJ-CIA in terms of TNF-α and IL-17. Since these results are analyzed only by qualitative observation, we do not know the quantitative amount of increased expression of these cytokines. Using quantification methods on immunohistochemically-stained sections, especially when observing cytokines that reside in the ECM and not necessarily intracellularly or attached to the cell surface, is very difficult. Even methods involving software to analyze the intensity of staining can be limited and flawed due changes in lighting and conditions when photomicrographs are taken. In order to attempt to understand how LIPUS may have had this effect on the expression of these cytokines, we can first consider how LIPUS affects the intracellular pathways in chondrocytes and synovial cells. In healthy chondrocytes LIPUS has been shown to stimulate cell surface integrin, initiating the activation of the MAPK and PI3K/Akt pathways within these cells. As each cellular component within these pathways become activated (phosphorylated), transcriptional factors induce the increased production of ECM components toward chondrocyte differentiation and maturation [Sekino et al., 2018; Takeuchi et al., 2008]. However, when LIPUS is applied to chondrocytes that have been stimulated by IL-1β, the effect on the MAPK pathway is different and there is downregulation of ERK1/2, which is normally upregulated in this same pathway in healthy chondrocytes [Zhang et al., 2017]. Similarly, depending on the environment or condition of the synovial cells that are stimulated with LIPUS, LIPUS has a different intracellular signalling effect. In healthy synovial cells, the MAPK pathway is stimulated with an upregulation of ERK1/2, but there is no reported

effect on how ERK1/2 responds when LIPUS is used to stimulate synovial cells that have been stimulated with IL-1β [Sato et al., 2014; Nakamura et al., 2010]. Because of these reasons, it still appears to be unclear what effect LIPUS has on these intracellular pathways when LIPUS is applied *in vivo* to TMJ tissues that contain synovial cells in the synovium and chondrocytes in the cartilage. Although it was expected that LIPUS would have a similar effect *in vivo* as it does *in vitro* in the previous studies, we can speculate that this is not the case. Because we do not know how LIPUS affects these intracellular signalling pathways *in vivo*, this suggests a further need for future studies to evaluate each component of these pathways *in vivo* in a growing CIA model of TMJ arthritis.

Additionally, we used ELISAs to measure cytokine levels systemically within the blood serum and plasma and locally in the articular disc homogenate. Our results revealed that there were no detectable levels of IL-1β in the serum and disc homogenate and of IL-6 in the disc homogenate. Then, we measured the levels of TGF-β1 in its active and inactive (bound to LAP) forms in the blood plasma. Our obtained data for TGF-β1 in its active form contained multiple 'zero' data points. Since TGF-β1 is highly expressed in most tissues, including blood plasma, it is highly unlikely that our samples did not have any levels of this protein. We potentially obtained these 'zero' data points due to human error involving pipetting or plate washing. Because of this obtained data, we recoded our data into ordinal data for analysis. Our results show that there were no significant differences between any groups for either form (active or inactive) of this growth factor. Interestingly, there were significantly more TNF-α in the serum from the Saline group with delayed LIPUS compared to the Saline group that received only delayed isoflurane. Again, LIPUS may have increased the production of this cytokine, as shown when analyzing the immunohistochemically-stained sections of cartilage and synovium. When

we analyze the trend of the serum levels of TNF-α, in general, these levels are lower in the rats with immediate treatment that appeared to have increased expression of TNF-α in the localized tissue. It may be possible that after performing the CIA injections, there is increased acute inflammation locally, which then gradually decreases via regulatory immune responses. But there may be a delayed effect systemically as shown by a trend of increased TNF-α serum levels in the older rats. Further time-dependent studies are needed to evaluate if a localized inflammatory response begins to diminish in TMJ tissues in CIA rats, and if a systemic inflammatory response begins after the local inflammatory responses start to decrease. Moreover, it may be suggested that LIPUS may have a different effect on specific cell types, such as chondrocytes and synovial cells, and their production of cytokines and growth factors depending on the environment in which these cells reside *in vivo*. If we consider this, then it may be possible that LIPUS, when applied to healthy TMJ tissues (Saline injections only), increases the production of TNF-α. Farrugia & Baron (2016) discuss the conflicting literature regarding the exact role of TNF-α in RA. They explain that the diverse roles of TNF-α may exist as two different forms of this cytokine. A membrane-bound TNF-α may exist in the localized TMJ tissue, whereas a soluble form may be released into the blood stream. The two forms of this protein may bind TNF-α receptors (ie. TNF-RI and TNF-RII) and transduce signals with potentially opposite outcomes. As well, they identify clinical studies in which anti-TNF-α therapies increased inflammation and autoimmunity, even in patients with JIA. Our study and these studies clearly demonstrate that we still do not fully understand how TNF-α functions in different tissues in patients or animal models of RA or JIA, or even in healthy tissues. Although our study provides contradictory outcomes regarding its effect on TNF-α, it does identify the need for further study on this topic.

Finally, we performed MicroCT analysis to evaluate if LIPUS could stimulate growth of the mandible in growing rats with TMJ arthritis. Our results show that LIPUS had a significant effect on stimulating mandibular growth in CIA rats. To help identify if this stimulatory effect was due to volumetric increases in the condylar bone, we measure condylar growth volume-wise. We expected that the condylar volume in the groups with CIA and no LIPUS treatment would have the least condylar growth since the majority of mandibular growth occurs in the condyle. However, upon analysis we found that the groups with immediate LIPUS treatment had the smallest increase in condylar volume. When we measured change in condylar volume in the rats with delayed treatments, delayed LIPUS treatment resulted in significantly greater condylar volume in the CIA group compared to the Saline group. To help explain the small increases in condylar volume in the groups that received immediate LIPUS treatment compared to the groups that received immediate isoflurane only, we need to consider how the condylar volume was measured. In this study using our MicroCT software, we made virtual linear cuts across the condyle from the deepest point of the superior notch to the deepest point of the inferior notch. If these notches were shallower in the rats in these groups, then it would be expected that the calculated volume of these condyles would be less. Likewise, if these notches were deeper, then the condylar volume would be greater. Because of this speculation, further analysis to measure condylar length and width, as well as notch depth, would need to be considered to rule out these possibilities. It is recommended that future studies consider these to further understand how LIPUS and CIA may affect changes in condylar volume. Further analysis of changes in the condyle is required to more fully understand how LIPUS has had its stimulatory effect on the growth of the mandible in CIA rats.

In summary our results demonstrate that LIPUS had more positive effect on the TMJ when it was applied immediately compared to after 4 weeks when considering the cartilage thickness results, immunostaining for Col-II, Col-X, MMP-13, VEGF, TGF-β1, and IL-1β, and the mandibular growth results. This may be due to decreased inflammation in the TMJ over time. Since the rats in the delayed treatment groups had decreased or minimal evidence of inflammation and their mandibles were close to the period of growth cessation in rats, LIPUS's effect on these TMJs and mandibles were only minimal. In this study, we may have observed a correlation in increased TGF-β1 expression in the condyle and an increase in mandibular growth in the CIA rats that received immediate LIPUS treatment. In CIA rats with only immediate isoflurane, there was less TGF-β1 expression and decreased mandibular growth. Although there was an acute inflammatory response in the CIA group (isoflurane only) demonstrated as cartilage thickening, shown by increased chondrocyte hypertrophy and increased VEGF expression, this chondrocyte hypertrophy and VEGF production did not result in increased mandibular growth. Further studies are needed to understand the relationships between VEGF, chondrocyte hypertrophy, and mandibular growth in TMJ arthritis.

4.6 *Conclusion*

In conclusion this study demonstrated that CIA in the TMJ was more prevalent within the first 4 weeks and evidence of inflammation after 8 weeks was minimal. LIPUS had a greater positive effect on TMJ-CIA-induced arthritis and the mandible in the first 4 weeks when acute inflammation was present. CIA prevented normal mandibular growth, but LIPUS prevented or reversed this deduction in mandibular growth due to CIA. LIPUS increased cartilage expression

of Col-II, Col-X, and TGF-β1, and decreased the expression of MMP-13 and VEGF in CIA TMJs.

4.7 *References*

Aref-Eshghi E, Liu M, Harper P, Doré J, Martin G, Furey A, Green R, Rahman P, Zhai G. Overexpression of MMP13 in human osteoarthritic cartilage is associated with the SMAD-independent TGF-β signalling pathway. Arthritis Research & Therapy. 2015; 17: 264-271.

Arita A, Yonemitsu I, Ikeda Y Miyazaki M, Ono T. Low-intensity pulsed ultrasound stimulation for mandibular condyle osteoarthritis lesions in rats. *Oral Diseases.* 2018; 24: 600-610.

Bendele A. Animal models of rheumatoid arthritis. J Musculoskel Neuron Interact 2001;1:377-385.

Brand D, Kang A, Rosloniec E. Immunopathogenesis of collagen arthritis. Spring Semin Immunopathol. 2003; 25: 3-18.

Brand D, Latham K, Rosloniec E. Collagen-induced arthritis. Nature Protocols 2007;2:1269-1275.

Carrasco R. Juvenile idiopathic arthritis overview and involvement of the temporomandibular joint – prevalence, systemic therapy. *Oral Maxillofacial Surg Clin N Am.* 2015; 27: 1-10.

Crossman J, Alzaheri N, Abdallah M, Tamimi F, Flood P, Alhadainy H, El-Bialy T. Low intensity pulsed ultrasound increases mandibular height and Col-II and VEGF expression in arthritic mice. Archives of Oral Biology. 2019; 104: 112-118.

Crossman J, Lai H, Kulka M, Jomha N, Flood P, El-Bialy T. Collagen-induced temporomandibular joint arthritis juvenile rat animal model. *Tissue Engineering: Part C.* 2021; 27 (2): 115-123.

Demoruelle M, Deane K, Holers M. When and where does inflammation begin in rheumatoid arthritis? *Curr Opin Rheumatol.* 2014; 26 (1): 64-71.

Farrugia M, Baron B. The role of TNF-α in rheumatoid arthritis – a focus on regulatory T cells. Journal of Clinical and Translational Research. 2016; 2 (3): 84-90.

He D, An Y, Li Y, Wang J, Wu G, Chen G, Zhu G. RNA sequencing reveals target genes of temporomandibular joint osteoarthritis in rats after the treatment of low-intensity pulsed ultrasound. *Gene.* 2018; 672: 126-136.

Iwabuchi Y, Tanimoto K, Tanne Y, Inubushi T, Kamiya T, Kunimatsu R, Hirose N, Mitsuyoshi T, Su S, Tanaka E, Tanne K. Effects of low-intensity pulsed ultrasound on the expression of

cyclooxygenase-2 in mandibular condylar chondrocytes. *Journal of Oral & Facial Pain and Headache.* 2014; 28(3): 261-268.

Kaur H, Uludağ H, Dederich D, El-Bialy T. Effect of increasing low-intensity pulsed ultrasound and a functional appliance on the mandibular condyle in growing rats. *J Ultrasound Med.* 2017; 36: 109-120.

Kinne R, Bräuer R, Stuhlmüller B, Palombo-Kinne E, Burmester G. Macrophages in rheumatoid arthritis. *Arthritis Res.* 2000; 2: 189-202.

Li J, Chang W, Lin J, Ruaan R, Liu H, Sun J. Cytokine release from osteoblasts in response to ultrasound stimulation. *Biomaterials.* 2003; 24: 2379-2385.

Li X, Li J, Cheng K, Lin Q, Wang D, Zhang H, An H, Gao M, Chen A. Effect of low-intensity pulsed ultrasound on MMP-13 and MAPKs signaling pathway in rabbit knee osteoarthritis. *Cell Biochem Biophys.* 2011; 61: 427-434.

Liu W, Xu Z, Li Z, Zhang Y, Han B. RANKL, OPG and CTR mRNA expression in the temporomandibular joint in rheumatoid arthritis. *Experimental and therapeutic medicine*. 2015; 10: 895-900.

Maldonado M, Nam J. The role of changes in extracellular matrix of cartilage in the presence of inflammation on the pathology of osteoarthritis. Biomed Research International. 2013; 2013: 1-10.

Melo R, D'Avila H, Wan H, Bozza P, Dvorak A, Weller P. Lipid bodies in inflammatory cells: structure, function, and current imaging techniques. J Histochem Cytochem. 2011; 59: 540-556.

Mizoguchi I, Toriya N, Nakao Y. Growth of the mandible and biological characteristics of the mandibular condylar cartilage. Japanese Dental Science Review 2013;49:139-150.

Morel M, Ruscitto A, Pylawka S, Reeve G, Embree M. Extracellular matrix turnover and inflammation in chemicall-induced TMJ arthritis mouse models. PLoS ONE. 2019; 14 (10): e0223244 (1-22).

Mukai S, Ito H, Nakagawa Y, Akiyama H, Miyamoto M, Nakamura T. Transforming growth factor-β1 mediates the effects of low-intensity pulsed ultrasound in chondrocytes. Ultrasound in Med. & Biol. 2005; 31 (12): 1713-1721.

Nakamura T, Fujihara S, Katsura T, Yamamoto K Inubushi T, Tanimoto K, Tanaka E. Effects of low-intensity pulsed ultrasound on the expression and activity of hyaluronan synthase and hyaluronidase in IL-1β-stimulated synovial cells. *Annals of Biomedical Engineering.* 2010; 38 (11): 3363-3370.

Nakamura T, Fujihara S, Yamamoto-Nagata K, Katsura T, Inubushi T, Tanaka E. Low-intensity pulsed ultrasound reduces the inflammatory activity of synovitis. *Annals of Biomedical Engineering.* 2011; 39(12): 2964-2971.

Nejad S, Kobezda T, Tar I, Szekanecz Z. Development of temporomandibular joint arthritis: the use of animal models. Joint Bone Spine. 2017; 84: 145-151.

Ohashi N, Ejiri S, Hanada K, Ozawa H. Changes in type I, II, and X collagen immunoreactivity of the mandibular condylar cartilage in a naturally aging rat model. J Bone Miner Metab. 1997; 15: 77-83.

Oyonarte R, Zárate M, Rodriguez F. Low-intensity pulsed ultrasound stimulation of condylar growth in rats. *Angle Orthodontist.* 2009; 79 (5): 964-970.

Pedersen T, Jensen J, Melsen B, Herlin T. Resorption of the temporomandibular condylar bone according to subtypes of juvenile chronic arthritis. *The Journal of Rheumatology*. 2001; 28 (9): 2109-2115.

Prahalad S and Glass D. Is juvenile rheumatoid arthritis/juvenile idiopathic arthritis different from rheumatoid arthritis? *Arthritis Res.* 2002; 4 (suppl 3): 303-310.

Sato M, Nagata K, Kuroda S, Horiuchi S, Nakamura T, Karima M, Inubushi T, Tanaka E. Low-intensity pulsed ultrasound activates integrin-mediated mechanotransduction pathway in synovial cells. *Annals of Biomedical Engineering.* 2014; 40(10): 2156-2163.

Sekino J, Nagao M, Kato S, Sakai M, Abe K, Nakayama E, Sato M, Nagashima, Y, Hino H, Tanabe N, Kawato T, Maeno M, Suzuki N, Ueda K. Low-intensity pulsed ultrasound induces cartilage matrix synthesis and reduced MMP13 expression in chondrocytes. *Biochemical and Biophysical Research Communications.* 2018; 506: 290-297.

Shen P, Jiao Z, Zhen J, Xu W, Zhang S, Qin A, Yang C. Injecting vascular endothelial growth factor into the temporomandibular joint induces osteoarthritis in mice. Scientific Reports. 2015; 5: 16244 (1-11).

Takeuchi R, Ryo A, Komitsu N, Mikuni-Takagaki Y, Fukui A, Takagi Y, Shiraishi T, Morishita S, Yamazaki Y, Kumagai K, Aoki I, Saito T. Low-intensity pulsed ultrasound activates the phosphatidylinositol 3 kinase/Akt pathway and stimulates the growth of chondrocytes in three-dimensional cultures: a basic science study. *Arthritis Research & Therapy.* 2008; 10 (4): 1-11.

Tang C, Yang R, Huang T, Lu D, Chuang W, Huang T, Fu W. Ultrasound stimulates cyclooxygenase-2 expression and increases bone formation through integrin, focal adhesion kinase, phosphatidylinositol 3-kinase, and Akt pathway in osteoblasts. *Molecular Pharmacology.* 2006; 69 (6): 2047-2057.

Utreja A, Dyment N, Yadav S, Villa M, Li Y, Jiang X, Nanda R, Rowe D. Cell and matrix response of temporomandibular cartilage to mechanical loading. Osteoarthritis and Cartilage. 2016; 24: 335-344.

Wang W, Rigueur D, Lyons K. TGFβ signaling in cartilage development and maintenance. Birth Defects Res C Embryo Today. 2014; 102 (1): 37-51.

Wang X, Kou X, He D, Zeng M, Meng Z, Bi R, Liu Y, Zhang J, Gan Y, Zhou Y. Progression of cartilage degradation, bone resorption and pain in rat temporomandibular joint osteoarthritis induced by injection iodoacetate. PLoS ONE 2012; 7 (9): e45036 (1-12).

Zhang L. Effect of LIPUS on inflammatory factors, cell apoptosis and integrin signaling pathway in osteoarthritis animal models. Journal of Hainan Medical University. 2017; 23 (9): 17-20.

CHAPTER 5: GENERAL DISCUSSION AND CONCLUSION

This thesis included two parts, Parts 1 and 2. The objective of Part 1 was to validate the TMJ-CIA juvenile rat model, and the objective of Part 2 was the investigate the effect of LIPUS on TMJ-CIA in juvenile rats. We hypothesized that the CIA that would be induced in the TMJs of growing rats would develop arthritic changes in the TMJ as shown by TMJ inflammation and reduced mandibular growth. Additionally, we expected that LIPUS would reduce TMJ inflammation and stimulate mandibular growth.

The results for Part 1 of this thesis were published in the journal Tissue Engineering: Part C in February 2021. We demonstrated how inducing CIA in the TMJ in juvenile rats prevented normal mandibular growth. As well, we observed inflamed synovial tissue, cartilage invaginations, and lipid accumulation. Proteoglycan production and Col-II expression were reduced in the CIA cartilage, and the expressions of IL-1β, MMP-13 and TNF-α were greater in the CIA cartilage.

Because of our results in Part 1, we continued to use this rat model of TMJ arthritis, the CIA juvenile rat, to study the effect of LIPUS on TMJ arthritis. We investigated a potential preventive effect of LIPUS by immediately applying LIPUS to the TMJ after CIA induction in the TMJ in juvenile rats. We applied this treatment for 20 minutes/day for 4 weeks. Additionally, we investigated a potential treatment effect of LIPUS by applying this treatment beginning 4 weeks after the TMJ injections that were used to induce CIA. We were able to not only compare between these groups receiving LIPUS treatment beginning at different stages of disease, but we were also able to further study how CIA affects the TMJs beyond the 4 weeks that were studied in our published article (Part 1).

Considering the effects of CIA on the TMJ in the absence of any treatment, our study that validated this model clearly demonstrated that CIA rats had reduced mandibular growth. We

were able to confirm this result in Part 2 as well because our CIA rats again had reduced mandibular growth. This mandibular growth was normalized when LIPUS was applied to the TMJs either immediately after TMJ injections or after 4 weeks after these injections. In our validation study, we did not evaluate condylar volume, but we were able to do this evaluation in Part 2 of this thesis. Because of the reduced mandibular growth in the CIA groups that did not receive LIPUS treatment, we expected that this reduction in growth would be solely due to condylar erosion and therefore reduced condylar volume. This was not supported by our condylar volume data. After obtaining these results and considering the methods used to perform such measurements, this discrepancy may potentially be due to how condylar volume was measured, as previously discussed in this thesis. This part of the study helped to identify how these volumetric measurements could be improved for future studies that would help to more fully understand how LIPUS has had this effect on stimulating mandibular growth.

We performed histological analyses in both parts of the study to measure the thicknesses of the four cartilage cell layers. In Part 1 we demonstrated how the hypertrophic cell layer was significantly thicker in the CIA group, and in Part 2 we were able to confirm these results. An increase in hypertrophy in chondrocytes may result in increased mandibular growth, but this was not the case in the CIA groups. It is suspected that this increase in cartilage thickness may be an acute response to induced arthritis in the TMJ, as previously discussed. As well, we showed how LIPUS could prevent these acute responses of inappropriate cartilage thickening.

We obtained similar results between the studies concerning T.B. staining and immunostaining for Col-II and MMP-13. When LIPUS was applied to CIA TMJs, the production of proteoglycans and the expression of Col-II appear to be greater. However, when we observed the results of immunohistochemical-staining of TNF-α from each part of the thesis, our results do

not support each other. In Part 1 TNF-α expression was significantly greater in the CIA cartilage, but when we observed the same staining in Part 2, the CIA groups with only isoflurane did not demonstrate similar expression. Surprisingly, the LIPUS groups appeared to have increased expression. Since the effect of LIPUS on the expression of TNF-α in cartilage in TMJs with induced CIA has never been studied, we attempted to understand these results by considering the effect of LIPUS on different cell types in different conditions (healthy vs. inflamed, *in vivo* vs. *ex vivo*), as previously discussed. Additionally, there is conflicting literature regarding the exact role of TNF-α in RA or JIA [Farrugia & Baron, 2016]. TNF-α exists in two different forms – a membrane bound form and a soluble form – and these two forms are associated with binding different receptors to transduce intracellular signals. As well, there is evidence in the literature of clinical studies investigating anti-TNF-α therapies on inflammation and autoimmunity that demonstrate that these therapies worsen these conditions. Because of the results from our study and these clinical studies with contradictory results, more studies are needed to understand how TNF-α functions across different tissues, in different forms, and systemically in patients as well as in animal models of RA and JIA, like the TMJ-CIA juvenile rat model.

Furthermore, although our results may show some acute inflammation in terms of expression of pro-inflammatory cytokines in TMJ tissues, this inflammation does not appear to be sustained at 8 weeks (delayed treatment groups) within these tissues. Because of this, the mechanisms of how LIPUS could have an anti-inflammatory treatment effect on TMJ arthritis cannot be fully understood from our results. More studies need to investigate the long-term effects of CIA in the TMJ of juvenile rats in a time-dependent manner, understanding when inflammation subsides and if there is any relapse. This animal model may be a better model for

analyzing the short-term treatment effects of LIPUS on TMJ arthritis. Further investigation is needed to study long-term effects of both LIPUS and TMJ-CIA in this juvenile rat model.

To help summarize and explain the results from Part 1 and Part 2 of this study, two diagrams have been created. Figure 5.1 demonstrates a proposed mechanism describing the results from Part 1.

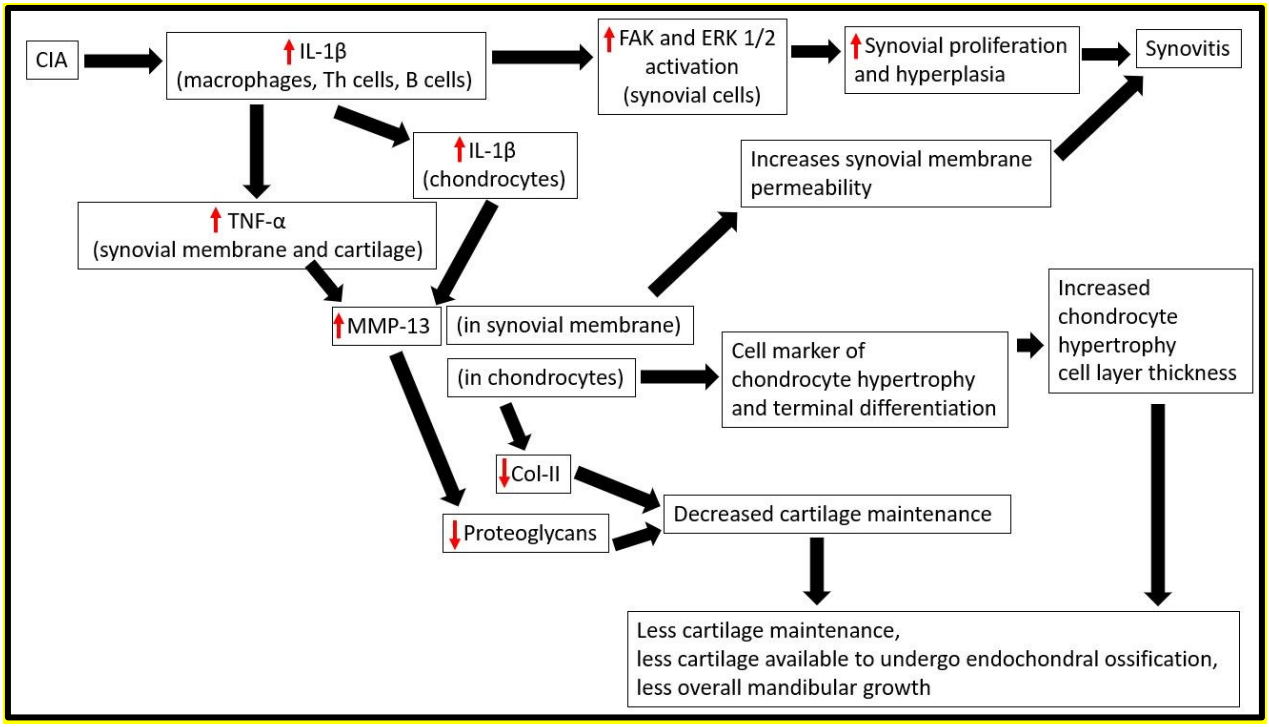

Figure 5.1: Illustration of proposed mechanism of the effect of CIA on the TMJ and mandibular growth in Part 1.

One of the most prominent proinflammatory cytokines involved in CIA is IL-1β. This cytokine can be produced by activated macrophages that reside in the local tissues, among other cells [Burmester et al., 1997]. Synovial hyperplasia, and therefore synovial cell proliferation, describe a main pathophysiologic feature of RA and CIA, has been associated with IL-1β. When

synovial cells are stimulated with IL-1β, it has been shown that COX-2 expression increases in these cells [Iwabuchi et al., 2014]. An increase in COX-2 expression occurs mainly through intracellular signalling involving activation of the FAK/MAPK pathway, including activation/phosphorylation of FAK and ERK 1/2. Additionally, the stimulation of this pathway can result in an increase in cell proliferation [Nakamura et al., 2011]. This may explain how CIA results in an increase in the observation of synovial cell hyperplasia, a characteristic of synovitis.

Another effect of the increased production of IL-1β induced by CIA in the TMJ may be an increased production and expression of TNF-α in the synovial membrane and the cartilage, and an increased expression of IL-β in the cartilage. We demonstrated in Part 1 an increased expression of TNF-α and IL-1β in TMJ condylar cartilage. It has been demonstrated that IL-1β stimulation in chondrocytes increased the production of MMPs, and the results in Part 1 show how MMP-13 expression was increased in the CIA cartilage [Iwabuchi et al., 2014]. Although we did not analyze any expression of MMPs in the synovial tissue, an increase in MMPs in this tissue increases synovial membrane permeability, which is a characteristic of synovitis [Scanzello &Goldring, 2012]. MMP-13 is a biomarker of chondrocyte hypertrophy and terminal differentiation, so therefore theoretically we should also observe increase in chondrocyte hypertrophy. We measured the hypertrophic chondrocyte cell layer thickness and found that this cell layer in the CIA group was significantly thicker. Also, MMP-13 expression is involved in cartilage degradation through breakdown of the ECM that includes proteoglycans and Col-II. This study showed that the expression of proteoglycans and Col-II were decreased in the CIA cartilage. A decrease in cartilage proteoglycan and Col-II production demonstrates a decrease in cartilage integrity and potentially lead to a decrease in cartilage maintenance over time. When considering decreased cartilage integrity and maintenance and an overall increase in chondrocyte

hypertrophy, then this should theoretically lead to less cartilage that would be available to undergo endochondral ossification, resulting in less mandibular growth. In Part 1 we did observe significantly less mandibular growth in the CIA group.

Figure 5.2 illustrates a proposed mechanism that may explain how immediate LIPUS treatment affected protein expression in the synovial tissue and cartilage in the CIA rats, leading to a prevention of mandibular growth disturbances that were observed in CIA-TMJs with no LIPUS treatment.

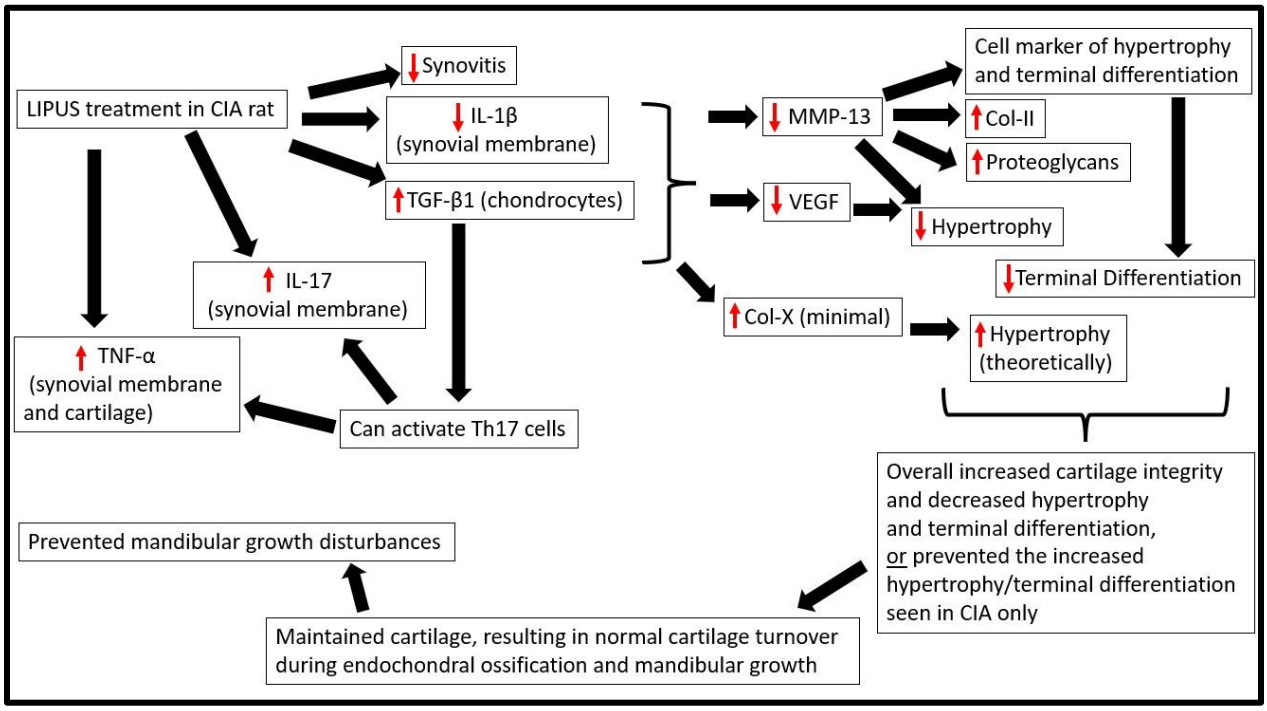

Figure 5.2: Illustration of proposed mechanism of the effect of immediate LIPUS treatment on CIA in the TMJ and mandibular growth in Part 2.

Previously in the proposed mechanism of how CIA in the TMJ results in synovitis, the induction of CIA increases the production of IL-1β. LIPUS has been shown to reduce the levels

of IL-1β in knee cartilage in an animal model of arthritis. In Part 2 of this study, we demonstrated how immediate LIPUS treatment decreased the expression of IL-1β in the synovial membrane in CIA TMJs. If LIPUS decreases this expression in the synovial membrane, then theoretically this should result in a decrease in synovitis, which we already observed in the TMJs of CIA rats that also received LIPUS treatment. Previously we described how an increase in IL-1β results in an increase in MMP-13 production. So, a decrease in IL-1β expression should lead to a decrease in MMP-13 expression. We demonstrated this in Part 2. Since MMP-13 expression is decreased, then we should expect to see an increase in the expression of components of the ECM, including proteoglycans and Col-II, which we did observe. As mentioned, MMP-13 is a marker of chondrocyte hypertrophy. Another marker of chondrocyte hypertrophy is VEGF. We found that LIPUS decreased the expression of VEGF. So, if we are observing less expression of the two markers of chondrocyte hypertrophy, then we should also observe a decrease in the thickness of the hypertrophic chondrocyte cell layer. We demonstrated this in Part 2.

Another important factor that we studied was TGF-β1. TGF-β1 plays an important role in regulating mandibular growth. Previous studies describe how LIPUS increased the production of TGF-β1 in chondrocytes, and we observed this in Part 2 [Li et al., 2003]. Another study demonstrated how exogenous TGF-β1 increased the expression of Col-II and decreased the expression of Col-X in chondrocytes [Mukai et al., 2005]. Although we did observe an increase in Col-II expression, we also observed an increase in Col-X expression instead of this expected decrease. However, in Part 2 the increase in Col-X expression in CIA cartilage was very subtle. Since Col-X is also a marker of chondrocyte hypertrophy, we would expect that this slight increase in Col-X expression would mean a minimal increase in chondrocyte hypertrophy in the CIA group that received immediate LIPUS treatment. However, the overall effect of LIPUS on

MMP-13 and VEGF was greater than that on Col-X, so we should expect that LIPUS decreased chondrocyte hypertrophy in CIA cartilage. This was demonstrated in our hypertrophic chondrocyte cell layer thickness measurements. So overall, we demonstrated how LIPUS increased cartilage integrity in CIA cartilage by increasing Col-II and proteoglycan expression and chondrocyte hypertrophy, and decreasing MMP-13 and VEGF expression. These results may also be interpreted as preventing the negative effect of CIA on TMJ cartilage. Since the TMJ cartilage may be better maintained, resulting in normal cartilage turnover during endochondral ossification and mandibular growth in CIA rats with LIPUS treatment, we would expect to see normal mandibular growth or prevention of these growth disturbances see in CIA rats without LIPUS treatment. We demonstrated that mandibular growth was increased in the LIPUS groups compared to the CIA-only groups, and that there were no differences in mandibular growth between normal healthy rats (Saline and no LIPUS) and CIA rats with LIPUS treatment.

In Part 2 we also observed some unexpected results when we studied the expression of TNF-α and IL-17. Our results show that the expression of these cytokines increased when LIPUS was applied to CIA TMJs. To help explain what may be happening, we must consider the expression of TGF-β1. It has been demonstrated that TGF-β1 can activate Th-17 cells [Zhang et al., 2018]. Activated Th-17 cells can produce both IL-17 and TNF-α [Tesmer et al., 2008]. So, this may explain how the expression of the cytokines increased when LIPUS was applied, however, how these cytokines had an effect on the TMJ tissues is still not fully understood. Future studies should consider studying this phenomenon.

5.1 *Limitations and Future Studies*

Identifying this study's limitations can help to understand this research's shortfalls as well as to help improve future studies. As mentioned, although we had previously studied the effect of CIA on the TMJ in juvenile rats, this study's timeline only consisted of 4 weeks beyond the TMJ injections. So, when we continued to use the model to study the effect of LIPUS on TMJ arthritis, we did not know how CIA could be observed in the older rats that continued in the study until 8 weeks after these TMJ injections. For our histological analyses, most of our observations were qualitative. Future studies should develop and use an appropriate disease scoring system for rats. This scoring system could allow for quantitative data to be obtained and statistically analyzed. Likewise, our immunohistochemical analyses were also qualitative. Improvements in the options of how to perform quantitative analyses in immunohistochemistry are required since many of the options are not valid. Our analysis of the expression of TNF-α in Part 1 of our study allowed for quantitative analysis because of the specific localized staining of this cytokine. Upon observation of the same staining in Part 2, this was not an option because the staining did not appear to be associated with immuno-positive cells but in the extracellular matrix instead. Additionally, in this study we used an anti-MMP13 antibody to analyze the expression of MMP-13 in the cartilage. This particular antibody used does recognize the proenzyme and active form of the enzyme MMP-13. Although from only the IHC immunostaining, it cannot be concluded that we only saw an increase in the active form since both forms of the enzyme are recognized by this antibody, we do see an increase in Col-II when MMP-13 expression was decreased. Therefore, this change may be due to changes in MMP-13 enzymatic activity, but we cannot be absolutely certain of this. Future studies should also consider using an antibody that is specific for the active form, or should consider isolating the

MMP-13 enzyme from the cartilage and using laboratory techniques to test the proteolytic activity of MMP-13 on degrading Col-II in vitro.

This study also mainly focused on changes within the cartilage, however, it is recommended that future studies further consider the effect of CIA and/or LIPUS on the subchondral bone. Many studies, including this one, assume that it's the effect of the cartilage that has a subsequent effect on the underlying bone, however, the opposite should also be considered – the changes within the subchondral bone affecting the overlying cartilage. Future studies should also measure condylar bone quality, such as bone mineral density, ratio of bone volume to total volume, trabeculae number, and trabeculae separation.

Finally, this study only included analyses of expressed protein and did not include any gene expression analysis to help further understand the effect of LIPUS on TMJ-CIA. RT-qPCR assays were planned but due to inappropriate tissue preservation, this method could not be performed properly. Future studies should include this type of analysis.

5.2 *Reference*

Burmester G, Stuhlmüller B, Keyszer G, Kinne R. Mononuclear phagocytes and rheumatoid arthritis. Mastermind of workhorse in arthritis? *Arthritis & Rheumatism.* 1997; 40 (1): 5-18.

Farrugia M, Baron B. The role of TNF-α in rheumatoid arthritis – a focus on regulatory T cells. Journal of Clinical and Translational Research. 2016; 2 (3): 84-90.

Iwabuchi Y, Tanimoto K, Tanne Y, Inubushi T, Kamiya T, Kunimatsu R, Hirose N, Mitsuyoshi T, Su S. Effects of low-intensity pulsed ultrasound on the expression of cyclooxygenase-2 in mandibular condylar chondrocytes. *J Oral Facial Pain Headache.* 2014; 28: 261-268.

Li J, Chang W, Lin J, Ruaan R, Liu H, Sun J. Cytokine release from osteoblasts in response to ultrasound stimulation. *Biomaterials.* 2003; 24: 2379-2385.

Mukai S, Ito H, Nakagawa Y, Akiyama H, Miyamoto M, Nakamura T. Transforming growth factor-β1 mediates the effects of low-intensity pulsed ultrasound in chondrocytes. Ultrasound in Med. & Biol. 2005; 31 (12): 1713-1721.

Nakamura T, Fujihara S, Yamamoto-Nagata K, Katsura T, Inubushi T, Tanaka E. Low-intensity pulsed ultrasound reduces the inflammatory activity of synovitis. *Annals of Biomedical Engineering.* 2011; 39 (12): 2964-2971.

Scanzello C, Goldring S. The role of synovitis in osteoarthritis pathogenesis. *Bone.* 2012; 51 (2): 249-257.

Tesmer L, Lundy S, Sarkar S, Fox D. Th17 cells in human disease. *Immunology.* 2008; 223: 87-113.

Zhang S. The role of transforming growth factor β in T helper 17 differentiation. *Immunology.* 2018; 155: 24-35.

BIBLIOGRAPHY

Ahmed N, Ptersson A, Irinel Catrina A, Mustafa H, Alstergren P. Tumor necrosis factor mediates temporomandibular joint bone tissue resorption in rheumatoid arthritis. Acta Odontologica Scandinavica. 2015; 73: 232-240.

Aho K, Palosuo T, Raunio V, Puska P, Aromaa A, Salonen J. When does rheumatoid disease start? *Arthritis and Rheumatism.* 1985; 28 (5): 485-489.

Arabshahi B and Cron R. Temporomandibular joint arthritis in juvenile idiopathic arthritis: the forgotten joint. Curr Opin Rheumatol. 2006; 18: 490-495.

Aref-Eshghi E, Liu M, Harper P, Doré J, Martin G, Furey A, Green R, Rahman P, Zhai G. Overexpression of MMP13 in human osteoarthritic cartilage is associated with the SMAD-independent TGF-β signalling pathway. Arthritis Research & Therapy. 2015; 17: 264-271.

Arita A, Yonemitsu I, Ikeda Y Miyazaki M, Ono T. Low-intensity pulsed ultrasound stimulation for mandibular condyle osteoarthritis lesions in rats. Oral Diseases. 2018; 24: 600-610.

Azuma Y, Ito Y, Harada Y, Takagi H, Ohta T, Jingushi S. Low-intensity pulsed ultrasound accelerates rat femoral fracture healing by acting on the various cellular reactions in the fracture callus. Journal of Bone and Mineral Research. 2001; 16(4): 671-680.

Banken R. Low-intensity ultrasound (Exogen^{TM}) for the treatment of fractures. Technology brief prepared by Reiner Banken (AETMIS 03-05). Montreal: AETMIS. 2004; x-15.

Barnes G, Kostenuik P, Gerstenfeld L, Einhorn T. Growth factor regulation of fracture repair. *Journal of Bone and Mineral Research.* 1999; 14 (11): 1805-1815.

Bendele A. Animal models of rheumatoid arthritis. J Musculoskel Neuron Interact. 2001; 1: 377-385.

Brand D, Kang A, Rosloniec E. Immunopathogenesis of collagen arthritis. Spring Semin Immunopathol. 2003; 25: 3-18.

Burmester G, Stuhlmüller B, Keyszer G, Kinne R. Mononuclear phagocytes and rheumatoid arthritis. Mastermind of workhorse in arthritis? *Arthritis & Rheumatism.* 1997; 40 (1): 5-18.

Carrasco R. Juvenile idiopathic arthritis overview and involvement of the temporomandibular joint – prevalence, systemic therapy. Oral Maxillofacial Surg Clin N Am. 2015; 27: 1-10.

Catrina A, Svensson C, Malmström V, Schett G, Klareskog L. Mechanisms leading from systemic autoimmunity to joint-specific disease in rheumatoid arthritis. *Nature Review. Rheumatology.* 2017; 13 (2): 79-86.

Cordeiro P, Guimaraes J, de Souza V, Dias I, Silva J, Devito K, Bonato L. Temporomandibular joint involvement in rheumatoid arthritis patients: association between clinical and tomographic data. Acta Odontol. Latinoam. 2016; 29 (3): 219-224.

Crossman J, Alzaheri N, Abdallah M, Tamimi F, Flood P, Alhadainy H, El-Bialy T. Low intensity pulsed ultrasound increases mandibular height and Col-II and VEGF expression in arthritic mice. Archives of Oral Biology. 2019; 104: 112-118.

Crossman J, Lai H, Kulka M, Jomha N, Flood P, El-Bialy T. Collagen-induced temporomandibular joint arthritis juvenile rat animal model. Tissue Engineering: Part C. 2021; 27 (2): 115-123.

D'Angelo M, Yan Z, Nooreyazdan M, Pacifici M, et al. MMP-13 is induced during chondrocyte hypertrophy. Journal of Cellular Biochemistry 2000;77:678-693.

Delatte M, Von den Hoff J, van Rheden R, Kuijpers-Jagtman A. Primary and secondary cartilages of the neonatal rat: the femoral head and the mandibular condyle. Eur J Oral Sci 2004;112:156-162.

Demoruelle M, Deane K, Holers M. When and where does inflammation begin in rheumatoid arthritis? Curr Opin Rheumatol. 2014; 26 (1): 64-71.

Einhorn T, Majeska R, Rush E, Levine P, Horowitz M. The expression of cytokine activity by fracture callus. *Journal of Bone and Mineral Research.* 1995; 10 (8): 1272-1281.

Farrugia M, Baron B. The role of TNF-α in rheumatoid arthritis – a focus on regulatory T cells. Journal of Clinical and Translational Research. 2016; 2 (3): 84-90.

Freeman T, Patel P, Parvizi J, Antoci V, Shapiro I. Micro-CT analysis with multiple thresholds allows detection of bone formation and resorption during ultrasound-treated fracture healing. Journal of Orthopaedic Research. 2009; 27: 673-679.

Griffiths M, Cremer M, Harper D, McCall S, Cannon G. Immunogenetics of collagen-induced arthritis in rats. Both MHC and non-MHC gene products determine the epitope specificity of immune response to bovine and chick type II collagens. The Journal of Immunology. 1992; 149 (1): 309-316.

Guo Q, Wang Y, Xu D, Nossent J, Pavlos N, Xu J. Rheumatoid arthritis: pathological mechanisms and modern pharmacologic therapies. Bone Research. 2018; 6 (15): 1-14.

Harrison A, Lin S, Pounder N, Mikuni-Takagaki Y. Mode & mechanism of low intensity pulsed ultrasound (LIPUS) in fracture repair. Ultrasonics. 2016; 7-: 45-52.

He D, An Y, Li Y, Wang J, Wu G, Chen G, Zhu G. RNA sequencing reveals target genes of temporomandibular joint osteoarthritis in rats after the treatment of low-intensity pulsed ultrasound. Gene. 2018; 672: 126-136.

Holmdahl R, Bockermann R, Bäcklund J, Yamada H. The molecular pathogenesis of collagen-induced arthritis in mice – a model for rheumatoid arthritis. Ageing Research Reviews. 2002; 1: 135-147.

Holwegner C, Reinhardt A, Schmid M, Marx D, Reinhardt R. Impact of local steroid or statin treatment of experimental temporomandibular joint arthritis on bone growth in young rats. American Journal of Orthodontics and Dentofacial Orthopedics. 2015; 147: 80-88.

Ishimi Y, Miyaura C, Jin C, Akatsu T, Abe E, Nakamura Y, Yamaguchi A, Yoshiki S, Matsuda T, Hirano T. Il-6 is produced by osteoblasts and induces bone resorption. *J Immunol.* 1990; 145: 3297-3303.

Iwabuchi Y, Tanimoto K, Tanne Y, Inubushi T, Kamiya T, Kunimatsu R, Hirose N, Mitsuyoshi T, Su S. Effects of low-intensity pulsed ultrasound on the expression of cyclooxygenase-2 in mandibular condylar chondrocytes. J Oral Facial Pain Headache. 2014; 28: 261-268.

Kartha S, Zhou T, Granquist E, Winkelstein B. Development of a rat model of mechanically induced tunable pain and associated temporomandibular joint responses. J Oral Maxillofac Surg. 2016; 74: 54e1-54e10.

Kaur H, Uludağ H, Dederich D, El-Bialy T. Effect of increasing low-intensity pulsed ultrasound and a functional appliance on the mandibular condyle in growing rats. J Ultrasound Med. 2017; 36: 109-120.

Kinne R, Bräuer R, Stuhlmüller B, Palombo-Kinne E, Burmester G. Macrophages in rheumatoid arthritis. Arthritis Res. 2000; 2: 189-202.

Kotake S, Udagawa N, Takahashi N, Matsuzaki K, Itoh K, Ishiyama S, Saito S, Inoue K, Kamatani N, Gillespie M, Martin T, Suda T. IL-17 in synovial fluids from patients with rheumatoid arthritis is a potent stimulator of osteoclastogenesis. J Clin Invest. 1999; 103: 1345-1352.

Li H, Wang D, Yuan Y, Min J. New insights on the MMP-13 regulatory network in the pathogenesis of early osteoarthritis. Arthritis Research & Therapy. 2017; 19: 1-12.

Li J, Chang W, Lin J, Ruaan R, Liu H, Sun J. Cytokine release from osteoblasts in response to ultrasound stimulation. Biomaterials. 2003; 24: 2379-2385.

Li X, Li J, Cheng K, Lin Q, Wang D, Zhang H, An H, Gao M, Chen A. Effect of low-intensity pulsed ultrasound on MMP-13 and MAPKs signaling pathway in rabbit knee osteoarthritis. Cell Biochem Biophys. 2011; 61: 427-434.

Lim W, Toothman J, Miller J, Tallents R, et al. IL-1β inhibits TGFβ in the temporomandibular joint. J Dent Res. 2009; 88: 557-562.

Liu J, Dai J, Wang Y, Lai S, Wang S. Significance of new blood vessels in the pathogenesis of temporomandibular joint osteoarthritis. Experimental and Therapeutic Medicine. 2017; 13: 2325-2331.

Liu W, Xu A, Li Z, Zhang Y, Han B. RANKL, OPG and CTR mRNA expression in the temporomandibular joint in rheumatoid arthritis. Experimental and Therapeutic Medicine. 2015; 10: 895-900.

Losken A, Mooney M, Siegel M. A comparative study of mandibular growth patterns in seven animal models. J Oral Maxillofac Surg. 1992; 50: 490-495.

Lutter A, Hempel U, Anderer U, Dieter P. Biphasic influence of PGE_2 on the resorption activity of osteoclast-like cells derived from human peripheral blood monocytes and mouse RAW264.7 cells. *Protaglandins, Leukotrienes and Essential Fatty Acids.* 2016; 111: 1-7.

Maldonado M, Nam J. The role of changes in extracellular matrix of cartilage in the presence of inflammation on the pathology of osteoarthritis. Biomed Research International. 2013; 2013: 1-10.

McNamee K, Williams R, Seed M. Animal models of rheumatoid arthritis: How informative are they? European Journal of Pharmacology. 2015; 759: 278-286.

Melo R, D'Avila H, Wan H, Bozza P, Dvorak A, Weller P. Lipid bodies in inflammatory cells: structure, function, and current imaging techniques. J Histochem Cytochem. 2011; 59: 540-556.

Miller D, Smith N, Bailey M, Czarnota G, Hynynen K, Makin I. Overview of therapeutic ultrasound application and safety considerations. J Ultrasound Med. 2012; 31: 623-634.

Mizoguchi I, Toriya N, Nakao Y. Growth of the mandible and biological characteristics of the mandibular condylar cartilage. Japanese Dental Science Review. 2013; 49: 139-150.

Moos V, Fickert S, Müller B, Weber U, Sieper J. Immunohistological analysis of cytokine expression in human osteoarthritic and healthy cartilage. J Rheumatology. 1999; 26: 870-879.

Morel M, Ruscitto A, Pylawka S, Reeve G, Embree M. Extracellular matrix turnover and inflammation in chemicall-induced TMJ arthritis mouse models. PLoS ONE. 2019; 14 (10): e0223244 (1-22).

Mukai S, Ito H, Nakagawa Y, Akiyama H, Miyamoto M, Nakamura T. Transforming growth factor-β1 mediates the effects of low-intensity pulsed ultrasound in chondrocytes. Ultrasound in Med. & Biol. 2005; 31 (12): 1713-1721.

Mulari M, Qu Q, Härkönen P, Väänänen H. Osteoblast-like cells complete osteoclastic bone resorption and form new mineralized bone matrix in vitro. *Calcif Tissue Int.* 2004; 75: 252-261.

Nakamura T, Fujihara S, Katsura T, Yamamoto K Inubushi T, Tanimoto K, Tanaka E. Effects of low-intensity pulsed ultrasound on the expression and activity of hyaluronan synthase and hyaluronidase in IL-1β-stimulated synovial cells. Annals of Biomedical Engineering. 2010; 38 (11): 3363-3370.

Nakamura T, Fujihara S, Yamamoto-Nagata K, Katsura T, Inubushi T, Tanaka E. Low-intensity pulsed ultrasound reduces the inflammatory activity of synovitis. Annals of Biomedical Engineering. 2011; 39 (12): 2964-2971.

Nandakumar K, Svensson L, Holmdahl R. Collagen type II-specific monoclonal antibody-induced arthritis in mice. Description of the disease and the influence of age, sex, and genes. American Journal of Pathology. 2003; 163 (5): 1827-1837.

Naruse K, Sekya H, Harada Y, Iwabuchi S, Kozai Y, Kawamata R, Kashima I, Uchida K, Urabe K, Seto K, Itoman M, Mikuni-Takagaki Y. Prolonged endochondral bone healing in senescence is shortened by low-intensity pulsed ultrasound in a manner dependent on Cox-2. Ultrasound in Med. &. Biol. 2010; 36 (7): 1098-1108.

Nejad S, Kobezda T, Tar I, Szekanecz Z. Development of temporomandibular joint arthritis: the use of animal models. Joint Bone Spine. 2017; 84: 145-151.

Nigrovic P, Raychaudhuri S, Thompson S. Genetics and the classification of arthritis in adults and children. Arthritis Rheumatol. 2018; 70 (1): 7-17.

Ohashi N, Ejiri S, Hanada K, Ozawa H. Changes in type I, II, and X collagen immunoreactivity of the mandibular condylar cartilage in a naturally aging rat model. J Bone Miner Metab. 1997; 15: 77-83.

Oyonarte R, Zárate M, Rodriguez F. Low-intensity pulsed ultrasound stimulation of condylar growth in rats. Angle Orthodontist. 2009; 79 (5): 964-970.

Palanisamy P, Alam M, Li S, Chow S, Zheng Y. Low-intensity pulsed ultrasound stimulation for bone fractures healing. *Journal of Ultrasound in Medicine.* 2021; 9999: 1-17.

Pedersen T, Jensen J, Melsen B, Herlin T. Resorption of the temporomandibular condylar bone according to subtypes of juvenile chronic arthritis. The Journal of Rheumatology. 2001; 28 (9): 2109-2115.

Phadke K, Fouts R, Parrish J. Collagen-induced and adjuvant-induced arthritis in rats. Arthritis and Rheumatism. 1984; 27: 797-806.

Prahalad S and Glass D. Is juvenile rheumatoid arthritis/juvenile idiopathic arthritis different from rheumatoid arthritis? Arthritis Res. 2002; 4 (suppl 3): 303-310.

Repacholi M, Grandolfo M, Rindi A. (1987). Ultrasound: Medical application, biological effects, and hazard potential. Plenum Press.

Ringold S, Cron R. The temporomandibular joint in juvenile idiopathic arthritis: frequently used and frequently arthritic. *Pediatric Rheumatology.* 2009; 7 (11): 1-9.

Rose B, Kooyman D. A tale of two joint: The role of matrix metalloproteases in cartilage biology. Disease Markers. 2016; 2016: 1-7.

Sato M, Nagata K, Kuroda S, Horiuchi S, Nakamura T, Karima M, Inubushi T, Tanaka E. Low-intensity pulsed ultrasound activates integrin-mediated mechanotransduction pathway in synovial cells. Annals of Biomedical Engineering. 2014; 40 (10): 2156-2163.

Scanzello C, Goldring S. The role of synovitis in osteoarthritis pathogenesis. *Bone.* 2012; 51 (2): 249-257.

Schindeler A, McDonald M, Bokko P, Little D. Bone remodeling during fracture repair: the cellular picture. Seminars in Cell & Developmental Biology. 2008; 19: 459-466.

Scott D, Wolfe F, Huizinga T. Rheumatoid arthritis. Lancet. 2010; 376: 1094-1108.

Sekino J, Nagao M, Kato S, Sakai M, Abe K, Nakayama E, Sato M, Nagashima Y, Hino H, Tanabe N, Kawato T, Maeno M, Suzuki N, Ueda K. Low-intensity pulsed ultrasound induces cartilage matrix synthesis and reduced MMP13 expression in chondrocytes. Biochemical and Biophysical Research Communications. 2018; 506: 290-297.

Shen P, Jiao Z, Zhen J, Xu W, Zhang S, Qin A, Yang C. Injecting vascular endothelial growth factor into the temporomandibular joint induces osteoarthritis in mice. Scientific Reports. 2015; 5: 16244 (1-11).

Snir O, Widhe M, Hermansson M, von Spee C, Lindber J, Hensen S, Lundberg K, Engström Å, Venables P, Toes R, Holmdahl R, Klareskog L, Malmström V. Antibodies to several citrullinated antigens are enriched in the joints of rheumatoid arthritis patients. *Arthritis & Rheumatism.* 2010; 62 (1): 44-52.

Stocum D, Roberts W. Part I: development and physiology of the temporomandibular joint. Curr Osteoporos Rep. 2018; 16 (4): 360-368.

Stroustrup P, Kristensen K, Küseler A, Pedersen T, Herlin T. Temporomandibular joint steroid injections in patients with juvenile idiopathic arthritis: an observation study on the long-term effect on signs and symptoms. Rheumatology. 2015; 13: 1-6.

Stuart J, Cremer M, Kang A, Townes A. Collagen-induced arthritis in rats. Arthritis and Rheumatism. 1979; 22 (12): 1344-1351.

Sun J, Hong R, Chang W, Chen L, Lin F, Liu H. In vitro effects of low-intensity ultrasound stimulation on the bone cells. J Biomed Mater Res. 2001; 57: 449-456.

Svensson L, Jirholt J, Holmdahl R, Jansson L. B cell-deficient mice do not develop type II collagen-induced arthritis (CIA). Clin Exp Immunol. 1998; 111: 521-526.

Takeuchi R, Ryo A, Komitsu N, Mikuni-Takagaki Y, Fukui A, Takagi Y, Shiraishi T, Morishita S, Yamazaki Y, Kumagai K, Aoki I, Saito T. Low-intensity pulsed ultrasound activates the phosphatidylinositol 3 kinase/Akt pathway and stimulates the growth of chondrocytes in three-dimensional cultures: a basic science study. Arthritis Research & Therapy. 2008; 10 (4): 1-11.

Tang C, Yang R, Huang T, Lu D, Chuang W, Huang T, Fu W. Ultrasound stimulates cyclooxygenase-2 expression and increases bone formation through integrin, focal adhesion kinase, phosphatidylinositol 3-kinase, and Akt pathway in osteoblasts. Molecular Pharmacology. 2006; 69 (6): 2047-2057.

Terato K, Hasty K, Reife R, Cremer M, Kang A, Stuart J. Induction of arthritis with monoclonal antibodies to collagen. J Immunol. 1992; 148: 2103-2108.

Trentham D, Townes A, Kang A. Autoimmunity to type II collagen: an experimental model of arthritis. The Journal of Experimental Medicine. 1977; 146: 857-868.

Utreja A, Dyment N, Yadav S, Villa M, Li Y, Jiang X, Nanda R, Rowe D. Cell and matrix response of temporomandibular cartilage to mechanical loading. Osteoarthritis and Cartilage. 2016; 24: 335-344.
Wang W, Rigueur D, Lyons K. TGFβ signaling in cartilage development and maintenance. Birth Defects Res C Embryo Today. 2014; 102 (1): 37-51.

Van de Sande M, de Hair M, van der Leij C, Klarenbeek P, Bos W, Smith M, Maas M, de Vries N, van Schaardenburg D, Dijkmans B, Gerlag D, Tak P. Different stages of rheumatoid arthritis: features of the synovium in the preclinical phase. *Ann Rheum Dis.* 2011; 70: 772-777.

Wang X, Kou X, He D, Zeng M, Meng Z, Bi R, Liu Y, Zhang J, Gan Y, Zhou Y. Progression of cartilage degradation, bone resorption and pain in rat temporomandibular joint osteoarthritis induced by injection iodoacetate. PLoS ONE. 2012; 7 (9): e45036 (1-12).

Wells P. Ultrasonics in medicine and biology. *Phys. Med. Biol.* 1977; 22 (4): 629-669.

Wilson-Gerwing T, Pratt I, Cooper D, Silver T, Rosenberg A. Age-related differences in collagen-induced arthritis: Clinical and imaging correlations. Comparative Medicine. 2013; 63(6): 498-502.

Wojdasiewicz P, Poniatowski L, Szukiewicz D. The role of inflammatory and anti-inflammatory cytokines in the pathogenesis of osteoarthritis. Mediators of Inflammation. 2014; 2014: 1-19.

Wu G, Zhu S, Sun X, Hu J. Subchondral bone changes and chondrogenic capacity of progenitor cells from subchondral bone in the collagenase-induced temporomandibular joints osteoarthritis rabbit model. Int J Clin Exp Pathol. 2015; 8: 9782-9789.

Yap H, Tee S, Wong M, Chow S, Peh S, Teow S. Pathogenic role of immune cells in rheumatoid arthritis: implications in clinical treatment and biomarker development. Cells. 2018; 7 (161): 1-19.

Yokoyama U, Iwatsubo K, Umemura M, Fujita T, Ishikawa Y. The prostanoid EP4 receptor and its signaling pathway. Pharmacol Rev. 2013; 65: 1010-1052.

Zhang L. Effect of LIPUS on inflammatory factors, cell apoptosis and integrin signaling pathway in osteoarthritis animal models. Journal of Hainan Medical University. 2017. 23 (9): 17-20.

Zhong X, Wang H, Jian X. Expression of matrix metalloproteinases-8 and -9 and their tissue inhibitor in the condyles of diabetic rats with mandibular advancement. *Experimental and Therapeutic Medicine.* 2014; 8: 1357-1364.

Zoetis T. Tassinari M, Bagi C, Walthall K, Hurtt M. Species comparison of postnatal bone growth and development. Birth Defects Research. 2003; 68: 86-110.